HEC MONTRÉAL
École affiliée à l'Université de Montréal

Outils d'aide à la décision pour la mise en place d'un réseau de transports en commun électriques

par
Pierre Vendé

Thèse présentée en vue de l'obtention du grade de Ph. D. en administration
(spécialisation Gestion des opérations et de la logistique)

Mai 2024

HEC MONTRÉAL
École affiliée à l'Université de Montréal

Cette thèse intitulée :

Outils d'aide à la décision pour la mise en place d'un réseau de transports en commun électriques

Présentée par :

Pierre Vendé

a été évaluée par un jury composé des personnes suivantes :

Guy Desaulniers
Polytechnique Montréal
Président-rapporteur

Jorge E. Mendoza
HEC Montréal
Directeur de recherche

Michel Gendreau
Polytechnique Montréal
Codirecteur de recherche

Emmanuel Néron
Université de Tours
Codirecteur de la cotutelle

Marilène Cherkesly
Université du Québec à Montréal – École des Sciences de la Gestion
Membre du jury

Caroline Prodhon
Université de Technologie de Troyes
Examinatrice externe

Jorge E. Mendoza
HEC Montréal
Représentant du directeur de HEC Montréal

Résumé

L'intégration de bus électriques dans les réseaux de transport en commun représente une solution pour limiter les émissions de gaz à effet de serre. Cependant, la mise en place d'une flotte de bus électriques soulève des questions d'organisation et de dimensionnement, notamment sur les aspects d'infrastructures pour la recharge des batteries des bus. Cette thèse vise à répondre à certaines de ces questions en étudiant et résolvant les problématiques liées aux différentes stratégies de recharge (nocturne ou en route) et de localisation et dimensionnement des chargeurs. Tout d'abord, le premier chapitre de la thèse aborde un problème d'emplacement de chargeurs dans un réseau de transport, utilisant des bus hybrides, dont les chargeurs sont placés sur le long des lignes et partagées entre les différentes lignes. Le problème consiste à trouver où placer des chargeurs, combien en installer, et comment les utiliser. Les deux fonctions objectif considérées sont : la maximisation de la distance parcourue en utilisant le mode électrique et la minimisation des coûts d'installation. Des perspectives managériales sont présentées et portent sur les bénéfices opérationnels et économiques d'utiliser des chargeurs partagés et les bénéfices économiques d'utiliser des bus hybrides à la place de bus électriques. Le deuxième chapitre aborde un problème d'affectation de bus électriques et d'ordonnancement de la recharge nocturne sur plusieurs jours. En considérant un ensemble de bloc véhicules (suites programmées de trajets effectués par le même bus sur une journée) sur plusieurs jours, un ensemble de bus électriques identiques, et un ensemble de chargeurs disponibles au dépôt, le problème consiste à affecter un bus électrique à chaque bloc et à planifier la recharge nocturne au dépôt. L'objectif est de minimiser le coût total de recharge tout en préservant

la durée de vie de la batterie à long terme. Les expérimentations réalisées montrent l'intérêt de considérer un horizon de plusieurs jours ainsi que celui bien gérer l'état de charge de la batterie. Le dernier chapitre de cette thèse étend les travaux du deuxième chapitre en considérant qu'il possible d'ajouter des opérations de recharges de batterie d'un bus lors de son trajet durant la journée. En plus des décisions prises dans le problème de départ, il faut également ordonnancer les opérations de recharge en route. Les expérimentations numériques conduites montrent l'intérêt d'utiliser une combinaison de stratégies de recharge mais aussi celui de limiter le nombre d'événements de recharge. Pour chacun des problèmes, des MILP et des méthodes de résolution ont été développées.

Mots-clés

Recherche opérationnelle ; Bus électriques ; Réseau de transport ; Emplacement de chargeurs ; Ordonnancement de la recharge ; Programmation linéaire ; Branch-and-check ; Matheuristique

Méthodes de recherche

Programmation linéaire ; Branch-and-check ; Matheuristique

Abstract

The integration of electric buses into public transit networks is a solution to limit greenhouse gas emissions. However, deploying an electric bus fleet raises organizational and sizing questions, especially regarding infrastructure for battery charging. This thesis aims to address some of these questions by studying and solving issues related to different charging strategies (overnight or en-route) and the location and sizing of chargers. The first chapter addresses a charger location problem in a transit network using hybrid buses, where chargers are placed along routes and shared between different lines. The problem involves determining charger location, quantity, and how to use those chargers. The two objective functions considered are : maximizing the distance traveled using electric mode and minimizing installation costs. Managerial perspectives highlight the operational and economic benefits of using shared chargers and the economic benefits of using hybrid buses instead of electric ones. The second chapter tackles a multi-day electric bus assignment and an overnight charging scheduling problem. The goal is to assign an electric bus to each vehicle block (pre-computed route sequence performed by the same bus in a day) and plan overnight charging at the depot to minimize total charging costs while preserving battery lifespan. Experimentation shows the importance of considering a multi-day planning horizon and effectively managing battery state of charge. The final chapter extends the work of the second one by considering the addition of battery charging operations during a bus trip throughout the day. In addition to decisions made in the initial problem, en-route charging operations need to be scheduled. Numerical experiments demonstrate the benefits of using a combination of charging strategies and limiting the number of

charging events. For each of the problems, MILP formulations and solution methods have been developed.

Keywords

Operational research ; Electric buses ; Transit network ; Charger location ; Charging Scheduling ; Linear programming ; Branch-and-check ; Matheuristic

Research Methods

Linear programming ; Branch-and-check ; Matheuristic

Table des matières

Liste des tableaux

Liste des figures

Liste des abréviations

AtS Assign-then-schedule

BC Branch-and-check

CCNUCC Convention-cadre des Nations unies sur les changements climatiques

CLP Charging location problem

COP Conférence des parties

CSP Charging scheduling problem

CS Charging station

D-AtS Daily-assign-then-schedule

EB Electric bus

FCLP-HB Fast-charging infrastructure location problem in networks operated with hybrid buses

FTP Fleet transformation problem

GES Gaz à effet de serre

GIEC Groupe d'experts intergouvernemental sur l'évolution du climat

HBC Branch-and-check-based heuristic

HB Hybrid bus

ITPM Iterative two-phase matheuristic

Max-SS Maximum short-sighted

MDEBARSP Multi-day EB assignment and recharge scheduling problem

MDEBAOSP Multi-day EB assignment and overnight recharge scheduling problem

MILP Mixed-integer linear program

Min-SS Minimum short-sighted

SAP Sequence assignment problem

SoC State of charge

VSP Vehicle scheduling problem

Remerciements

Cette période du doctorat fut une période de transition, de la vie étudiante vers la vie professionnelle. À l'image de Sacha après ses cinq années d'aventures sur le continent où il a débuté pour devenir le meilleur dresseur, j'ai moi aussi pris le large pour mon Hoenn personnel afin de devenir le meilleur chercheur. Cette transition s'est effectuée à travers bien des épreuves. J'ai changé de pays et de continent, ce qui m'a fait traverser la COVID dans un monde rempli d'inconnu. J'ai découvert d'autres environnements de travail, d'autres manières d'enseigner, mais aussi d'apprendre, et tout cela a grandement aidé à faire de moi le chercheur que je suis devenu. Toutes ces épreuves auraient été bien plus difficiles à surmonter sans le soutien de nombreuses personnes.

Je souhaite tout d'abord remercier l'école du HEC Montréal de m'avoir accueilli dans ses locaux et de m'avoir fait découvrir le monde des écoles de gestion. Les cours que j'ai pu y suivre ont une philosophie bien différente de celle des cours que j'ai connus en école d'ingénieur et cela m'a permis d'acquérir une plus grande ouverture d'esprit sur les méthodes d'enseignement. Je remercie également Martin de m'avoir fait confiance pour l'aider dans son enseignement dès que je suis arrivé à l'école. Ayant réalisé mon doctorat en co-tutelle, j'ai eu la chance de pouvoir effectuer la seconde moitié de mon doctorat dans mon alma mater, l'École Polytechnique de l'Université de Tours. Je remercie Ameur et Vincent de m'avoir donné l'opportunité d'enseigner des cours que j'avais moi-même aimés suivre en tant qu'élève-ingénieur. Toutes ces expériences d'enseignement ont confirmé mon souhait de continuer l'enseignement à l'avenir. Ce retour dans l'établissement où j'avais fait mes études m'a permis de rester jeune et étudiant quelques

années supplémentaires. Je remercie donc les étudiants de l'école d'avoir joué le jeu en m'intégrant dans les activités étudiantes pendant ces années que ce soit à travers ma participation à la K'fet (Bachar, Hénorie et Jaafar), je resterai toujours votre responsable retraite si le besoin s'en fait sentir, ou pendant les heures passées au baby-foot (Mallory, Mathieu et Noé). Ces moments furent des parenthèses de détente fort bienvenues dans des moments pas toujours évidents. Ce doctorat m'a permis de découvrir d'autres aspects de l'école, à savoir l'aspect recherche. Je remercie donc tous les membres et personnels du Laboratoire d'Informatique Fondamentale et Appliquée de Tours pour les moments passés ensemble, et en particulier les doctorants du laboratoire (Antoine, Félix, Hao, Quentin, Simon, Thomas, Tom et Xavier) pour les moments de pause passés au restaurant universitaire ou autour du baby-foot. Échanger avec vous au quotidien m'a fait grandement relativiser sur notre vie de doctorant en informatique.

L'ambiance avec les autres membres de l'établissement est primordiale dans le bon déroulement d'une thèse, tout autant que la relation avec les encadrants. Je remercie donc Guy et Michel d'avoir rejoint mon équipe d'encadrement au long de mon doctorat. Les discussions que nous avions étaient toujours très enrichissantes, que ce soit d'un point de vue professionnel ou personnel et j'ai pu beaucoup apprendre grâce à vous. Cependant, toute cette aventure n'aurait probablement jamais commencé sans Jorge et Yannick que je ne pourrai jamais assez remercier. Avoir accepté de me prendre en stage pour l'été 2018 a changé ma vie à jamais. Ce stage a été suivi d'un projet de fin d'étude qui a débouché sur cette thèse. J'étais destiné à devenir un ingénieur qui place des boutons sur un logiciel toute la journée. Mais grâce à vous, je sais qu'il n'existe aucune limite dans ce que je peux faire dans la vie et je me sens prêt à affronter tous les défis que je rencontrerai à l'avenir. Les réunions de travail avec mes encadrants ont toujours été des moments que j'attendais impatiemment et j'ai énormément apprécié être le Perceval de nos réunions de chevaliers de la table ronde. J'espère sincèrement que l'avenir nous permettra de travailler à nouveau ensemble. Je remercie également le reste des membres du jury (Caroline, Dominique, Emmanuel et Marilène) pour avoir accepté de suivre et de juger mon travail, parfois depuis plusieurs années.

Bien que le doctorat soit un travail à plein temps, il est important d'avoir une vie en dehors et rien de mieux qu'une bande d'amis pour ça. Je remercie donc toutes les personnes que j'ai pu rencontrer par le biais du comité PhD de l'Association des Étudiants aux Cycles Supérieurs du HEC Montréal, et en particulier Colombine, Dr Florian pour nos samedis matin travail puis restaurant, Francis, Julie, Justine-Anne, Nicolas pour nos discussions politiques des plus passionnantes, Dr Patrick, et bien évidemment Sara-Maude pour nos délicieux moments passés ensemble en compagnie du beau Mario. La COVID a écourté nos expériences de sortie à Montréal mais vous m'avez montré un aspect du Québec que je n'aurais jamais pu découvrir autrement. J'ai également eu l'opportunité de continuer le théâtre pendant le début de ma thèse, avant que la COVID ne mette fin à cette activité. Je remercie donc la troupe de théâtre du club Artistes en Affaires du HEC Montréal pour ces moments artistiques passés ensemble. Je n'aurais jamais cru finir ma carrière d'acteur en jouant devant une salle comble de 200 personnes. Je remercie également toutes les personnes que j'ai pu rencontrer par le biais de l'Association des Doctorants de l'Université de Tours dont j'ai eu l'honneur d'être le trésorier pendant un an, et en particulier Adam, Dr Antonin, Dre Pico, Dr Romain, Dr Thomas et Yohan pour nos sorties (trop ?) régulières au Shamrock, les soirées pétanque, les plans Guinguette, le eau-ou-vodka, le Piccolo Grande, le Cragnac, les soirées jeux des Velpotes, le marathon en équipe et tant d'autres moments passés ensemble. Vous êtes vraiment le *best group* dont j'avais besoin pour faire ma thèse. Promis, un jour, on ira tous ensemble au Milord. Je remercie également ma famille (mes parents, ma sœur et mon grand-père) pour leur soutien inconditionnel envers mes aventures sur le globe à grands coups d'éclairs au chocolat. Je remercie Alexandre et François de leurs encouragements constants pendant ma thèse bien qu'ils aient tous deux étés physiquement très loin de moi et Dre Camille pour m'avoir montré la voie à suivre, et surtout celle à ne pas suivre, pour faire un doctorat. Je ne pouvais pas finir ces remerciements sans remercier Paul, mon side-kick depuis toujours, le Leonard de mon Sheldon, sans qui j'aurais difficilement pu aller au bout de cette thèse, toujours là dans les bons moments et surtout dans les plus mauvais. Merci pour les moments passés ensemble, les soirées chocolat chaud et jeux vidéo, les journées

Minecraft et les matchs de baby-foot (où il faut admettre que j'ai fini par te surclasser).

Pour finir, je souhaite remercier toutes les personnes qui m'ont soutenu de près ou de loin pendant cette période. Je n'ai pas pu citer tout le monde mais vous vous reconnaitrez. Aujourd'hui n'est pas seulement la fin de mon doctorat mais la fin de 10 ans de bons et loyaux services à Polytech Tours. Pendant cette période de ma vie, j'ai découvert l'informatique, je suis devenu ingénieur et j'ai obtenu deux doctorats. Je suis finalement devenu le Dr Sheldon Cooper que je regardais avant de commencer cette aventure. Je me suis mis à courir derrière mes objectifs (à une vitesse de 5 minutes au kilomètre), j'ai développé un mental d'acier pour ne jamais rien abandonner, prêt à affronter tous les défis qui se dresseront devant moi, et je suis actuellement la meilleure version de moi-même. Depuis aussi loin que je me souvienne, j'ai toujours eu un plan précis de ce qui allait m'attendre à moyen terme et pour une fois je ne sais pas ce qui m'attend pour la suite. Cette situation est à la fois terrifiante mais excitante car cela veut dire que tout peut arriver lors de mes aventures à Sinnoh.

En espérant que votre lecture de ce manuscrit soit aussi palpitante que mes expériences vécues pendant mes années de doctorat.

Pierre « Dr Potter » Vendé, PhD, PhD

Introduction générale

“ Notre maison brûle et nous regardons ailleurs ”, ainsi furent les mots prononcés par le président Chirac lors du IV^{e} Sommet de la Terre à Johannesburg en 2002, afin de dénoncer l’inaction des États face aux effets du réchauffement climatique sur l’environnement.

Les sommets de la Terre sont des rencontres décennales organisées par l’Organisation des Nations unies (ONU ou UN en anglais), où les dirigeants des différents pays se réunissent pour parler environnement et développement durable. L’objectif principal de ces conférences est de mettre en avant la coopération mondiale afin de résoudre les problèmes environnementaux et les problèmes de développement (UN, 2024). Ils ont été créés pour répondre aux nouveaux défis qui menacent la planète tels que le changement climatique, la perte de la biodiversité et la désertification. La réponse à ces défis passe par la création d’accords et de plans d’action sur le long terme, afin de préserver la planète et d’assurer un avenir durable. Ils rassemblent des représentants de gouvernements, d’organisations internationales, d’ONG et du secteur privé pour trouver des solutions à ces défis mondiaux.

Depuis la mise en place de ces conférences sur l’environnement, des conférences non-régulières ont également fait leur apparition. En effet, se rencontrer une fois tous les 10 ans est trop peu comparativement à la vitesse du changement de l’environnement. Bien que le thème de ces conférences soit général à travers l’environnement et le développement durable, le climat fait régulièrement partie des sujets de préoccupation de la communauté internationale. Lors de ces conférences, des plans d’action et des conventions ont été mises en place par l'ONU, dont la convention-cadre des Nations unies sur les changements climatiques (CCNUCC ou UNFCCC en anglais) (UN, 1992). C'est dans le cadre de cette convention que se réunissent les États à travers des conférences des parties (COP). Les COP sont des réunions internationales où les pays participants à la CCNUCC se réunissent pour discuter des actions à entreprendre pour lutter contre le changement climatique (UNFCCC, 2024). Les COP ont pour objectif de coordonner les efforts mondiaux pour réduire les émissions de gaz à effet de serre (GES), adapter les sociétés aux impacts du changement climatique, et mobiliser des financements pour soutenir les pays en développement dans leurs efforts en matière de lutte contre les changements climatiques.

Afin de prendre des décisions lors de ces différents sommets, les États utilisent des rapports provenant d'organismes tels que le groupe d'experts intergouvernemental sur l'évolution du climat (GIEC ou IPCC en anglais). Le GIEC est une organisation scientifique internationale chargée d'identifier les causes et les conséquences du changement climatique actuel (IPCC, 2024). Le GIEC fournit des rapports réguliers basés sur les dernières recherches climatiques pour informer les décideurs politiques et le public sur les impacts du changement climatique, les risques associés et la manière dont on peut réduire les effets de ce changement ou comment s'y adapter.

Le dernier rapport du GIEC en date est le 6^{e} rapport d'évaluation publié en 2023 (IPCC, 2023). Ce rapport met en lumière plusieurs observations clés. Il indique que le changement climatique s'accélère. En effet, sur la période 2013–2022 (période d'étude du rapport), la température mondiale à la surface de la planète est 1.15°C plus élevée que lors de la période 1850–1900 (période de référence). On note que depuis la précédente période d'observation (2003–2012), l'augmentation a été de 0.19°C. Ainsi, l'augmentation observée pendant la période du 6^{e} rapport correspond à une hausse de près de 20% de l'augmentation entre la période de référence et celle du 5^{e} rapport. Si les politiques actuelles de lutte contre le réchauffement climatique ne sont pas renforcées, la hausse depuis la période de référence pourra être jusqu'à 3.2°C lors de la période 2081–2100, et jusqu'à 4.4°C si ces politiques sont assouplies ou même supprimées. Ces augmentations de température ont déjà un impact sur l'écosystème. Depuis les années 1950, les canicules sont devenues plus fréquentes sur l'entièreté des surfaces terrestres et les épisodes de grand froid plus rares. Les sécheresses sont également plus répétées dues à l'évaporation massive des sols et le nombre de cyclones tropicaux a significativement augmenté pendant les 40 dernières années. Ces épisodes météorologiques dégradent les sols, les rendant moins adaptés à l'agriculture. On observe donc une diminution des rendements. La baisse de la production agricole suite à ces événements crée à terme des risques pour la sécurité alimentaire des populations locales. L'assèchement des sols les a rendu imperméables et on observe des inondations plus fréquentes. Ces inondations et les phénomènes extrêmes tels que les tempêtes causent de forts dommages aux infrastructures. Toutes ces modifications de l'environnement rendent certaines régions moins propices au développement. Certaines populations décident de migrer afin de vivre dans des zones plus habitables. Une autre conséquence de ces changements climatiques est donc l'augmentation significative des réfugiés climatiques. Le dérèglement du climat provient de l'augmentation significative des émissions de GES, majoritairement du CO_2, provenant principalement des activités humaines telles que la combustion de combustibles fossiles, pour l'énergie, et le déboisement, pour l'agriculture, ainsi que des secteurs-clés liés au développement tels que l'industrie et le transport. Ce sont également ces émissions de GES qui sont le moteur principal de l'augmentation de température. En 2019, l'énergie représentait 34% des émissions de GES, l'industrie en produisait 24%, l'agriculture était responsable de 22% et le transport de 15%.

Les rapports d'évaluation du GIEC ne présentent pas seulement les causes et les conséquences du changement climatique. Ils proposent aussi des solutions afin de limiter ou d'inverser ces changements. Ce 6^{e} rapport insiste sur l'urgence d'actions rapides et décisives pour réduire les émissions de GES, s'adapter aux impacts du changement climatique et limiter les dommages futurs. Ces actions ont pour but de limiter l'augmentation à 1.5°C. Le rapport propose des actions dans les principaux secteurs d'émissions de GES : l'énergie, l'industrie, l'agriculture, et le transport. Dans le domaine de l'énergie, il faut réduire la part des énergies fossiles (charbon, pétrole et gaz) dans le mix énergétique et privilégier les énergies décarbonées (solaire, éolien, hydraulique, nucléaire). Dans le domaine de l'industrie, il est préconisé de changer les processus de production afin de les orienter vers des processus moins polluants. Cela peut se faire par l'utilisation de matériaux plus efficaces, mais aussi en promouvant l'économie circulaire et le recyclage des déchets issus de la production vers d'autres systèmes de production. L'objectif est de limiter les flux d'entrée et de sortie des systèmes industriels et ainsi de diminuer la consommation des matières premières et la production de déchets ainsi que les transports qui en résultent. Dans le domaine de l'agriculture, le rapport conseille tout d'abord de réduire la conversion des écosystèmes naturels, responsable de la moitié des émissions du domaine agricole. Cette action de contrôle de ces écosystèmes peut même aller jusqu'à un processus de reforestation, les arbres pouvant capturer naturellement le CO_2. Un autre axe d'action est le changement des régimes alimentaires des populations. L'industrie de la viande est un grand domaine producteur de GES, de l'élevage des animaux jusqu'à sa mise sur le marché. Changer les habitudes de consommation changerait les besoins de production et donc diminuerait les émissions de GES du secteur. Pour finir, dans le domaine du transport, le principal axe d'amélioration passe par une réduction de la quantité de mouvement des biens et des personnes. Une baisse de la distance parcourue dans les systèmes de transports réduit d'une part les émissions, mais aussi encourage les mobilités décarbonées qui ne sont parfois pas envisageables sur les longues distances. Si les usagers n'ont pas besoin de parcourir de longues distances, ils peuvent se réorienter soit vers des transports plus propres tels que la marche ou le vélo, soit vers les transports en commun pour limiter la quantité d'émission par personne et retirer des véhicules du système de transport. Le rapport insiste également sur la création de synergies entre les différents domaines. Par exemple, en utilisant des circuits courts et de proximité pour la distribution de productions agricoles, une action est réalisée entre les domaines agricoles et du transport. Dans le cas du transport et de l'énergie, une électrification massive des réseaux de transport en commun à travers l'utilisation de véhicules électriques permet de réduire les émissions de GES. Ainsi, il est nécessaire d'intégrer l'impact environnemental dans toutes les décisions politiques, en créant des synergies dans les différents domaines d'activité, afin d'obtenir un effet systémique pour la réduction des émissions de GES. Ces actions peuvent être catalysées par un investissement massif dans la recherche. Le résultat de ces recherches doit pouvoir être transmis à tous les États, permettant de globaliser l'action et observer plus rapidement les conséquences.

Le secteur du transport est un des principaux secteurs responsables des émissions de GES. Une action que les gouvernements peuvent promouvoir pour réduire ces émissions est l'électrification du transport. Pour le transport en commun, cela se traduit par l'utilisation des bus électriques dans les réseaux urbains. L'électrification du transport public pose cependant des défis stratégiques, tactiques mais aussi opérationnels. De plus, les bus diesels représentent encore une forte proportion des flottes actuelles de transports publics, et les remplacer par des bus électriques est un processus complexe qui soulève des problématiques organisationnelles. Les bus électriques ont une portée de conduite opérationnelle limitée et ont donc besoin d'être rechargés régulièrement, entre leurs tournées ou bien pendant la tournée (selon la technologie, la longueur de la ligne, etc.). Une première stratégie de recharge des bus est l'échange de batteries (AN et al., 2020 ; AYAD et al., 2021). Pendant ou à la fin de la tournée, les bus passent à des stations d'échange pour remplacer leur batterie vide avec une batterie pleine et ainsi continuer la tournée. L'avantage de cette stratégie est que le temps de recharge du bus est constant et rapide, le temps de changer la batterie, ce qui permet une bonne estimation connue à l'avance de la durée de l'opération. Cependant, cela nécessite d'avoir une réserve de batteries pleines prêtes à être utilisées. Un facteur important de la conservation de la durée de vie d'une batterie est son état de charge. Le stockage des batteries à des états de charge élevés pendant de longues périodes réduit significativement la durée de vie de la batterie (PELLETIER et al., 2017). Les batteries utilisées avec une stratégie d'échange ont donc besoin d'être remplacées plus régulièrement, augmentant considérablement le coût opérationnel de la recharge du système de transport. Une seconde stratégie de recharge consiste à recharger les batteries directement sur les bus. Pour cela, les autorités organisatrices des transports doivent déployer des infrastructures de recharge installées à des arrêts de bus, dans des terminaux en fin de ligne ou bien dans des dépôts. Dans ce contexte, deux principales stratégies existent pour recharger les bus : la recharge nocturne (HOUBBADI et al., 2019 ; VENDÉ, DESAULNIERS, KERGOSIEN & MENDOZA, 2023) et la recharge en route (Y. WANG et al., 2017 ; XYLIA et al., 2017). Lors de la recharge nocturne, les bus sont rechargés uniquement au dépôt, principalement pendant la nuit. Afin d'implémenter cette stratégie, les bus ont besoin d'une portée opérationnelle plus grande, capable de tenir toute la journée. Ainsi, les bus doivent être équipés de batteries à grande capacité, qui sont plus onéreuses. De plus, les batteries possédant une capacité pouvant tenir toute une journée sont peu courantes. Pour surmonter ce problème, les compagnies de transport doivent s'assurer qu'elles ont plusieurs bus pour couvrir chaque ligne du réseau, permettant aux conducteurs de changer rapidement de bus quand la batterie est vide. Le nombre additionnel de bus augmente le coût d'investissement de la flotte. De plus, la stratégie de recharge nocturne implique de nombreuses recharges de batterie de bus pendant la nuit. Ainsi, un grand nombre d'opérations de recharge peuvent se dérouler en simultané, ce qui se traduit par une infrastructure de recharge onéreuse. La recharge en route implémente la stratégie opposée. Lors de la recharge en route, les bus sont chargés pendant leurs activités quotidiennes à des terminaux en fin de ligne ou à des arrêts spécifiques (points de transfert entre des lignes par exemple). Étant donné que les bus ont besoin de recharger rapidement leur batterie plusieurs fois par jour, la recharge en route nécessite un fort investissement initial dans l'infrastructure de recharge (chargeurs rapides, lignes à haute tension, transformateurs haute tension, etc.), complexifie les opérations quotidiennes et peut ajouter de l'incertitude. Cependant, le nombre important d'opportunités de recharge permet d'utiliser des bus avec des batteries à capacité plus réduite, ce qui réduit le coût d'investissement dans la flotte (GOEHLICH et al., 2013). Un facteur important de la conservation de la durée de vie d'une batterie est son nombre de cycles de recharge. À la construction, une batterie a un nombre prédéterminé de cycles de recharge qu'elle peut endurer (BLOOMBERG NEW ENERGY FINANCE, 2018). La recharge en route, nécessitant un plus grand nombre de cycles de recharge, réduit la durée de vie des batteries en général augmentant ainsi considérablement le coût opérationnel de la recharge du système de transport. Il existe une variante de la stratégie de recharge en route appelée recharge d'opportunité (KUNITH et al., 2017). Lors de la recharge d'opportunité, les bus peuvent recharger sur des chargeurs installés directement le long de la ligne. Ainsi, le bus n'a pas besoin d'attendre pour la recharge ni même de dévier de sa trajectoire. Cela permet de ne pas modifier les tournées des bus lorsque la flotte est électrifiée. Cependant, les recharges doivent être encore plus rapides que pour la recharge en route classique et les bus doivent recharger plus régulièrement. Il faut donc installer davantage de chargeurs, qui sont d'autant plus onéreux, pour assurer également la disponibilité du service de recharge. De plus, la technologie de stockage de l'énergie est différente pour pouvoir supporter cette forte intensité de recharge. On utilise des condensateurs à la place de batteries classiques. L'utilisation de cette stratégie peut s'avérer incompatible avec les autres stratégies car les supports pour stocker l'énergie sont différents. Pour finir, on peut également penser à une combinaison de la recharge nocturne et de la recharge en route (WEI et al., 2018). L'idée de cette stratégie est de charger suffisamment les bus pendant la nuit pour qu'ils puissent atteindre un chargeur installé sur le circuit pendant la tournée. Cette stratégie hybride fournit les avantages de la recharge en route d'un point de vue du dimensionnement des batteries et du coût de la flotte, et permet de réduire le nombre de chargeurs installés au dépôt.

Suite aux dernières conférences sur le climat, des États ont commencé à imposer aux autorités organisatrices de transports de renouveler leurs flottes de véhicules avec des bus propres. Ainsi, les autorités organisatrices de transports sont confrontées au renouvellement de leurs flottes de véhicules diesel en véhicules électriques ou hybrides (RATP, 2023 ; SUSTAINABLE BUS, 2023). Ce renouvellement pose de nombreuses problématiques décisionnelles tant au niveau stratégique qu'au niveau opérationnel. Quelle technologie associant les bornes de recharge et les bus électriques choisir ? Où placer les bornes de recharge ? Comment gérer l'efficacité des bus ? Quel type de bus est à affecter à quelle ligne et à quelle heure ? Et encore bien d'autres questions organisationnelles et de planification. À ces questions s'ajoutent des enjeux économiques et des enjeux de qualité de services à assurer. Les décisions qui doivent être prises nécessitent la résolution de problèmes complexes d'optimisation à résoudre dont la combinatoire augmente significativement lorsque la taille de la flotte de véhicules est importante. L'objectif de cette thèse est de proposer des outils d'aide à la décision pour répondre à ces problématiques en utilisant les techniques de la recherche opérationnelle. Étant donné que l'électrification fait face à des enjeux différents selon la politique de recharge choisie, chaque chapitre de cette thèse explore une des politiques présentées.

Cette thèse, intitulée *Outils d'aide à la décision pour la mise en place d'un réseau de transports en commun électrique*, a pour but de répondre aux problématiques d'électrifications présentées précédemment. Elle est réalisée en cotutelle entre l'Université de Tours et HEC Montréal, au format "thèse par articles". Ainsi, chaque chapitre correspond à un article destiné à une publication en revue internationale. Cette thèse a été dirigée par Jorge E. Mendoza (HEC Montréal), Michel Gendreau (Polytechnique Montréal), et par Emmanuel Néron (Université de Tours). Cette thèse a également été encadrée par Yannick Kergosien (Université de Tours) et Guy Desaulniers (Polytechnique Montréal). Les différents problèmes abordés pendant cette thèse ont été présentés lors de quatre conférences nationales : ROADEF 2021 (VENDÉ et al., 2021), ROADEF 2022 (VENDÉ et al., 2022b), ROADEF 2023 (VENDÉ, DESAULNIERS, GENDREAU et al., 2023), et ROADEF 2024 (VENDÉ et al., 2024b) ; et deux conférences internationales : VeRoLog 2022 (VENDÉ et al., 2022a), et EURO 2024 (VENDÉ et al., 2024a). Le chapitre 1 a été soumis dans le journal Transportation Research Part E. Le chapitre 2 a donné lieu à une publication dans le journal Transportation Research Part C (VENDÉ, DESAULNIERS, KERGOSIEN & MENDOZA, 2023).

La suite de ce manuscrit se compose de la manière suivante. Le chapitre 1 traite d'un problème d'emplacement d'une infrastructure de recharge rapide dans un réseau de transport public. Des bus hybrides (présence d'un moteur diesel et d'un moteur électrique) sont considérés dans ce réseau, les chargeurs sont partagés entre les bus, et une politique de recharge d'opportunité est appliquée. À partir d'un ensemble de lignes caractérisées par une séquence d'arrêts desservis par des bus hybrides à des fréquences données, le problème consiste à trouver où placer des stations de recharge qui peuvent être partagées par plusieurs lignes, combien en installer, et comment les utiliser en s'assurant qu'un certain niveau de service soit respecté et qu'un ordonnancement réalisable pour toutes les tâches de rechargement existe. Nous considérons deux fonctions objectifs : la maximisation de la distance parcourue en utilisant le mode électrique et la minimisation des coûts d'installation. L'objectif de l'étude de ce problème est de montrer l'intérêt d'utiliser les bus hybrides et du partage des chargeurs entre plusieurs lignes de bus. Nous proposons un programme linéaire en nombres entiers (PLNE) et une méthode basée sur le branch-and-check pour résoudre efficacement le problème. Nous proposons également des perspectives managériales en présentant les avantages opérationnels et économiques de partager les chargeurs entre les lignes ainsi que les compromis entre l'augmentation du budget et la réalisation d'une plus grande électrification. Le chapitre 2 traite d'un problème d'affectation de bus électriques et d'ordonnancement de la recharge nocturne sur plusieurs jours, dans lequel une politique de recharge nocturne est appliquée. Le problème considère un ensemble de bloc véhicules (suites programmées de trajets en bus effectués par le même bus sur une journée) devant être effectués sur plusieurs jours, un ensemble de bus électriques identiques, et un ensemble de chargeurs disponibles au dépôt. L'objectif est d'affecter un bus électrique à chaque bloc et à planifier la recharge nocturne au dépôt en s'assurant que les bus ne soient jamais à court d'énergie et que la capacité de recharge au dépôt ne soit jamais dépassée. Ces décisions sont prises de manière à minimiser le coût total de recharge tout en préservant la durée de vie de la batterie à long terme. L'objectif de l'étude de ce problème est de montrer l'intérêt de considérer un horizon de planification de plusieurs jours dans un contexte de recharge de véhicules électriques ainsi que l'impact économique de la mauvaise gestion de la recharge de la flotte pendant la nuit. Ce problème est modélisé sous la forme d'un PLNE. Nous proposons deux matheuristiques basées sur le modèle de PLNE pour résoudre le problème. Afin de montrer l'intérêt de considérer un horizon de plusieurs jours, nous présentons deux autres méthodes mimant les pratiques industrielles actuelles et résolvent le problème séquentiellement, un jour à la fois. Ces méthodes ont pour but de montrer l'intérêt de considérer un horizon de planification de plusieurs jours lors de la recharge, en comparant les résultats avec ceux des matheuristiques proposées. Le chapitre 3 est une extension du problème étudié dans le deuxième chapitre. Cette extension remet en cause les activités journalières effectuées par les bus en introduisant des événements de recharge en route effectués pendant la journée. Ainsi, une politique de combinaison de recharge nocturne et de recharge en route est appliquée. Les bloc véhicules sont dorénavant vus comme des suites sécables de trajets en bus effectués par le même bus sur une journée. Entre ces différents trajets, les bus peuvent effectuer des opérations de recharge en route sur des chargeurs installés sur le réseau de transport. En plus des décisions prises dans le problème original, nous ordonnançons les opérations de recharge en journée en s'assurant que les contraintes des différentes ressources soient respectées : disponibilité et état de charge des bus, et capacité des stations de recharge. Deux objectifs sont considérés : minimiser le coût total de recharge ainsi que l'impact des décisions de recharge sur la vie de la batterie à long terme. L'objectif de l'étude de ce problème est de montrer l'intérêt de diminuer le nombre d'opérations de recharge pendant la journée. En premier lieu, nous avons modélisé le problème sous la forme d'un PLNE. Ensuite, nous avons développé une matheuristique dans laquelle, à chaque itération de la méthode, une partie de la solution est détruite puis reconstruite à l'aide de la partie restante de la solution. Nous avons effectué des analyses pour quantifier l'impact du nombre d'opérations de recharge effectuées pendant la journée et montrer l'intérêt d'utiliser une combinaison de ces deux stratégies de recharge. Le chapitre 3.6 apporte une conclusion sur les problèmes présentés et discute de nouvelles orientations de recherche possibles concernant ces problématiques d'électrification des réseaux de transport en commun.

Chapitre 1

Deploying fast-charging infrastructure on urban transit networks

Résumé

L'électrification des bus circulant sur les réseaux de transport urbain est l'un des nombreux outils dans la lutte pour limiter les émissions de gaz à effet de serre. Les bus diesel existants peuvent être remplacés par de nouveaux bus totalement électriques ou transformés en bus hybrides. Cette dernière solution est intéressante sur les marchés où les budgets consacrés à l'électrification sont limités. Les bus hybrides peuvent fonctionner à la fois au diesel et à l'électricité. Ils sont généralement équipés de dispositifs de stockage d'énergie à faible capacité mais à charge rapide. Par conséquent, leur autonomie électrique est limitée, mais ils peuvent se recharger rapidement en cours de route pendant qu'ils effectuent leurs tâches. Dans cet article, nous proposons un modèle de programmation en nombres entiers et deux versions d'un algorithme de type branch-and-check pour installer des chargeurs sur les réseaux de bus qui utilisent des bus hybrides. Plus précisément, nos méthodes décident du nombre de chargeurs à installer à chaque emplacement candidat et du mode de transport sur chaque segment de chaque ligne du réseau. L'objectif est de maximiser la distance totale parcourue en mode électrique et de minimiser le coût de déploiement de l'infrastructure de recharge. L'une des nouveautés de nos approches est qu'elles permettent le partage des chargeurs entre les lignes. Ce dernier permet une électrification plus rentable du réseau, mais rend le problème plus difficile à résoudre car les contraintes de niveau de service des lignes et de faisabilité de l'horaire s'entremêlent. Nous présentons des expériences approfondies sur un ensemble de 210 instances basées sur le réseau de transport en commun de la ville de Tours (France). Nous fournissons des perspectives managériales sur les avantages opérationnels et économiques du partage des chargeurs et sur les compromis entre l'augmentation du budget et la réalisation d'une plus grande électrification.

Abstract

The electrification of buses running on urban transit networks is one of the many weapons in the battle to limit greenhouse gas emissions. Existing diesel buses can be replaced by new 100% electric buses or retrofitted to become hybrid. The latter is an interesting alternative in markets where electrification budgets are limited. Hybrid buses can run both on diesel and electric train modes. They are typically equipped with low-capacity-but-fast-charging energy storage devices. As a result, their electric range is limited, but they can quickly charge en-route while executing their tasks. In this paper we device a mix integer programming model and two versions of a branch-and-check algorithm to locate chargers on multi-line hybrid bus transit networks. More specifically, our methods decide how many chargers to install at each candidate location and what should be the train mode on each segment of each line in the network. The objective is to maximize the total distance driven using the electric mode and minimize the cost of deploying the charging infrastructure. One novelty of our approaches, is that they allow for charger sharing between lines. The latter allows for a more cost-effective electrification of the network but makes the problem more difficult to solve as line service level and time tabling feasibility constraints become intertwined. We discuss extensive computational experiments on a set of 210 instances based on the transit network of the city of Tours (France). We provide ma-

nagerial insights into the operational and economic benefits of allowing charger sharing and the trade-offs between increasing the budget and achieving greater electrification.

1.1 Introduction

Greenhouse-gas emissions increased by 80% between 1970 and 2010 (INSEE RÉFÉRENCES, 2019). This increase is mainly owing to the development of energy-intensive sectors, such as manufacturing and transportation. According to the COP21 report (UNFCCC, 2016), if no action is performed to stop this rise by 2100, the global temperature is expected to increase by up to 5°Celsius. This strong rise could have dramatic consequences such as, acidification of the oceans, loss of biodiversity, and the rise of climate refugees. To limit this temperature increase, countries reunited during the COP21 climate conference committed to reduce emissions of CO_2, which account for 70% of greenhouse gases released into the atmosphere each year.

The transportation sector is responsible for nearly 30% of the European Union CO_2 emissions (IPCC, 2014). One leverage that governments can use to reduce these emissions is the electrification of public transit. However, transitioning from diesel-powered buses, which still constitute a significant portion of current fleets, to electric buses (EBs) raises several strategic, tactical, and operational challenges. EBs have a considerably limited driving range, necessitating frequent recharging to execute their tasks. Two primary charging strategies exist : overnight charging (HOUBBADI et al., 2019 ; VENDÉ, DESAULNIERS, KERGOSIEN & MENDOZA, 2023) and opportunity charging (Y. WANG et al., 2017 ; XYLIA et al., 2017). With overnight charging, EBs are charged only at the depots, typically during the night. This strategy requires larger batteries, increasing vehicle upfront costs and reducing payload capacity. Additionally, transit agencies often require extra buses to rotate during the day while others charge, further increasing fleet costs. Concentrating charging operations during the night also necessitates more expensive infrastructure and leads to higher electricity bills (because of power-related costs). In contrast, opportunity charging involves charging EBs during regular operation at end-of-line terminals or long-term stops. While this strategy requires a high upfront investment in charging infrastructure, it allows for smaller batteries, reducing fleet costs (GOEHLICH et al., 2013). However, it adds complexity to daytime operations and may introduce additional uncertainty. Some transit agencies have implemented combinations of overnight and opportunity charging to leverage the advantages of both strategies (WEI et al., 2018). In this study, we focus on transportation systems that utilize the opportunity charging strategy.

The charging infrastructure needed to support an opportunity charging strategy represents a significant capital investment. For instance, according to PELLETIER et al., 2019, the prices of end-of-line and fast en-route EB chargers are currently in the ranges of USD 100,000 and USD 700,000, respectively. Owing to limited budgets, transit authorities may not be able to install as many chargers as they need to run the system on 100%-electric buses. In this context, hybrid buses (HB) emerge as a valid alternative. As the name suggests, HBs are equipped with both an electric engine and a diesel-powered engine. They provide more flexibility to transit agencies and can lower the upfront cost of the fleet because they can be obtained by retrofitting existing diesel-powered vehicles (TOPAL, 2023). Deploying opportunity-charging infrastructure for HBs leads to a challenging optimization problem. Transit agencies must simultaneously determine i) how many chargers to install and where to install them, and ii) what drive mode to use (electric or diesel) on each segment of each line in the network to maximize the benefits of electrification (e.g., the total distance travelled by HBs in electric mode). While these decisions are mostly strategic (number and location of the chargers) and tactical (drive mode), they must be taken considering the operational and managerial constraints of the transit system (e.g., service frequency, inconvenience for the passengers). The latter is especially relevant when chargers are shared by HBs covering different lines. This practice is cost-efficient because it allows for greater levels of electrification at lower costs, but it complexities the problem because congestion at the chargers must be taken into account when making location and mode selection decisions.

In this paper, we investigate the fast-charging infrastructure location problem in networks operated with HBs (FCLP-HB). This problem involves optimizing the placement of fast chargers, scheduling charging events (i.e., determining where and how much HBs operating on each line must charge), and specifying the drive mode for each segment of each line. The goal is to maximize the total distance covered by HBs operating in electric mode. Solutions must adhere to a set of operational and managerial constraints, including : a maximum electrification budget, a minimum service frequency on each line, stop-dependent maximum charging times, and mandatory electric-mode segments on some lines. Our main contributions are five fold :

— We introduce a new, challenging, and practically relevant optimization problem (the FCLP-HB) to the transportation community.

— We propose a non-trivial mixed-integer linear program (MILP) formulation that can solve small-sized instances of the problem using a commercial solver.

— We devise both exact and heuristic versions of a branch-and-check algorithm to efficiently solve the problem.

— We introduce a set of realistic instances built based on real data from the city of Tours (France).

— We present extensive computational experiments assessing the efficiency and effectiveness of our approaches and provide managerial insights on the benefits of considering HBs on the total electrification costs and the advantages of allowing charger sharing between lines in large transit networks.

The remainder of this paper is organized as follows. Section 1.2 presents a literature review related to the fast-charging location problem in HB networks. Section 1.3 formally defines the FCLP-HB. Section 1.4 provides a mixed-integer linear program model. Section 1.5 describes the two version of the branch-and-check algorithm. Section 1.6 presents the results of the computational experiments and provides managerial insights. Finally, Section 1.7 concludes the paper and discusses possible future research directions.

1.2 Literature review

The adoption of EBs in urban transit networks has led to the study of several optimization problems, including the fleet transformation problem (FTP), the sequence assignment problem (SAP), the vehicle scheduling problem (VSP), and the charging location problem (CLP). We will briefly describe these problems and their relevance to ours, directing interested readers to DIRKS et al., 2022 for a more detailed description and literature review. The FTP focuses on creating a multi-period plan to replace a fleet of diesel-powered buses with EBs. This involves decisions on purchasing new EBs, retiring old diesel-powered buses, and acquiring charging stations for the EBs in the new fleet, all aimed at minimizing operational and acquisition costs (DIRKS et al., 2021 ; PELLETIER et al., 2019). The SAP involves assembling sequences of trips assigned to EBs, with charging events scheduled between consecutive trips to ensure feasibility (ROGGE et al., 2018 ; SASSI-BEN SALAH & OULAMARA, 2017). Deadheading and detours may be considered based on the charging strategy, and the objective is to minimize charging costs. The VSP aims to determine the minimum number of buses required to perform a set of trips (JANOVEC & KOHÁNI, 2019 ; T. LIU & CEDER, 2020). This problem is similar to the SAP, except that the number of buses used is also a decision variable and the objective function is to minimize the charging and bus purchase costs. Finally, the CLP considers an existing fleet of EBs and a given urban bus network, and aims to find the locations of the charging stations in order to efficiently power the fleet (KUNITH et al., 2017 ; LOTFI et al., 2020). The CLP and its variants typically arise as a result of adopting an opportunity charging strategy. Chargers can be located at bus stops, terminals, or hubs in a network. In addition to the location, the type (e.g., charging speed) of each charger type can also be a decision variable. The objective function typically minimizes the acquisition costs of the charging stations and batteries. Our problem belongs to the family of CLPs

With the increasing prominence of electric vehicles (EVs), CLPs have garnered substantial attention in recent literature. For a comprehensive discussion of recent papers on these topics, we recommend referring to the works of SHEN et al., 2019, KCHAOU-

BOUJELBEN, 2021, and MAJHI et al., 2021. Most studies have focused on personal EVs, utilizing coverage models to determine optimal charger locations based on factors such as traffic flows and population distribution (FRADE et al., 2011 ; HE et al., 2016). However, in the context of urban bus networks, EBs operate according to daily schedules and predefined trips, which alters the structure of the charger location problem.

In CLPs for EBs, chargers can be installed at three primary locations : the depot, hubs, or bus stops (including terminals). Installing chargers at the depot allows EBs to charge after their trips, typically overnight. In this scenario, the decisions focus on determining the number of chargers required for the nightly charging plan, rather than the specific charger locations (ROGGE et al., 2018). With chargers limited to the depot, EBs are seldom charged more than once a day, necessitating short trips constrained by battery range and potentially increasing the need for a larger fleet to meet demand. To extend EB trip duration and reduce fleet size, en-route charging can be implemented without returning to the depot. En-route charging typically occurs at strategic hub locations (SOLTANPOUR et al., 2022 ; Y. WANG et al., 2022). Unlike depot-based charging, en-route charging involves considering multiple candidate locations and determining the number of chargers at each site. While en-route charging at hubs extends trip duration, the detours required for charging consume additional time and energy, resulting in added costs. Furthermore, shared (among different lines) charging hubs introduce complex scheduling challenges (YE et al., 2022).

An alternative approach is to install chargers at bus stops, where chargers can be managed in two ways : either dedicated to a single line or shared by electric buses (EBs) serving different lines. KUNITH et al., 2017 proposed a mathematical model for deploying line-exclusive chargers. Their objective is to determine charger locations, battery capacity for EBs on each line, and the energy charged by each EB at every charging stop. The charging function is modeled using a piecewise linear function with two segments : a high-power segment when the state of charge (SOC) of the bus is below a certain threshold and a low-power segment otherwise. In this model, EBs are charged during predefined dwell times between consecutive bus trips, ensuring no impact on the bus timetable. However, this model does not consider the potential for charger sharing among EBs from different lines, leading to a potentially higher number of installed chargers.

X. WANG et al., 2017 also studied a CLP within the context of an urban public bus system. The problem focuses on determining the optimal bus stops for placing charging stations with the objective of minimizing total installation costs. Each stop can accommodate only one charger, which is shared among all-electric buses (EBs). However, the approach proposed in this study overlooks certain operational constraints such as the scheduling of charging operations (to prevent overlapping charging tasks on the same charger), line service frequencies, and timetables. The authors developed a backtracking algorithm to optimally solve the special case of a single line. The core idea of this algorithm is to identify the maximum number of stops that a bus can visit after stopping at the charging station and then explore all possible charger location solutions using a search tree. In the case of multiple bus lines, they introduced two heuristic approaches : a greedy algorithm and a multiple backtracking algorithm based on the first case.

Similarly, Z. LIU et al., 2018 addressed a comparable problem. Similarly to X. WANG et al., 2017 they did not specifically consider the scheduling of charging operations. On the other hand, they focused on various types of batteries, charging stations, and uncertainties related to energy consumption. Their objective function aimed to minimize the overall costs of batteries and the installation of fast-charging stations. Each candidate location, such as a bus stop, base station, or terminal station, could accommodate only one charger of each type. They proposed a robust optimization model using a mixed-integer linear program to tackle this problem. Their approach underwent testing in a case study involving a downtown bus system in Salt Lake City, Utah (U.S.).

ZHOU et al., 2022 presented a model that integrates the planning of charging infrastructure deployment with the scheduling of charging operations, building upon the work of KUNITH et al., 2017 by allowing chargers to be shared along lines. Chargers are positioned at end-of-line terminals, and EBs utilize them during predefined dwell times between two consecutive trips. The objective is to determine the optimal number of chargers at each terminal, the appropriate battery size for each EB, and the charging schedule for each charger while minimizing the total acquisition costs of chargers and batteries as well as the charging costs. The proposed model includes several practical considerations, such as a minimum charging requirement and time-dependent charging costs that account for peak and off-peak prices. The model also accounts for various factors affecting energy consumption during a trip, such as EB type, route, battery weight, onboard passengers, and varying charging power. The authors introduced deterministic and robust optimization models to address energy consumption uncertainties, utilizing the box uncertainty set, budgeted uncertainty set, and ellipsoidal uncertainty set. To validate their approach, computational experiments were conducted using real data from a case study based on tower transit data in Singapore.

GAIROLA et NEZAMUDDIN, 2022 introduced a charging infrastructure planning problem that addresses the installation of chargers both at the depot using plug-in slow chargers and at end-of-line terminals using fast opportunity chargers. This problem encompasses both overnight and opportunity charging scenarios. Similar to the studies mentioned earlier, electric buses (EBs) are only allowed to utilize the chargers during designated dwell times. The model incorporates time-limitation constraints that restrict charging events at fast-opportunity chargers to predefined time windows. Furthermore, capacity constraints at the chargers are considered using queuing models. The proposed stochastic optimization model, solved using the Lagrangian relaxation method, aims to determine the optimal size of bus batteries and the required charging infrastructure. This approach takes into account various operational and managerial constraints to ensure efficient and effective utilization of the charging infrastructure.

QUINTANA et al., 2022 tackled a charger location problem where chargers are installed at bus stops, and charging operations must be scheduled for each charger. Each bus stop can accommodate only one charging station, and the charging rate is assumed to be a linear function of the charging time. Charging times at the stops are constrained by minimal deviations from the original timetables, ensuring that the absolute difference between expected and actual arrival times remains below a specified threshold. The authors introduced an iterative local search method to address this problem. The method initiates by opening all potential charging stations, and then the neighborhood operator selectively removes charging stations while maintaining feasibility. To avoid local minima, a perturbation phase randomly reopens previously removed charging stations.

While there exists a substantial volume of research on charger location problems within urban bus networks, limited attention has been given to shared chargers among lines and the explicit handling of timetabling constraints. To the best of our knowledge, this study is the first to address a fleet of HBs, shared chargers for opportunity charging, the scheduling of charging operations on each charger, and service frequency constraints for each bus line (as opposed to fixed timetables). This approach offers enhanced flexibility regarding charging times, marking a step forward in the field of charging infrastructure planning in public transit systems.

1.3 Problem description

Let $G(V,A)$ be an oriented graph representing a public transit network, where V is the set of nodes representing bus stops (on-street bus stops or terminals), and A is the set of arcs representing paths connecting two stops on the road network. Define L as the set of bus lines on the network, and let $G_l(V_l,A_l)$ be the sub-graph of G representing line $l \in L$. Line l corresponds to a set of continuous segments connecting two stops running at a given frequency. It is assumed that the timetable for line l can be adjusted (with respect to the current one) as long as the current frequency $(\frac{1}{f_l})$ is maintained. In other words, after the electrification of the line, a timetable prescribing that an HB will stop at each stop of the line every f_l units of time must exist. The transit network operates with a homogeneous fleet of HBs, each with a battery capacity of Q. We assume that the fleet is large enough to run the network meeting all demand and service constraints. The HBs can switch driving modes (between electric and diesel) at any stop $i \in V$ but cannot switch modes while traveling between stops. HBs can recharge their batteries at any stop of the line they are covering if the latter is equipped with a *charging station* (CS). A CS has one or more chargers. To limit inconvenience to users, HBs cannot charge at stop i for more than $w_{l,i}$ time units. These maximum waiting times are computed offline by the transit authority, taking into account factors such as the expected number of passengers at that stop. Charging operations start as soon as the HBs arrive at the CS. In other words, HBs never wait for a charger.

The maximum budget allocated for the deployment of charging infrastructure is denoted by B. The cost of equipping a CS located at stop $i \in V$ with a charger is denoted by $cost_i$. The installation costs for chargers are stop-dependent to account for differences in civil and landscaping work required for installation at different locations. Setting $cost_i = B + 1$ prevents the installation of a CS at a given stop. Each arc $(i, i') \in A$ is associated with distance $d_{i,i'}$, travel time $tt_{i,i'}$ (including time required to pick up passengers), and electric energy consumption $e_{i,i'}$. Additionally, each arc (i, i') is associated with a boolean parameter $m_{i,i'}$ indicating if the use of the electric mode is mandatory between stops i and i'. The latter allows transit agencies to limit pollution, noise, and vibrations in specific geographic areas such as old towns and school zones. Note that setting $m_{i,i'} = 1$ for every pair $(i, i') \in A$ converts the problem into a charger location problem for a fleet of EBs (instead of HBs). Table 1.1 summarizes the notation.

The problem entails determining (i) the number of chargers to install at each stop (infrastructure decisions), (ii) the driving mode on each segment of each line (mode decisions), and (iii) the duration of charging operations at each stop of each line (charging and scheduling decisions). We approach this as a multi-objective problem using a lexicographic method. Our primary objective is to maximize the total distance covered by the fleet operating in electric mode, while our secondary objective is to minimize electrification costs.

Figure 1.1 illustrates a solution to an instance involving two lines (blue and red). The solution recommends installing a CS with a single charger at the only stop shared between the blue and red lines. It also specifies that the HBs must operate in electric mode over seven arcs in the network. The bottom part of the figure displays a feasible schedule for the charging operations of HBs serving the two lines.

TABLE 1.1 – Sets and parameters of the problem

Sets	
V	Set of bus stops
A	Set of arcs between stops
L	Set of bus lines
V_l	Set of bus stops of line l
A_l	Set of arcs between stops of line l
P_i	Set of bus lines that stop at i
C_i	Set of potential chargers at the CS located at stop i
J_l	Set of charging operations of line l at each charging stop
K_i	Set of charging operations carried out at the CS located at stop i
Parameters	
Q	Battery capacity of a bus
R	Charging speed rate of the chargers
f_l	Time between two consecutive bus arrivals at each stop of line l
st_l	Index of the first stop of line l
lt_l	Index of the last stop of line l
$w_{l,i}$	Maximum stop duration at stop i for an HB servicing line l
B	Maximum budget allocated for the deployment of charging infrastructure
$cost_i$	Installation cost of a charger at stop i
$d_{i,i'}$	Distance between stops i and i'
$tt_{i,i'}$	Travel time between stops i and i'
$e_{i,i'}$	Electric energy consumption between stops i and i'
$m_{i,i'}$	Whether the segment connecting stops i and i' must be driven in electric mode
λ	Length of the scheduling cycle
n_l	Number of charging operations of line l at each charging stop

1.4 Mixed-integer programming formulation

We model the problem introduced in Section 1.3 as a mixed-integer linear program (MILP) using eight types of variables. The positive integer decision variables x_i indicate the number of chargers installed at a CS located at stop i. The binary decision variables $y_{l,i,i'}$ take value one if the HBs operating on Line l travel on electric mode between stops i and i', and zero otherwise. The positive real decision variables $q_{l,i}$ represent the SoC of the HBs operating Line l when they arrive at Stop i. The positive integer decision variables $t_{l,i}$ represent the charging time at Stop i of HBs operating Line l. Let $C_i = \{1, \cdots, \left\lfloor \frac{B}{cost_i} \right\rfloor\}$

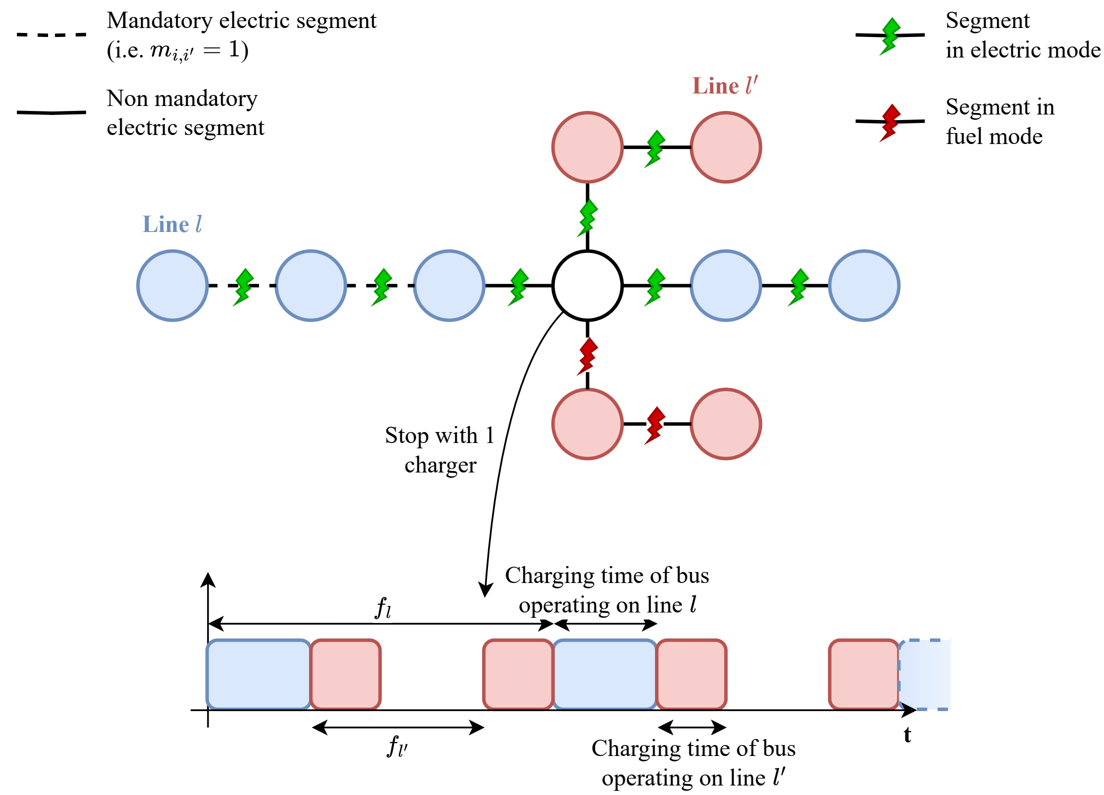

FIGURE 1.1 – Solution to an instance with 2 lines and 10 stops

be the set of potential chargers at the CS located at Stop i, the binary decision variables $u_{i,c}$ take value one if Charger $c \in C_i$ is installed at the CS of Stop i, and zero otherwise.

The next subset of variables is used to model the scheduling of charging operations at the CSs. Note that because a CS can be used by multiple lines and the service frequency $\frac{1}{f_l}$ of every line may be different, the constraints preventing the overlapping of charging operations on a charger must be verified over a cyclic period equal to $\lambda = LCM_{l \in L}(f_l)$, where the LCM is the least common multiple of a set of numbers. The number of charging operations to schedule for HBs operating on Line l at Stop i is given by $n_l = \frac{\lambda}{f_l} + 1$. The first $n_l - 2$ operations have a duration equal to the value of decision variable $t_{l,i}$. Each corresponds to a distinct HB stop for charging at l. On the other hand, operations $n_l - 1$ and n_l correspond to the same HB stop. They model charging operations that start in one scheduling cycle and finish in the next. As it stands, their combined duration is equal to $t_{l,i}$. Figure 1.2 illustrates these concepts.

The figure shows a feasible charging schedule involving four lines (l_1, l_2, l_3, l_4). Lines l_1, l_2, and l_3 share a stop (Stop i), so do lines l_3 and l_4 (Stop i'). The time between the arrival of two consecutive HBs (i.e., the inverse of the frequency) for each line is listed in Table 1.2. In this example, a CS with two chargers is installed at Stop i and a CS with one charger is installed at Stop i'. The charging times at each stop are listed in Table 1.2. For simplicity, in this example, the charging operations of a given line at a given CS are always scheduled on the same charger, but this is not a constraint in our problem. The duration of the charging cycle is $\lambda = LCM(6,6,4,4) = 12$. For the sake of briefness, we will refer to the starting time of the cycle depicted in the figure as time 0. Lines l_1 and l_2 stop for charging at the first charger (Charger α) of the CS located at stop i, whereas Line l_3 does it at the second charger (Charger β).

The number of charging operations to schedule in Charger α is equal to $n_{l_1,i} = \frac{\lambda}{f_l} + 1 = \frac{12}{6} + 1 = 3$ and $n_{l_1,i} = 3$, for lines l_1 and l_2, respectively. Note, however, that the duration of the last operation for each line is equal to 0. This is not the case l_3. The number of operations scheduled at charger β is $n_{l_3,i} = 4$. The first two operations have a duration of 3 units of time. They correspond to the stops for charging of HBs A and B. The last two operations (3 and 4) correspond to the stop of bus C. Note that their combined duration is also 3 units of time.

TABLE 1.2 – Instance data with four lines

Line	1	2	3	4
f_l	6	6	4	4
$t_{l,i}$	2	4	3	/
$t_{l,i'}$	/	/	2	2

We define $J_l = \{1, \cdots, n_l\}$ as the set of charging operations of Line $l \in L$ and $K_i = \{1, \cdots, \min\{\lambda, \sum_{\substack{l \in L:\\ i \in l}} |J_l|\}\}$ as the set of charging operations carried out at the CS located at Stop i. The positive real decision variables $s_{l,i,j}$ indicate the starting time of the j^{th} charging operation of Line l at the CS of Stop i. The binary decision variables $p^{c,k}_{l,i,j}$ take value one if the j^{th} charging operation of Line l at the CS of Stop i is scheduled on Charger c in position k, and zero otherwise. Finally, we use auxiliary variables $\theta_{l,i}$ to link

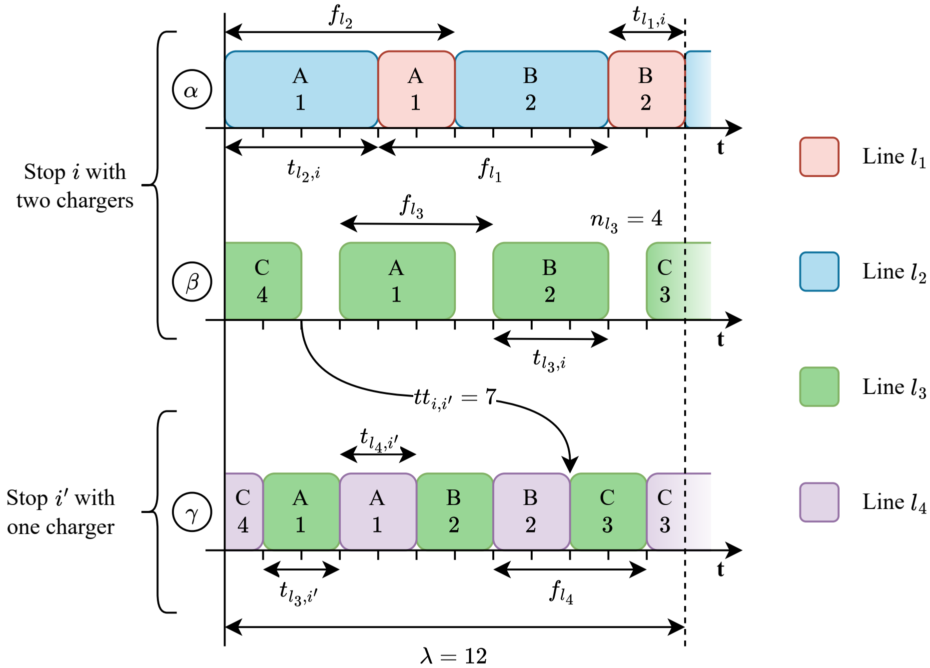

FIGURE 1.2 – Feasible schedule considering four lines and three chargers at two stops

the charging start times at different stops of the same line l and ensure that there are at least $\frac{\lambda}{f_l}$ to schedule on every cycle. The example in Figure 1.2 also illustrates the use of the $\theta_{l,i}$ variables.

The charging operations of HBs servicing Line l_3 at stops i and i' are linked by the travel time between i and i'. Take, for instance, the first charging operation scheduled at Charger β of Stop i (denoted as 4). This operation started in the previous scheduling cycle (at Time -1) and it is completed at Time 2. The HB (bus C) then continues servicing l_3 until it reaches Stop i' (at Time 9) where it charges for 2 units of time. The next HB servicing l_3 (bus A) leaves Stop i at Time 6 after completing its charging operation (denoted as 1). The HB arrives at Stop i' at Time 13, which is out of the depicted scheduling cycle. To couple the HB's charging operations at chargers β and γ while framing them within a single scheduling cycle, we use the $\theta_{l_3,i'}$ auxiliary variable. More specifically, we set $s_{l_3,i',j} = s_{l_3,i,j} + t_{l_3,i} + tt_{i,i'} - f_{l_3} \cdot \theta_{l_3,i'}\ \forall j \in J_{l_3}$. In our previous example, that is $s_{l_3,i',1} = 3+3+7-4\cdot\theta_{l_3,i'}$. By setting $\theta_{l_3,i'}$ equal to three, we obtain $s_{l_3,i',1} = 1$.

The FCLP-HB can be formulated as a MILP as follows (Table 1.3 summarizes all the variables).

TABLE 1.3 – Variables of the model

Variables	
x_i	Positive integer decision variable indicating the number of chargers to install at the CS located at stop $i \in V$
$y_{l,i,i'}$	Binary decision variable indicating whether the segment connecting stops $i \in V_l$ and $i' \in V_l$ driven by a bus operating on line $l \in L$ is driven in electric mode
$q_{l,i}$	Positive decision variable indicating the SoC of an HB operating on line $l \in L$ at arrival at stop $i \in V_l$
$t_{l,i}$	Positive integer decision variable indicating the charging time of a bus operating on line $l \in L$ at stop $i \in V_l$
$u_{i,c}$	Binary decision variable indicating if the charger $c \in C_i$ is installed at the CS located at stop $i \in V$
$s_{l,i,j}$	Positive decision variable indicating the starting time of the $j^{th} \in J_l$ charging operation of line $l \in L$ at stop $i \in V_l$
$p_{l,i,j}^{c,k}$	Binary decision variable indicating whether the $j^{th} \in J_l$ charging operation of line $l \in L$ is scheduled at position $k \in K_i$ on charger $c \in C_i$ of the CS located at stop $i \in V_l$
$\theta_{l,i}$	Positive integer auxiliary decision variable

$$\max \quad \sum_{l\in L}\sum_{(i,i')\in A_l} \frac{d_{i,i'}}{f_l} \cdot y_{l,i,i'} \tag{1.1}$$

$$\min \quad \sum_{i\in V} cost_i \cdot x_i \tag{1.2}$$

Subject to :

$$\sum_{i\in V} cost_i \cdot x_i \leq B \tag{1.3}$$

$$t_{l,i} \leq w_{l,i} \qquad \forall l \in L,\ \forall i \in V_l \tag{1.4}$$

$$y_{l,i,i'} = 1 \qquad \forall l \in L,\ \forall (i,i') \in A_l : m_{i,i'} = 1 \tag{1.5}$$

$$q_{l,i} + t_{l,i} \cdot R - e_{i,i'} \cdot y_{l,i,i'} = q_{l,i'} \qquad \forall l \in L,\ \forall (i,i') \in A_l \tag{1.6}$$

$$q_{l,i} + t_{l,i} \cdot R \leq Q \qquad \forall l \in L,\ \forall i \in V_l \tag{1.7}$$

$$q_{l,st_l} \leq q_{l,lt_l} \qquad \forall l \in L \tag{1.8}$$

$$s_{l,i,1} \leq f_l - 1 \qquad \forall l \in L,\ \forall i \in V_l \tag{1.9}$$

$$s_{l,i,n_l} = 0 \qquad \forall l \in L,\ \forall i \in V_l \tag{1.10}$$

$$s_{l,i,j} + f_l = s_{l,i,j+1} \qquad \forall l \in L,\ \forall i \in V_l,\ \forall j, j+1 \in J_l \backslash \{n_l\} \tag{1.11}$$

$$s_{l,i,1} + t_{l,i} + tt_{i,i'} = s_{l,i',1} + f_l \cdot \theta_{l,i'} \qquad \forall l \in L,\ \forall (i,i') \in A_l \tag{1.12}$$

$$\sum_{c \in C_i} u_{i,c} \leq x_i, \qquad \forall i \in V \tag{1.13}$$

$$u_{i,c} \geq u_{i,c+1}, \qquad \forall i \in V,\ \forall c, c+1 \in C_i \tag{1.14}$$

$$\sum_{l \in P_i} \sum_{j \in J_l} \sum_{k \in K_i} p_{l,i,j}^{c,k} \leq \lambda \cdot u_{i,c} \qquad \forall i \in V,\ \forall c \in C_i \tag{1.15}$$

$$\sum_{c \in C_i} \sum_{k \in K_i} p_{l,i,j}^{c,k} \leq 1 \qquad \forall l \in L,\ \forall i \in V_l,\ \forall j \in J_l \tag{1.16}$$

$$\sum_{l \in P_i} \sum_{j \in J_l} p_{l,i,j}^{c,k} \leq 1 \qquad \forall i \in V,\ \forall c \in C_i,\ \forall k \in K_i \tag{1.17}$$

$$\sum_{l \in P_i} \sum_{j \in J_l} p_{l,i,j}^{c,k+1} \leq \sum_{l \in P_i} \sum_{j \in J_l} p_{l,i,j}^{c,k} \qquad \forall i \in V, c \in C_i,\ \forall k, k+1 \in K_i \tag{1.18}$$

$$\sum_{k \in K_i} p_{l,i,n_l-1}^{c,k} = \sum_{k \in K_i} p_{l,i,n_l}^{c,k} \qquad \forall l \in L,\ \forall i \in V_l,\ \forall c \in C_i \tag{1.19}$$

$$\sum_{c \in C_i} \sum_{k \in K_i} p_{l,i,j}^{c,k} \geq \frac{R \cdot t_{l,i}}{Q} \qquad \forall l \in L,\ \forall i \in V_l,\ \forall j \in J_l \tag{1.20}$$

$$s_{l,i,j} + t_{l,i} \leq s_{l',i,j'} + \lambda(2 - p_{l,i,j}^{c,k} - p_{l',i,j'}^{c,k+1}) \qquad \forall l, l' \in L,\ \forall i \in V_l \cap V_{l'},\ \forall j' \in J_{l'}, \tag{1.21}$$

$$\forall j \in J_l \backslash \{n_l\},\ \forall c \in C_i,\ \forall k, k+1 \in K_i$$

$$s_{l,i,n_l-1} + t_{l,i} - \lambda \leq s_{l',i,j'} + \lambda(2 - p_{l,i,n_l}^{c,k} - p_{l',i,j'}^{c,k+1}) \qquad \forall l, l' \in L,\ \forall i \in V_l \cap V_{l'},\ \forall j' \in J_{l'}, \tag{1.22}$$

$$\forall c \in C_i,\ \forall k, k+1 \in K_i$$

$$x_i \in \mathbb{N}_0 \qquad \forall i \in V \tag{1.23}$$

$$q_{l,i} \geq 0 \qquad \forall l \in L,\ \forall i \in V_l \tag{1.24}$$

$$y_{l,i,i'} \in \{0,1\} \qquad \forall l \in L,\ \forall (i,i') \in A_l \tag{1.25}$$

$$s_{l,i,j} \geq 0 \qquad \forall l \in L, i \in V_l,\ \forall j \in J_l \tag{1.26}$$

$$t_{l,i}, \theta_{l,i} \in \mathbb{N}_0 \qquad \forall l \in L,\ \forall i \in V_l \tag{1.27}$$

$$p_{l,i,j}^{c,k} \in \{0,1\} \qquad \forall l \in L,\ \forall i \in V_l,\ \forall j \in J_l, \tag{1.28}$$

$$c \in C_i,\ \forall k \in K_i$$

$$u_{i,c} \in \{0,1\} \qquad \forall i \in V,\ \forall c \in C_i \tag{1.29}$$

Objective function (1.1) maximizes the total distance traveled using the electric mode weighted by line frequency. For simplicity, hereafter we refer to this objective as weighted electric distance. Objective function (1.2) minimizes the total investment. Constraints (1.3) ensure that the electrification budget is respected. Constraints (1.4) ensure the maximum stop durations. Constraints (1.5) enforce the electric mode on certain (predefined) segments. Constraints (1.6) compute the SoC of HBs covering a given line when arriving at a given stop. Constraints (1.7) ensure that the SoC never exceeds the battery capacity. Constraints (1.8) imply that HBs complete the service of their lines with a higher state of charge than that they had at the beginning. The latter guarantees that no extra charging time is required to start servicing the same line again. Constraints (1.9) and (1.10) initialize the starting times of the first and last charging operations for each line. The starting times of the other charging tasks are separated by a fixed period f_l, as indicated by constraints (1.11). Constraints (1.12) link the starting times for all the operations at all stops belonging to the same line. Constraints (1.13) limit the number of chargers that can be used, depending on the number of installed chargers. Constraints (1.14) are symmetry-breaking constraints, enforcing the order in which the charges of a CS must be used. Constraints (1.15) imply that a charger is used if at least one charging operation is scheduled for it. Constraints (1.16) and (1.17) ensure that each charging operation is scheduled at most once and that at most one operation exists per position. Constraints (1.18) are symmetry-breaking constraints, mandating that the first positions are occupied and the last positions are empty. Constraints (1.19) force the last two charging operations to be scheduled on the same charger because they both represent a single charging operation. Constraints (1.20) ensure that the associated charging operations are scheduled for a given stop and line, if the charging time is not zero. Constraints (1.21) and (1.22) are non-overlap constraints for all charging operations scheduled on the same charger. Constraints (1.23)–(1.29) define the domain of the decision variables.

To address the multi-objective aspect, we used a lexicographic approach (ARORA, 2017). The primary objective is to maximize weighted electric distance. Then, we aim to meet that objective at a minimum cost. We implement the lexicographic approach as follows. First, we solve the problem using only the primary objective (1.1). Then, we set z_{dist} as the value of the retrieved solution. Next, we add the following constraint : $\sum_{l \in L} \sum_{(i,i') \in A_l} \frac{d_{i,i'}}{f_l} \cdot y_{l,i,i'} \geq z_{dist}$ and solve the model using (1.2) as the objective function. It is worth noting that this method always provides a Pareto-optimal solution.

1.5 Branch-and-check

To solve the FCLP-HB, we propose two version (one exact and one heuristic) of a branch-and-check method (THORSTEINSSON, 2001). Algorithm 1 presents the main steps in the branch-and-check framework. The main idea is to decompose the original problem into two smaller problems : the master problem and the subproblem. Both problems are easier to solve than the original one. During the process of solving the master problem, whenever an integer solution is found, we check whether this solution is also feasible for the subproblem. In the case of infeasibility, a cut capable of removing the infeasible solution is generated and added to the master problem. Note that a feasible solution for both the master problem and subproblem is feasible for the original problem. In a classic branch-and-check framework, the master problem is modeled as a mixed integer linear program, and the subproblem is modeled as constraint logic program. However, in our method, we used a binary linear programming model to solve the subproblem.

We decompose the problem as follows. The master problem consists of finding : i) the charger locations, ii) the segments that are driven in electric mode, and iii) the charging operations (where and how much to charge) that maximize the weighted electric distance (or that minimize the investment). Given a master problem solution, the subproblem checks whether at least one feasible schedule exists. More specifically, it checks that all the charging operations prescribed by the master problem's solution can be scheduled on all the chargers without overlapping. The check cannot be carried on independently for each charger. As shown on the example in Figure 1.2, the travel times between stops and the service frequencies of the lines induce coupling constraints between chargers. To implement the lexicographic approach, we run the branch-and-check twice : once for each

Algorithme 1 : Branch-and-check framework

best_solution ⟵ ∅
Start the master problem solving
while *the master problem is not solved to optimality* **do**
    if *an integral solution S to the master problem is found and is better than best_solution* **then**
        Solve the subproblem from S
        if *the subproblem is feasible* **then**
            best_solution ⟵ S
        else
            Generate and add a feasibility cut to the master problem
        end
    end
end

objective function. The best solution found in the first run (i.e., maximizing the distance travelled on electric mode) is used as a feasible initial solution for the second run (i.e., minimizing the investment). All the cuts generated during the first run are also transmitted to the second run.

1.5.1 Master problem

The master problem is a relaxation of the original problem in which the scheduling of the charging operations is not considered. Therefore, it uses only the x_i, $y_{l,i,i'}$, $q_{l,i}$, and $t_{l,i}$ decision variables (with the same definition than in the original problem. See Table 1.3). The mixed integer linear programming model of the master problem consists of objective functions (1.1) and (1.2), constraints (1.3)–(1.8), domain constraints (1.23)–(1.25), and two additional constraints (1.30) and (1.31). These constraints bound the charging time at each stop using the number of installed chargers.

$$\frac{t_{l,i}}{f_l} \leq x_i \qquad \forall l \in L, \forall i \in V_l \tag{1.30}$$

$$\sum_{l \in L} t_{l,i} \leq x_i \cdot \max_{l \in L}(f_l) \qquad \forall i \in V \tag{1.31}$$

We solve the master problem using the branch-and-bound algorithm embedded in a commercial solver (CPLEX). Every time the solver finds a new incumbent, we solve the subproblem to check whether a feasible charging schedule exists. If that is the case, we accept the new incumbent; otherwise, we ignore it. In the latter case, we also add a cut aiming to prevent the root cause of the infeasibility to reemerge in the later. Our cut generation procedure is discussed in Section 1.5.3.

1.5.2 Subproblem

Starting from a master problem solution fixing the values of the $\hat{x}_i$ (number and location of the chargers) and $\hat{t}_{l,i}$ (charging times for every line at every stop) variables, the subproblem consists in determining if there is a feasible way to schedule the prescribed charging operations on the installed chargers without violating the service frequency of the lines. It is worth noting that the subproblem can be decomposed by *clusters* of chargers. A cluster of chargers contains all the chargers installed at the stops belonging to a subset of lines sharing at least one charger. More formally, if $\exists i \in V : t_{l,i} > 0 \wedge t_{l',i} > 0$ all the chargers at stops belonging to l or l' belong to the same cluster. Note that a cluster may contain chargers from more than two lines, but a charger can only belong to one cluster. For example, in the toy-instance depicted in Figure 1.2, chargers α, β, and γ form a cluster.

The subproblem consists in determining solely the departure time of the first HB from the initial stop of each line. With these departure times, along with the line frequencies, travel times, and charging times (established by the solution to the master problem), we can infer the arrival time of each HB at every stop on every line. These arrival times most allow for the scheduling of all charging operations on the installed chargers, while adhering to the constraints of non-preemption and non-overlap. It's important to note that, akin to the initial mathematical model outlined in Section 1.4, these constraints need to be checked only over a cycle of λ time units.

To address the subproblem, we propose a MILP model aimed at selecting a bus timetable for each line from a feasible set. The bus timetable for a specific line, denoted as h_l, is fully represented by a single value : the departure time value for the first bus from the initial stop of line l. The feasible set of bus timetables, denoted as Ω_l, encompasses all potential departure time values for the first bus of line l. The cardinality of the set Ω_l is equivalent to f_l since the set of departure time values is $\{0, \cdots, f_l - 1\}$. From the timetable of a line, we can deduce the timing for all charging operations associated with that line. We denote $a_{l,i,t}^{h_l}$ as a Boolean variable, equal to one if a charging operation is executed at time $t \in 0, \cdots, \lambda - 1$ at a CS located at stop $i \in V$ on a bus operating on line $l \in L$ with timetable $h_l \in \Omega_l$, and zero otherwise.

The proposed mathematical model uses only binary variables $x_l^{h_l}$ taking the value of one if Line $l \in V$ is assigned to Timetable $h_l \in \Omega_l$, and zero otherwise. The subproblem can be formulated as the following MILP :

$$\sum_{h_l \in \Omega_l} x_l^{h_l} = 1 \qquad \forall l \in L \tag{1.32}$$

$$\sum_{l \in L} \sum_{h_l \in \Omega_l} a_{l,i,t}^{h_l} \cdot x_l^{h_l} \leq \hat{x}_i \qquad \forall i \in V,\ \forall t \in \{0, \cdots, \lambda - 1\} \tag{1.33}$$

$$x_l^{h_l} \in \{0, 1\} \qquad \forall l \in L,\ \forall\, h_l \in \Omega_l \tag{1.34}$$

Constraints (1.32) ensure that a single timetable is selected for each line. Constraints (1.33) bound the number of charging operations that can be performed simultaneously at each stop. The latter also guarantees the respect of non-preemption and non-overlap constraints. Constraints (1.34) define the domain of decision variables. Note that this model only checks the feasibility of the charging scheduling problem but does not solve it. In other words, after solving the subproblem we know that feasible charging schedules and timetables exists for every line, but we do not know the specific assignment of charging operations to chargers. However, determining these assignments can be done in polynomial time solving a tactical fixed job scheduling problem. The latter consists in finding the minimum number of machines to schedule N fixed tasks (preemption and overlap are not allowed) and can be solved in $O(N \cdot \log N)$ time (GUPTA et al., 1979).

1.5.3 Cut generation

As mentioned earlier, if a subproblem is found to be infeasible, we introduce a tailored no-good cut into the master problem to prevent the reoccurrence of infeasibility. These cuts are designed to not only cut the specific infeasible solution but, potentially, several other infeasible solutions. In cases where the subproblem is deemed infeasible, it is typically due to the master handing in a solution with i) an inadequate number of chargers at a given stop, ii) poorly located chargers, or iii) excessively long charging operations. Our cuts are crafted to address these underlying issues and minimize the likelihood of infeasibilities resurfacing later in the search. Given a solution o to the master problem, we denote $\hat{x}_i^o$ as the quantity of chargers to be installed at stop i, and $\hat{t}_{l,i}^o$ as the charging time at Stop i for an HB operating on Line l. To construct the cut to eliminate this solution o, additional decision variables are needed :

— $bx_i^o, \forall i \in V$: Binary decision variable taking the value of one if the value of decision variable x_i is strictly greater than a reference value $\hat{x}_i^o$, and zero otherwise.

— $bt_{l,i}^o, \forall l \in L\ \forall i \in V_l$: Binary decision variable taking the value of one if the value of decision variable $t_{l,i}$ is strictly lower than a reference value $\hat{t}_{l,i}^o$, and zero otherwise.

The cut is given by Expression 1.35 in combination with constraints 1.36–1.39.

$$\sum_{i \in V} bx_i^o + \sum_{l \in L\ i \in V_l} bt_{l,i}^o \geq 1 \tag{1.35}$$

$$bx_i^o < 1 + \frac{x_i - \hat{x}_i^o}{\lfloor \frac{B}{cost_i} \rfloor + 1} \qquad \forall i \in V \tag{1.36}$$

$$bt_{l,i}^o < 1 + \frac{\hat{t}_{l,i}^o - t_{l,i}}{w_{l,i} + 1} \qquad \forall l \in L\ \forall i \in V_l \tag{1.37}$$

$$bx_i^o \in \{0,1\} \qquad \forall i \in V \tag{1.38}$$

$$bt_{l,i}^o \in \{0,1\} \qquad \forall l \in L\ \forall i \in V_l \tag{1.39}$$

To adhere to constraint (1.35), either at least one additional charger must be added at one stop or at least one charging time must be reduced at one stop compared with the given values of solution o. In other words, this constraint eliminates not only solution o but also any other solution that would contain fewer chargers (with no additional charger at any stop) and longer charging times (with no reduction in the charging time at any stop) because if solution o is not feasible, then none of these solutions is feasible. Constraints (1.36) and (1.37) link the binary decision variables to the corresponding variables of the master problem (x_i and $t_{l,i}$). Constraints (1.38) and (1.39) define the domains of the additional variables.

From an implementation perspective, the master problem is not solved from scratch each time a new cut is generated. Instead, we add cuts as lazy constraints using a callback routine while solving the master problem. Lazy constraints are checked only when a new feasible integer solution is obtained during branch-and-bound tree search. In this step, if the integer solution is not feasible for the subproblem, the cut generation procedure consists in adding a new violated lazy constraint.

1.5.4 Branch-and-check-based heuristic

To converge to the optimal solution, the branch-and-check may need to generate a large number of no-good cuts, potentially leading to extended computational times. Therefore, we also implemented a heuristic version of our algorithm, denoted HBC, to obtain good solutions within a short computation time. HBC functions similarly to the original branch-and-check method. However, when an integer solution to the master problem is found that is not feasible for the subproblem, we simply reject the incumbent solution without adding a no-good cut or the associated variables/constraints. This results in a reduction in the exploration of the search tree as well as the loss of the optimality guarantee. When a solution found at a particular node is rejected, we do not explore the subtree connected to that node. However, it is possible to have a solution at a node that is not feasible for the subproblem, while another solution at the child node is feasible.

1.6 Computational experiments

The MILP model and the two version of the branch-and-check method were implemented in C++ using CPLEX 20.1 and its callback library. We set all the parameters in CPLEX to their default values, except for the number of threads which we set to one. For the branch-and-check metods we also switched off the dual preprocessing reductions to use the lazy constraint callback functions. We ran all the experiments on the workstations of the Digital Research Alliance of Canada's servers. They are equiped with an *Intel Gold 6148 Skylake, 2.4 GHz* processor and 50 Gigabyte of memory.

1.6.1 Instances generation

To test our methods we generated a set of instances using real-world data from the city of Tours (France). This data was provided by the French Ministry of the Ecological Transition (MINISTÈRE DE LA TANSITION ÉCOLOGIQUE, 2020). The instances are based on the main and most frequented lines of the Tours' network, namely, lines 2, 3a, 3b, 4, 5, 10, 11, 12, 14, 15, 16, and A. Bidirectional lines are consider as two different lines that may or not share stops. Therefore, we have a pool made up of 24 lines. On average, each line drives through 43 stops. We consider the theoretical transit offer (lines, stops, timetables) for several weeks. Based on these data, we determined the subgraphs G_l representing the bus lines and the distance between two stops $d_{i,i'}$. We considered the service frequency $\frac{1}{f_l}$ at three different times of the day. These correspond to early morning and late evening (5AM-7AM and 10PM-12PM) for low service frequency (one bus every $[30,60]$ min), evening (7PM-10PM) for mid service frequency (one bus every $[15,45]$ min), and working hours (7AM-7PM) for high service frequency (one bus every $[10,30]$ min). We set the portion of mandatory electric mode arcs to 10%. For each line, we selected these arcs such that they form a path in G_l. We set the maximum stop duration $w_{l,i}$ to 2 min for every stop. We compute the travel time between stops i and i' as $tt_{i,i'} = \frac{d_{i,i'}}{v}$, where v is the average speed of the bus in the network. We set the electric consumption of an arc connecting two stops as $e_{i,i'} = e \cdot d_{i,i'}$, where e is the average electric consumption in the network. After some discussion with public transit practitioners, we set $v = 18\ km.h^{-1}$ and $e = 1.22\ kWh.km^{-1}$. We computed the installation cost of a charger $cost_i$ as the base price of a charger, USD 230,000 (BLOOMBERG NEW ENERGY FINANCE, 2018), plus infrastructure set-up costs ranging between 30% and 50% of the cost of the charger. We set the charging speed rate R to 300 kW (PELLETIER et al., 2019) and the HB battery capacity to 19 kWh(BLOOMBERG NEW ENERGY FINANCE, 2018). Considering this fast charger, it takes a total 3 min 48 s to fully recharge the battery ; this value alights with current fast-opportunity charging standards observed in practice.

We built instances with $|L| = \{3, ..., 9\}$. For each instance, we selected the lines from the pool of 24 ensuring that the resulting bus network is a connected graph. To set the electrification budget, we used the following expression :

$$B = \frac{\sum_{l \in L} \sum_{(i,i') \in A_l} e_{i,i'}}{|L| \cdot Q} \cdot \bar{cost_i} \cdot \alpha \qquad \text{with} \qquad \bar{cost_i} = \frac{\sum_{i \in V} cost_i}{|V|} \tag{1.40}$$

The maximum budget B is computed from an average electric consumption per line, an average installation cost ($\bar{cost_i}$) and a parameter α. This parameter is a coefficient chosen empirically at 3.6, to set the possible number of chargers to be installed at consistent values (i.e., insufficient to electrify the entire network but sufficient to electrify more than half of the network). We generated 10 instances for each combination between number of lines (i.e., $|L|$) and service frequency (i.e., low, mid, high). Therefore, our set is made up of 210 instances ($= 7 \times 3 \times 10$). Our instances are publicly available at https://github.com/PVende/tmpRepoInstances.

1.6.2 Efficiency and effectiveness of the proposed methods

The first set of experiments compares the results delivered by MILP and those delivered by the exact (BC) and heuristic (HBC) version of the branch-and-check method. Recall that we use a lexicographic approach with two objectives. Therefore, we solved each instance twice using each method. In the first run we maximized the total weighted electric distance, and in the second, we minimize the total investment. We used 4 key performance metrics (KPIs) to assess the efficiency and effectiveness of the methods : i) the number of instances for which a feasible or optimal solution was found, ii) the value of the objective function, iii) the optimality gaps, and iv) the computation times.

MILP results

Table 1.4 and 1.5 delivered by the MILP formulation introduced in Section 1.4. In this experiment we set the time limit to 2h (for each instance and objective). Table 1.4 lists the results of the first run (i.e., maximizing the weighted electric distance). The first two columns indicate the instance family according to the number of lines and the service frequency. Each line in the table aggregates the results for ten instances. The next 5 columns report : the number of feasible solutions found (# Feasible), the number of optimal solutions found (# Optimal), the average objective values of the best solution found (the weighted electric distance), the average optimality gap in percentage given by CPLEX for instances for which no optimal solution is found (Optimality gap), and the average computation time when a feasible solution is found (Computation time).

The data in the table indicates that the solver provided an optimal solution for 116 out of the 210 instances (55%), a feasible-but-improvable-optimal solution for an additional 43 instances (20%), and was unable to find a feasible solution for the remaining 51 instances (24%). Additionally, the results reveal a degradation in the number of both optimal and feasible solutions, as well as in the optimality gap, as the size of the instances (in terms of the number of lines) increases. Indeed, as the number of lines increases, so does the number of charging events n_l, the number of shared stops between lines suitable for charger installation, and the number of charging operations on each charger $|K_i|$. Intuitively, in such circumstances, the model becomes larger and more challenging to solve. The data also presents a counterintuitive finding : the problem becomes harder to solve when the service frequency is mid compared to when it is either low or high. A plausible explanation for this phenomenon is that in the middle-ground situation, the scheduling component becomes more difficult to manage. When the service frequency is low, the scheduling problem is simpler because there is ample time between bus arrivals to accom-

TABLE 1.4 – MILP results - First run (weighted electric distance)

$\|L\|$	Service frequency	# Feasible	# Optimal	Avg. weighted electric distance	Avg. investment ($\times$1000 $)	Avg. optimality gap (%)	Avg. CPU time (s)
3	Low	10	10	19.6	919.8	–	55.1
	Mid	10	10	31.4	951.3	–	199.0
	High	10	10	42.0	960.5	–	54.9
4	Low	10	10	28.9	1139.7	–	710.4
	Mid	8	6	45.5	1107.5	0.9	2357.7
	High	10	10	61.0	1142.0	–	1062.9
5	Low	10	5	35.2	1037.3	2.3	4071.2
	Mid	7	2	56.2	1034.3	6.8	5674.9
	High	7	2	73.1	1070.8	2.9	5790.5
6	Low	9	6	36.5	922.3	1.3	2893.4
	Mid	3	2	46.5	854.8	10.4	3999.9
	High	8	7	77.2	922.9	0.1	1209.6
7	Low	10	8	37.9	957.7	0.9	2961.9
	Mid	6	5	56.5	937.6	21.3	2005.0
	High	9	7	83.5	948.1	3.5	3300.7
8	Low	10	7	46.0	1027.2	0.9	3958.3
	Mid	2	1	63.6	945.3	14.0	3851.5
	High	6	3	95.9	1064.1	0.6	4569.8
9	Low	10	5	52.2	1070.4	0.0	5009.2
	Mid	0	0	–	–	–	–
	High	4	0	108.1	1022.4	2.9	7200.0
Total / Average		159/210	116	51.1	1009.0	3.2	2725.3

modate charging operations. Conversely, when the service frequency is high, the solution space of the scheduling problem tightens, so the solver is more efficient to explore it.

Table 1.5 reports the results for the second run (i.e., minimizing the investment). Note that for this run the testbed is reduced to 159 instances ($= 116 + 43$). The first two columns indicate the instance family. The next 4 columns report the output depending on the nature of the solution found in the first run. Let F denotes a feasible-but-unproven-optimal solution and O a proven optimal solution. The third column (# F$\rightarrow$F) reports the number of F solutions obtained when the solution to the first run is an F solution. Similarly, the fourth column (# F$\rightarrow$O) reports the number of F solutions obtained when the solution the first run is an O solution. The fifth and sixth columns follow a similar logic. The last three columns report the average investment, the average optimality gap in percentage given by CPLEX for instances for which no optimal solution is found, and the average computation time when a feasible solution is found. Similar to Table 1.4, each row aggregates the results for multiple instances, but not necessarily the 10 belonging to each family.

TABLE 1.5 – MILP results - Second run (investment)

$\|L\|$	Service frequency	# F→F	# O→F	# F→O	# O→O	Avg. investment (×1000 $)	Avg. optimality gap (%)	Avg. CPU time (s)
3	Low	0	0	0	10	868.2	–	10.1
	Mid	0	0	0	10	868.2	–	37.0
	High	0	0	0	10	868.2	–	5.6
4	Low	0	1	0	9	1072.5	7.3	883.9
	Mid	0	1	2	5	1031.8	3.5	1597.7
	High	0	0	0	10	1102.4	–	330.9
5	Low	0	0	5	5	1026.9	–	150.3
	Mid	3	0	2	2	1018.6	12.4	3544.6
	High	0	0	5	2	1055.0	–	552.2
6	Low	0	0	3	6	908.5	–	1017.8
	Mid	1	0	0	2	843.3	13.0	3300.5
	High	0	0	1	7	904.8	–	165.9
7	Low	0	1	2	7	939.5	3.6	1927.7
	Mid	0	0	1	5	918.5	–	370.8
	High	0	1	2	6	935.6	5.4	1035.2
8	Low	1	2	2	5	1019.4	3.0	2666.6
	Mid	0	1	1	0	945.3	0.2	4466.1
	High	0	1	3	2	1054.9	5.1	2088.1
9	Low	1	2	4	3	1066.3	2.6	2965.7
	Mid	0	0	0	0	–	–	–
	High	1	0	3	0	1018.9	3.1	2111.7
Total / Average		7	10	36	106	976.5	5.6	1214.3

In most instances, when an optimal solution is found in the first run, an optimal solution is also found in the second run. Overall, the solver delivered optimal solutions to 142 out of the 159 instances (89%) and feasibile-but-unproven-optimal solutions to the remaining 17 (11%). These results suggest that the MILP formulation for the second run is easier to solve than that of the first run. The CPU times in the last column point in the same direction. The average CPU time over the whole testbed is nearly halved in the second run. This behaviour is not surprising, since i) the solution space for the MILP in the second run is smaller (because of the max weighted electric distance constraint) and ii) the solver starts from an initial solution.

A close examination of the Avg. Investment columns in tables 1.4 and 1.5 highlights the benefits of the lexicographic approach. As indicated by the overall average (last line in both tables), the second run results in potential savings of nearly 3.25% (32.5k USD). It's worth noting that this reduction in investment does not compromise the primary objective (the weighted electric distance).

Results of the Branch-and-Check method

The same computational experiments were conducted to evaluate the effectiveness of the branch-and-check method (BC) introduced in Section 1.5. Table 1.6 and Table 1.7 present the results obtained using the BC method with a time limit of 2 h for each instance and step in the lexicographic approach. Table 1.6 presents the results of the first step of the lexicographic approach. The first five columns have the same meaning as the first five columns in Table 1.4. The subsequent columns report the average optimality gap as a percentage given by the BC method for instances for which no optimal solution is found (Optimality gap), average gap with the MILP resolution if both methods provide a feasible solution for a same instance (MILP gap), average computational time (Comp. time), average number of calls to the sub-problem (# Call S.P.), and average total time spent solving the subproblem per instance (Total S.P. Comp. time). For each instance, the MILP gap is computed as $\frac{z_{MILP}-z_{BC}}{z_{MILP}}$, where z_{MILP} and z_{BC} are the objective functions of the solution returned by the MILP resolution and BC method, respectively.

Branch-and-Check results

We conducted a similar experiment to assess the effectiveness of BC. Tables 1.6 and 1.7 present, for the first and second run respectively, the results obtained after running the method for 2 h on each instance. In addition to the metrics reported for the fist run of the MILP, Table 1.6 also reports the average gap with respect to the MILP solution (Avg. MILP gap), the average number of calls to the sub-problem (Avg. # Call S.P.), and the average time spent solving the subproblem per call (Avg. S.P. CPU time). The gap with respect to the MILP is reported only if both methods provided a feasible solution for a same instance. It is computed as $\frac{z_{MILP}-z_{BC}}{z_{MILP}}$, where z_{MILP} and z_{BC} are the objective functions of the solution returned by the MILP and BC, respectively.

BC found a feasible solution for 200 out of the 210 instances (95%), 41 more than MILP (nearly 20%). Moreover, out of those feasible solutions, 128 are proven optimal, compared to 116 for MILP. A closer look at the Avg. MILP gap column reveals that both

TABLE 1.6 – BC Results - First run (weighted electric distance)

$\|L\|$	Service frequency	# Feasible	# Optimal	Avg. weighted electric distance	Avg. optimality gap (%)	Avg. MILP gap (%)	Avg. CPU time (s)	Avg. # Call S.P.	Avg. S.P. CPU time (s)
3	Low	10	9	19.6	0.5	0.0	1037.5	11.3	1.6
	Average	10	8	31.3	2.6	0.4	1674.2	271.8	1.2
	High	10	10	42.0	–	0.0	600.2	9.9	0.9
4	Low	10	10	28.9	–	0.0	785.9	15.0	5.1
	Average	10	10	45.9	–	-0.2	849.8	11.8	3.9
	High	10	10	61.0	–	0.0	410.5	12.4	3.1
5	Low	10	8	35.2	5.9	0.0	3137.7	27.2	10.9
	Average	10	4	55.7	5.2	-1.7	5537.3	182.4	9.6
	High	10	8	75.9	2.6	-0.5	3611.3	86.2	6.5
6	Low	9	6	36.4	12.1	0.3	4688.2	23.1	24.9
	Average	8	1	58.3	2.8	-3.0	6499.7	49.5	19.4
	High	7	1	79.0	5.8	1.4	6296.3	141.6	13.8
7	Low	10	5	37.8	1.8	0.1	5218.6	18.6	43.1
	Average	10	1	60.4	14.0	-0.1	7114.2	31.7	34.2
	High	9	5	82.6	3.0	0.9	4377.8	72.8	25.6
8	Low	10	7	46.0	0.0	0.0	4579.4	12.7	77.5
	Average	10	6	72.5	2.8	0.0	4867.4	19.0	64.4
	High	9	6	95.5	7.8	0.2	4240.7	45.0	56.3
9	Low	10	4	52.2	0.0	0.0	5965.2	13.0	157.1
	Average	10	6	84.6	1.4	–	5358.7	18.4	91.8
	High	8	3	107.7	15.5	14.6	5740.2	31.6	96.3
Total / Average		200/210	128	56.5	5.7	0.3	3846.2	51.6	35.5

methods deliver solutions of similar quality, at least for those instances in which both methods found a feasible solution. On the other hand, the data in the Avg. optimality gap and Avg. CPU time columns paint a more favorable picture for MILP. However, it is worth noting that these results for BC cover 41 more instances, including the largest and most challenging ones (the 9-line, mid-frequency family), where MILP could not find a single feasible solution. More generally, BC outperforms the MILP on larger instances (specially the difficult mid-frequency ones), while the latter is more effective on small instances (specially those with low service frequency).

The last two columns in Table 1.6 offer insights into the behavior of BC. As depicted in the table, with increasing instance size, the average number of calls to the subproblem decreases, while the average time spent solving a subproblem increases. This trend arises because as the number of bus lines increases, the total budget also increases, resulting in a higher number of installed chargers. Consequently, the number of charging operations to schedule tends to rise, as does the potential number of lines passing through each charger. This makes the sub-problem more challenging to solve. Another interesting observation emerges upon closer examination of the number of calls to the subproblem within each instance size. With a few notable exceptions (e.g., instances with 3 and 5 lines), the num-

TABLE 1.7 – BC results - Second run (investment)

$\|L\|$	Service frequency	# F→F	# O→F	# F→O	# O→O	Avg. investment (×1000 $)	Avg. optimality gap (%)	Avg. MILP gap (%)	Avg. CPU time (s)	Avg. # Call SP	Avg. S.P. CPU time (s)
	Low	0	0	1	9	868.2	–	0.0	18.5	2.7	1.0
3	Average	1	0	1	8	868.0	29.5	0.0	750.7	254.2	1.0
	High	0	0	0	10	868.2	–	0.0	28.9	3.1	1.0
	Low	0	0	0	10	1102.4	–	6.2	874.3	4.3	9.0
4	Average	0	0	0	10	1102.4	–	0.0	179.5	7.6	30.1
	High	0	0	0	10	1102.4	–	0.0	724.4	3.4	4.2
	Low	0	1	2	7	1026.9	0.7	0.0	793.7	2.0	4.2
5	Average	3	0	3	4	1023.7	12.2	–	2540.5	79.1	3.4
	High	0	0	2	8	1027.2	–	–	92.3	1.7	0.9
	Low	0	1	3	5	915.4	0.4	0.0	1061.1	1.9	2.1
6	Average	1	0	6	1	911.1	0.5	–	999.5	5.0	2.3
	High	2	0	4	1	944.0	1.7	–	3127.7	183.0	19.5
	Low	0	0	5	5	930.8	–	0.0	608.0	2.1	4.4
7	Average	4	0	5	1	936.6	3.2	0.0	3496.9	14.1	19.1
	High	1	3	3	2	932.0	2.2	1.0	3289.5	31.2	4.0
	Low	0	1	3	6	1012.5	2.2	0.0	1556.9	1.6	8.6
8	Average	1	2	3	4	1011.3	5.2	–	2947.6	6.5	13.3
	High	1	2	2	4	1011.7	5.2	–	2907.1	23.6	12.9
	Low	2	2	4	2	1069.5	2.7	−3.4	3414.2	1.2	13.8
9	Average	1	2	3	4	1063.8	2.9	–	2785.5	1.5	6.6
	High	2	0	3	3	1087.0	10.5	–	2249.5	21.4	30.9
Total / Average		19	14	53	114	992.3	5.1	0.9	1606.6	29.3	8.9

ber of calls to the subproblem increases with the service frequency. This suggests that as the frequency increases, the master problem is more likely to generate solutions that are infeasible. However, a quick look at column 10 reveals that the subproblem is more efficient in high-frequency instances. The latter phenomenon can be explained by the size of the subproblem's model. When the service frequencies are low, the size of set Ω_l (the possible timetables for a line) increases. Consequently, the model becomes larger to solve and, notably, to construct.

Table 1.7 displays the results of BC's second run. The first eight columns maintain the same meaning as those in Table 1.5. Following these, a column presents the average gap with the MILP solution, focusing on instances where both methods produce identical objective values after the first run and provide feasible solutions after the second run. This gap, calculated for each instance as $\frac{z_{BC}-z_{MILP}}{z_{MILP}}$, compares the objective functions of solutions from the MILP (z_{MILP}) and BC (z_{BC}). The final three columns retain the same significance as those in Table 1.6.

Out of the 200 instances, BC yielded a Pareto-optimal solution for 114. Additionally, for 53 instances, BC delivered a second-run optimal solution after after starting from a feasible-but-unproven first-run solution. Similar to the observations with the MILP, and for analogous reasons, the results of BC (especially the computation times) suggest that the second run tends to be easier to solve than the first. Notably, the number of calls to the sub-problem and the time spent solving it are significantly lower in the second run. This outcome can be attributed to i) retaining all cuts generated in the first run for the second run, thereby substantially reducing the feasible solution space and ii) the upper bound on the value of the first objective function. On average, the MILP gap stands at 0.9%, with many instances having a gap of zero. This indicates that when both methods find the same solutions after the first run, they also produce identical solutions after the second run.

Branch-and-check-based heuristic results

The HBC method introduced in Section 1.5.4 aims to find good solutions with shorter computation times compared to previous exact methods. To assess the benefits of using HBC, we conducted the same computational experiments, but this time, we set a time limit of 10 minutes for each instance and run of the lexicographic approach. Table 1.8 displays the results for the first run, featuring columns similar to those in Table 1.6. In addition, the table introduces columns 6 and 8, reporting the gap with respect to BC and the number of times where the method exceeds the time limit, respectively. For the sake of brevity, we do not report here the results for HBC's second run, but the interested reader can find the summary table in Appendix 3.6.

HBC provided feasible solutions for 191 instances in less than 10 minutes, surpassing MILP but falling short of BC's performance. However, the BC method is considerably more time-consuming. Notably, for nearly half of the instances, the HBC concluded before reaching the time limit. The quality of the solutions obtained by HBC was comparable to those obtained by the MILP and BC, with average gaps of 0.2% and 0.0% respectively. HBC even outperformed these methods for some instances, with a negative gap of up to 3.1%. The table also demonstrates that HBC makes a significantly larger number of calls to the subproblem compared to BC. This finding hints on the capacity of the cuts embedded in BC to eliminate not just one, but several infeasible solutions at once. Regarding HBC, we observed that : i) in most of the calls to the subproblem, the master problem solution ended up being infeasible, and ii) the solver efficiently identifies this infeasibi-

TABLE 1.8 – HBC results - First run (weighted electric distance)

$\|L\|$	Service frequency	# Feasible	Avg. weighted electric distance	Avg. MILP gap (%)	Avg. BC gap (%)	Avg. CPU time (s)	# Time limit exceeded	Avg. # Call S.P.	Avg. S.P. CPU time (s)
3	Low	10	19.6	0.0	0.0	221.4	3	8.0	0.0
	Average	10	31.4	0.0	−0.4	239.6	3	559.5	0.0
	High	10	42.0	0.0	0.0	188.0	3	11.1	0.0
4	Low	10	28.9	0.0	0.0	277.8	4	10.8	0.1
	Average	10	45.9	−0.2	0.0	304.5	4	18.6	0.1
	High	10	61.0	0.0	0.0	208.5	1	13.0	0.0
5	Low	10	34.9	0.8	0.8	396.9	4	26.5	0.1
	Average	10	55.9	−1.2	−0.3	438.6	6	380	0.1
	High	10	75.4	0.4	0.8	414.7	6	338.7	0.0
6	Low	9	36.4	0.5	0.1	600.0	9	21.1	0.1
	Average	9	58.1	−3.1	0.0	577.1	8	161.2	0.1
	High	8	78.7	2.8	1.5	548.8	7	1007.6	0.0
7	Low	10	37.8	0.2	0.0	560.2	9	16.9	0.1
	Average	9	59.3	1.5	0.4	537.6	7	215.9	0.1
	High	8	84.4	−0.2	−0.5	565.0	6	374.4	0.0
8	Low	10	46.0	0.0	0.0	459.6	3	15.8	0.1
	Average	10	72.3	0.0	0.1	544.6	7	24.2	0.1
	High	8	95.2	0.0	−0.7	472.5	4	201.8	0.0
9	Low	10	52.2	0.0	0.0	583.6	8	12.6	0.1
	Average	7	83.7	–	0.0	544.9	5	13.7	0.1
	High	3	124.8	–	−3.1	537.1	2	18.3	0.0
Total / Average		191/210	54.7	0.2	0.0	429.0	109.0	161.1	0.1

lity. This behavior is reflected numerically in columns 9 and 10. Upon closer examination of the results for each instance size, we note that, similar to BC, the number of calls to the subproblem increases with the service frequency. However, the average time spent solving the problem decreases, primarily because most of those subproblems are quickly identified as infeasible.

1.6.3 Managerial insights

In this section, we present the results of two additional computational experiments aimed at helping managers address two key questions : What is the trade-off between charging infrastructure investment and weighted electric distance ? and How much can the weighted electric distance be improved by allowing shared chargers between lines, given a fixed electrification budget ? We conducted all computational experiments reported in this section using the same set of instances described in Section 1.6.1.

The trade-off between investment and weighted electric distance

In this experiment, our aim is to measure the additional investment required in charging infrastructure to operate the network in fully electric mode and quantify the additional decarbonation benefits it represents. To accomplish our goal, we ran BC for 2 h on each instance in our testbed deactivating the budget constraint (constraint (1.3)) and forcing all segments to be driven in electric mode. In other words, we set

$$y_{l,i,i'} = 1 \qquad \forall l \in L,\ \forall (i,i') \tag{1.41}$$

Consequently, the resulting optimization problem is simpler than the original one because it involves fewer decisions. The objective function in this new scenario is the minimization of the investment (i.e., objective function (1.2)).

Table 1.9 presents a detailed overview of the results. The first two columns categorize instances by family. Following these, the subsequent columns detail the number of feasible solutions found (#Fea.), number of optimal solutions (#Opt.), average computation time on instances for which BC found a feasible solution (Avg. CPU time), average weighted electric distance, and average total investment required for full electrification. The last two columns compare the differences in terms of the average weighted electric distance and the average investment between the original full electrification scenarios. The deltas in the last two columns are computed as $\Delta X = \frac{z(X_{FE})-z(X_{HE})}{z(X_{HE})}$, where $z(X_{FE})$ and $z(X_{HE})$ represent the value of X for the best solution in the full electrification and original scenarios, respectively. Note that ΔX is computed only on instances for which BC provides a feasible solution in both scenarios.

The performance of BC in the full electrification scenario is comparable, both in terms of the number of feasible and optimal solutions, to that displayed in the original setup. More interestingly, the results in the last two columns suggest that the increase on the investment needed to run a fully electrified network disproportionately increases with respect to the benefits. This is specially true on larger instances. Take for instance the 9-line, low-frequency family. On average, in the solutions for the full electrification scenario, the fleet travels 24.3% more distance on electric mode. However, to accomplish that

TABLE 1.9 – Computational results - Full electrification scenario

$\|L\|$	Service frequency	Full electrification: # Fea.	# Opt.	Avg. CPU time (s)	Avg. weighted electric distance	Avg. investment ($\times$1000 \$)	Original set up: Δ Avg. weighted electric distance (%)	Δ Avg. investment (%)
3	Low	10	9	897.4	21.3	1047.7	11.2	21.7
	Mid	10	10	407.6	33.9	1047.7	11.5	21.7
	High	10	10	604.6	44.9	1047.7	10.8	21.7
4	Low	10	10	992.4	30.4	1245.2	5.0	14.7
	Mid	10	9	1328.6	48.0	1246.8	4.6	14.8
	High	10	10	1012.4	63.0	1245.2	3.5	14.7
5	Low	10	9	1124.1	36.9	1262.9	5.0	24.9
	Mid	10	8	2689.7	59.1	1267.3	6.1	25.7
	High	10	9	1322.5	78.7	1262.9	3.6	24.9
6	Low	10	4	4803.7	41.1	1625.2	15.6	80.1
	Mid	10	4	5389.9	65.6	1625.4	14.6	78.6
	High	10	1	6552.6	88.1	1735.8	10.7	91.0
7	Low	10	0	7200.0	47.2	1954.5	26.6	110.3
	Mid	9	0	7200.0	74.9	2256.0	25.8	142.2
	High	10	0	7200.0	102.6	2073.7	25.4	119.7
8	Low	10	0	7200.0	57.1	2040.8	25.4	102.7
	Mid	10	0	7200.0	90.0	2156.2	25.4	115.9
	High	10	1	6775.3	120.1	2141.3	27.8	114.7
9	Low	10	1	6915.1	64.4	2147.3	24.3	102.1
	Mid	10	1	6881.7	103.2	2228.5	22.5	109.9
	High	9	1	7137.7	139.1	2408.1	32.1	138.7
Total / Average		208/210	97	4298.2	66.7	1663.5	15.8	68.7

feat, a two fold investment in charging infrastructure is needed (102.1%). Overall, fully electrified networks translate into an average of 15.8% more electric distance but 68.7% more infrastructure investments. In markets where electrification budgets are thigh, BC can help analysts find a good balance between these two important KPIs.

The benefits of shared chargers

Allowing charger sharing between lines complicates the infrastructure location problem and adds complexity to the network's operation. In this experiment, our aim is to evaluate the advantages of this feature. To achieve this, we solved a new version of the problem in which each installed charger is strictly assigned to a single line. Consequently, only HBs servicing that line can utilize it. It is important to note that in this scenario, the charging operation scheduling component is absent. Therefore, our methods (MILP, BC, and HBC) are not suitable for solving the problem. Instead, we developed a new MILP model specifically for this case. For brevity, we do not present the model here, but readers can find a detailed description in Appendix 3.6. We executed the new model for 2 hours on a slightly modified version of each of our 210 instances. Specifically, for this expe-

TABLE 1.10 – Computational results - Non-shared charging stations scenario

$\|L\|$	Service frequency	Non-shared chargers # Fea.	# Opt.	Avg. CPU time (s)	Avg. weighted electric distance	Shared chargers Δ Avg. weighted electric distance (%)
3	Low	10	7	2856.3	13.0	−33.2
	Mid	10	7	3129.7	21.8	−29.7
	High	10	7	3303.3	30.2	−27.2
4	Low	10	6	4128.0	14.8	−48.7
	Mid	10	4	5442.1	25.2	−45.0
	High	10	2	6734.0	36.1	−40.9
5	Low	10	5	4908.6	15.3	−56.4
	Mid	10	4	5357.1	27.5	−50.3
	High	10	3	5670.0	39.7	−47.4
6	Low	10	10	1499.3	12.7	−63.7
	Mid	10	4	4531.5	22.9	−59.9
	High	10	2	5764.3	33.1	−57.1
7	Low	10	8	3265.7	13.7	−63.2
	Mid	10	0	7200.0	24.8	−58.2
	High	10	0	7200.0	36.8	−55.1
8	Low	10	7	2321.1	14.5	−68.5
	Mid	10	1	6494.4	26.6	−63.2
	High	10	1	6497.4	39.5	−58.2
9	Low	10	10	1054.1	15.5	−70.4
	Mid	10	2	6297.4	29.0	−65.8
	High	10	2	5841.5	43.3	−58.5
Total / Average		210/210	92	4737.9	25.5	−53.1

riment, we did not enforce the mandatory electric arcs (constraints (1.5)). This decision was made because, under that constraint, too many instances become infeasible due to the inability to share chargers while maintaining the budget unchanged. We compared the results delivered by the new MILP in the non-sharing scenario to those retrieved by BC in the charging sharing scenario.

Table 1.10 presents the results of this new scenario. The first six columns have the same meaning as those in Table 1.9. However, the last column reports the average degradation in weighted electric distance when chargers are not shared. These values are computed as $\Delta = \frac{z(X_{NS})-z(X_S)}{z(X_S)}$, where $z(X_{NS})$ and $z(X_S)$ represent the weighted electric distance in the solutions for the non-sharing and sharing scenarios, respectively.

As anticipated, the solver found feasible solutions for all instances because even a solution with no installed charger is feasible. Conversely, the new model reported optimal solutions for only 92 out of the 210 instances (43%). As indicated in the third column, the optimal/feasible ratio is better for instances with low service frequency, regardless of the instance size. Furthermore, as highlighted in the last column, forbidding charger sharing leads to an average 53.1% reduction in the weighted electric distance. In other words, by allowing this practice, we were able to double (on average) the total distance traveled in electric mode, without increasing the electrification budget. By using BC, analysts can overcome the difficulty of solving the more complex charger location and charging scheduling problem while benefiting from the higher electrification provided by the charger sharing policy.

1.7 Conclusion

In this paper, we explored a fast-charging location problem on hybrid electric bus networks, where charging stations can be shared among different bus lines. Our approach involves a lexicographic optimization strategy to first maximize the total distance traveled using the electric mode, weighted by the bus line frequency, and subsequently minimize the total investment on charger installation. This approach ensures the existence of a feasible charging schedule at each station. We proposed a mixed integer linear programming model alongside exact and heuristic methods based on a branch-and-check framework to efficiently solve the problem. Computational experiments conducted using a set of 210 instances derived from the urban transit network in Tours, France, revealed that the branch-and-check method outperformed the MILP, yielding more feasible and optimal solutions. Furthermore, our proposed heuristic generated solutions close to those obtained by exact methods, albeit within significantly shorter computation times. Additionally, we provide several managerial insights for decision-makers to evaluate the trade-offs between total installation costs and achieved electric distance, as well as the benefits of shared chargers versus non-shared ones in enhancing the distance traveled by buses in electric mode.

From a research perspective, extending the problem to incorporate various types of charging technology, assets (hybrid, full electric, etc.), and battery capacities could be valuable. Although this would increase the problem's complexity, it could provide transit agencies with a decision support tool that is more flexible to accommodate their specific needs. Another area for research could involve restructuring bus lines and schedules to reduce electric consumption and promote charger sharing. For example, the models could include decision variables to allow modifying a line to include a stop where chargers can be shared with other lines. However, any modifications should carefully consider factors such as customer demand, desired service levels, and potential disruptions to user habits. Additionally, exploring the placement of existing chargers and electrified bus lines presents another promising research direction. This approach would enable transit agencies to gradually electrify their networks over an extended planning horizon, ultimately contributing to the overall reduction of greenhouse gas emissions.

Acknowledgments

This research was partially funded by the Natural Sciences and Engineering Research Council of Canada, thought the discovery grants and by HEC Montreal through the research professorship on Clean Transportation Analytics. This research was enabled in part by support provided by Calcul Québec (www.calculquebec.ca) and Digital Research Alliance of Canada (www.alliancecan.ca).

References

ARORA, J. S. (2017). Chapter 18 - Multi-objective Optimum Design Concepts and Methods. In *Introduction to Optimum Design (Fourth Edition)*. Academic Press.

BLOOMBERG NEW ENERGY FINANCE. (2018). *Electric buses in cities : Driving towards cleaner air and lower CO2* (Report) (Visité en Mars 2024). on the behalf of : Financing Sustainable Cities Initiative, C40 Cities, World Resources Institute, Citi Foundation. https://data.bloomberglp.com/professional/sites/24/2018/05/Electric-Buses-in-Cities-Report-BNEF-C40-Citi.pdf

DIRKS, N., SCHIFFER, M., & WALTHER, G. (2022). On the integration of battery electric buses into urban bus networks. *Transportation Research Part C : Emerging Technologies*, *139*, 103628.

DIRKS, N., WAGNER, D., SCHIFFER, M., & WALTHER, G. (2021). A Concise Guide on the Integration of Battery Electric Buses into Urban Bus Networks. *arXiv preprints arXiv :2104.10752v1*.

FRADE, I., RIBEIRO, A., GONÇALVES, G., & ANTUNES, A. P. (2011). Optimal Location of Charging Stations for Electric Vehicles in a Neighborhood in Lisbon, Portugal. *Transportation Research Record*, *2252*(1), 91-98.

GAIROLA, P., & NEZAMUDDIN, N. (2022). Design of Battery Electric Bus System Considering Waiting Time Limitations. *Transportation Research Record*.

GOEHLICH, D., SPANGENBERG, F., & KUNITH, A. (2013). Stochastic total cost of ownership forecasting for innovative urban transport systems. *2013 IEEE International Conference on Industrial Engineering and Engineering Management*.

GUPTA, U. I., LEE, D., & LEUNG, J. Y. (1979). An Optimal Solution for the Channel-Assignment Problem. *IEEE Transactions on Computers*, *C-28*(11), 807-810.

HE, S. Y., KUO, Y.-H., & WU, D. (2016). Incorporating institutional and spatial factors in the selection of the optimal locations of public electric vehicle charging facilities : A case study of Beijing, China. *Transportation Research Part C : Emerging Technologies*, *67*, 131-148.

INSEE RÉFÉRENCES. (2019). *Changement climatique et effet de serre* (Report). Insee. https://www.insee.fr/fr/statistiques/3676581

IPCC. (2014). *Climate Change 2014 : AR5 Synthesis Report* (rapp. tech.).

JANOVEC, M., & KOHÁNI, M. (2019). Exact approach to the electric bus fleet scheduling. *Transportation Research Procedia*, *40*, 1380-1387.

KCHAOU-BOUJELBEN, M. (2021). Charging station location problem : A comprehensive review on models and solution approaches. *Transportation Research Part C : Emerging Technologies*, *132*, 103376.

KUNITH, A., MENDELEVITCH, R., & GOEHLICH, D. (2017). Electrification of a city bus network—An optimization model for cost-effective placing of charging infrastructure and battery sizing of fast-charging electric bus systems. *International Journal of Sustainable Transportation*, *11*(10), 707-720.

LIU, T., & CEDER, A. (2020). Battery-electric transit vehicle scheduling with optimal number of stationary chargers. *Transportation Research Part C : Emerging Technologies*, *114*, 118-139.

LIU, Z., SONG, Z., & HE, Y. (2018). Planning of Fast-Charging Stations for a Battery Electric Bus System under Energy Consumption Uncertainty. *Transportation Research Record*, *2672*(8), 96-107.

LOTFI, M., PEREIRA, P., PATERAKIS, N. G., GABBAR, H. A., & CATALÃO, J. P. S. (2020). Optimal Design of Electric Bus Transport Systems With Minimal Total Ownership Cost. *IEEE Access*, *8*.

MAJHI, R. C., RANJITKAR, P., SHENG, M., COVIC, G. A., & WILSON, D. J. (2021). A systematic review of charging infrastructure location problem for electric vehicles. *Transport Reviews*, *41*(4), 432-455.

MINISTÈRE DE LA TANSITION ÉCOLOGIQUE. (2020). Réseau urbain Fil Bleu - Jeu de données [Data about the theoretical transport offer of Fil Bleu network, Tours, France]. https://transport.data.gouv.fr/datasets/horaires-theoriques-du-reseau-fil-bleu-tours-metropole-gtfs

PELLETIER, S., JABALI, O., MENDOZA, J. E., & LAPORTE, G. (2019). The electric bus fleet transition problem. *Transportation Research Part C-Emerging Technologies*, *109*, 174-193.

QUINTANA, C. L., CLIMENT, L., & ARBELAEZ, A. (2022). Iterated Local Search for the eBuses Charging Location Problem. In G. RUDOLPH, A. V. KONONOVA, H. AGUIRRE, P. KERSCHKE, G. OCHOA & T. TUŠAR (Éd.), *Parallel Problem Solving from Nature – PPSN XVII*. Springer International Publishing.

ROGGE, M., van der HURK, E., LARSEN, A., & SAUER, D. U. (2018). Electric bus fleet size and mix problem with optimization of charging infrastructure. *Applied Energy*, *211*, 282-295.

SASSI-BEN SALAH, O., & OULAMARA, A. (2017). Electric vehicle scheduling and optimal charging problem : complexity, exact and heuristic approaches. *International Journal of Production Research*, *55*(2), 519-535.

SHEN, Z.-J. M., FENG, B., MAO, C., & RAN, L. (2019). Optimization models for electric vehicle service operations : A literature review. *Transportation Research Part B : Methodological*, *128*, 462-477.

SOLTANPOUR, A., GHAMAMI, M., NICKNAM, M., GANJI, M., & TIAN, W. (2022). Charging Infrastructure and Schedule Planning for a Public Transit Network with a Mixed Fleet of Electric and Diesel Buses. *Transportation Research Record*.

THORSTEINSSON, E. S. (2001). Branch-and-check : A hybrid framework integrating mixed integer programming and constraint logic programming. *International Conference on Principles and Practice of Constraint Programming*.

TOPAL, O. (2023). A novel on the retrofit from CNG buses to electric buses for rubber-tyred wheeled public transportation systems. *Proceedings of the Institution of Mechanical Engineers, Part D : Journal of Automobile Engineering*, *237*(7), 1738-1750.

UNFCCC. (2016). *Report of the Conference of the Parties on its twenty-first session, held in Paris from 30 November to 13 December 2015. Part one : Proceedings* (rapp. tech.).

WANG, X., YUEN, C., HASSAN, N. U., AN, N., & WU, W. (2017). Electric Vehicle Charging Station Placement for Urban Public Bus Systems. *IEEE Transactions on Intelligent Transportation Systems*, *18*(1), 128-139.

WANG, Y., LIAO, F., & LU, C. (2022). Integrated optimization of charger deployment and fleet scheduling for battery electric buses. *Transportation Research Part D : Transport and Environment*, *109*, 103382.

WANG, Y., HUANG, Y., XU, J., & BARCLAY, N. (2017). Optimal recharging scheduling for urban electric buses : A case study in Davis. *Transportation Research Part E : Logistics and Transportation Review*, *100*, 115-132.

WEI, R., LIU, X., OU, Y., & KIAVASH FAYYAZ, S. (2018). Optimizing the spatio-temporal deployment of battery electric bus system. *Journal of Transport Geography*, *68*, 160-168.

XYLIA, M., LEDUC, S., PATRIZIO, P., KRAXNER, F., & SILVEIRA, S. (2017). Locating charging infrastructure for electric buses in Stockholm. *Transportation Research Part C : Emerging Technologies*, *78*, 183-200.

YE, Z., YU, N., WEI, R., & LIU, X. C. (2022). Decarbonizing regional multi-model transportation system with shared electric charging hubs. *Transportation Research Part C : Emerging Technologies*, *144*, 103881.

ZHOU, Y., MENG, Q., & ONG, G. P. (2022). Electric Bus Charging Scheduling for a Single Public Transport Route Considering Nonlinear Charging Profile and Battery Degradation Effect. *Transportation Research Part B : Methodological*, *159*, 49-75.

Chapitre 2

Matheuristics for a multi-day electric bus assignment and overnight recharge scheduling problem

Résumé

Afin de limiter les émissions de gaz à effet de serre dans le secteur des transports publics, les autorités organisatrices des transports augmentent constamment la proportion de bus électriques dans leur flotte. En raison de contraintes d'espace et de budget, le nombre de chargeurs pouvant être installés dans les dépôts est généralement inférieur au nombre de bus électriques de la flotte. De plus, même s'il y a un chargeur pour chaque véhicule électrique, il est pratiquement impossible d'utiliser tous les chargeurs en même temps en raison des contraintes de puissance maximale pouvant être demandée au réseau électrique. Il est donc nécessaire de concevoir des techniques d'optimisation qui aident à recharger les bus de manière efficace, en tenant compte des contraintes de capacité de l'infrastructure de recharge. Dans cet article, nous considérons un problème d'affectation de bus électriques sur plusieurs jours et d'ordonnancement de la recharge nocturne qui peut être brièvement énoncé comme suit. Étant donné un ensemble de blocs véhicules (séquences de trajets programmés effectués par le même bus pendant un jour donné) parcourus sur plusieurs jours, un ensemble de bus électriques identiques et un ensemble de chargeurs disponibles au dépôt dont la fonction de recharge est une fonction linéaire par morceaux, le problème consiste à affecter un bus électrique à chaque bloc et à programmer les opérations de recharge nocturne au dépôt de telle sorte que les bus électriques ne manquent jamais d'énergie lorsqu'ils effectuent leurs blocs et que la capacité des chargeurs installés au dépôt ne soit jamais dépassée. L'objectif est double : minimiser les coûts de recharge totaux et minimiser l'impact des décisions de recharge sur la santé à long terme des batteries. Nous modélisons d'abord ce problème sous la forme d'un programme linéaire en nombres entiers (MILP) qui peut être résolu à l'aide d'un solveur commercial. Ensuite, afin d'obtenir des temps de calcul plus rapides, nous développons deux matheuristiques multiphases basées sur le MILP. Pour montrer l'intérêt de considérer un horizon de plusieurs jours, nous introduisons deux autres matheuristiques qui imitent les pratiques industrielles actuelles et résolvent le problème de manière séquentielle, un jour à la fois. Pour évaluer tous ces algorithmes, nous utilisons un ensemble de 264 instances générées à partir des données d'un opérateur de bus électriques.

Abstract

To limit greenhouse gas emissions in the public transportation sector, transit authorities are constantly increasing the proportion of electric buses (EBs) in their fleets. Due to space and budget constraints, more often than not, the number of chargers that can be installed at the depots is less than the number of EBs in the fleet. Moreover, even if there is one charger for each EB, it is virtually impossible to use all the chargers at the same time due to maximum power grid constraints. Thus, there is a need to devise optimization techniques that help to recharge the buses in an efficient and acute way, taking into account these charging infrastructure capacity constraints. In this study, we consider a multi-day electric bus assignment and overnight recharge scheduling problem that can be briefly stated as follows. Given a set of vehicle blocks (sequences of timetabled bus trips performed

by the same bus on a given day) to be operated over several days, a set of identical EBs, and a set of chargers available at the depot whose charging function is a piecewise linear function, the problem consists in assigning an EB to each block and to schedule the overnight recharging operations at the depot such that the EBs never run out of energy when performing their blocks and the depot charging capacity is never exceeded. The objective is twofold : minimizing the total charging costs and minimizing the impact of the charging decisions in the long-term health of the batteries. We first model this problem as a mixed integer linear program (MILP) that can be solved with a commercial solver. Then, to yield faster computational times, we develop two multi-phase matheuristics based on the MILP. To show the interest of considering a multiple-day horizon, we introduce two other matheuristics that mimic current industrial practices and solve the problem sequentially, one day at a time. To evaluate all these algorithms, we use a set of 264 instances generated from data of an EB operator.

2.1 Introduction

From 1970 to 2010, greenhouse gas emissions increased by 80% (INSEE RÉFÉRENCES, 2019). This increment is mainly due to the development of energy-intensive sectors such as manufacturing and transportation. According to the COP21 report (UNFCCC, 2016), if no action is taken to stop this rise by 2100, the global temperature is expected to increase by up to 5 °C. This strong rise could have dramatic consequences such as the acidification of the oceans, the loss of biodiversity, and the rise of climate refugees, among others. To limit this temperature increase, the countries reunited in the COP21 climate conference committed to reducing emissions of CO_2, which accounts for 70% of the greenhouse gases released into the atmosphere every year.

The transportation sector is responsible for almost 30% of the European Union CO_2 emissions (IPCC, 2014). One leverage that governments may use to reduce these emissions is the electrification of public transport, especially city buses. The electrification of transport systems raises several strategic, tactical, and operational challenges. Indeed, replacing classical diesel-powered buses with electric buses (EBs) is not straightforward. EBs have a considerably limited driving range and therefore often need to be recharged between services or even en route (depending on the technology, length of the line, loading time, etc.). To cope with these technological constraints, transport authorities must deploy charging infrastructure along the lines, as well as at end-of-line terminals and depots. There are two main policies for charging the EBs : opportunity charging (Y. WANG et al., 2017 ; XYLIA et al., 2017) and overnight charging (HOUBBADI et al., 2019). In the former, the buses are charged during their regular operation at end-of-line terminals or long stops (e.g., at transfer points between lines). Since buses must be charged fast and frequently, opportunity charging requires a high upfront investment in charging infrastructure (e.g., fast chargers, high tension power lines, high voltage transformers). On the other hand, for the same reasons, buses need smaller batteries, which reduces the upfront cost of the fleet and increases its payload. Overnight charging follows the opposite strategy. As the name suggests, buses are charged at the depots during the night (or more broadly, between shifts) using slow chargers. Needless to say, to implement the overnight charging strategy, the buses must be equipped with larger, thus more expensive, batteries but the purchasing and installing cost of slow chargers is much lower than that of fast chargers (BLOOMBERG NEW ENERGY FINANCE, 2018). In this paper, we focus on transportation systems exploiting the overnight charging strategy.

Today, because EBs account for only a small fraction of the vehicles in a fleet and slow chargers are relatively inexpensive, transit operators can often dedicate one charger to each EB during overnight charging operations. However, the participation of EBs in the global fleet is expected to grow up to 50% by 2025 (CAUGHILL, 2018). Due to this drastic change and the tight budget and space constraints that operators typically face, the one-charger-per-vehicle practice is not sustainable in the long run. Moreover, even in cases where these constraints are not critical and the operator can devote one charger to each EB, it is virtually impossible to use all the chargers at the same time due to maximum power grid constraints. As a consequence, operators need to develop strategies to schedule overnight EB charging operations taking into account these charging infrastructure capacity constraints.

In general, the overnight EB charging scheduling process works as follows. First, sequences of timetabled trips, called vehicle blocks, are computed for each day of a planning horizon (e.g., a week) by solving a vehicle scheduling problem (VSP) or a multi-depot VSP (BUNTE & KLIEWER, 2009 ; KLIEWER et al., 2006 ; LÖBEL, 1999). Second, every night, the EBs are assigned to the vehicle blocks to be operated from their depot on the next day, taking into account their current state of charge (SoC). Third, each EB is recharged overnight just enough to be able to perform its assigned block. While this day-by-day process is simple to understand and implement, it may be unsuitable in many practical situations. For instance, imagine a simplified situation with one EB and two days, each with a single block (for simplicity Block 1 and Block 2). Now, assume that Block 1 consumes 50% of a full battery charge and Block 2 consumes 90%. Assume also that the EB always keeps a charge equivalent to 10% of its battery capacity as a safety buffer. A myopic single-day scheduler may prescribe charging the EB up to 60% of its capacity the night before Day 1. Then, the EB will return to the depot with a SoC of 10% after executing Block 1. If Block 1 finishes late at night and Block 2 starts early in the morning, the inter-block period may not be long enough to fully charge the battery (which is required to execute Block 2 and meet the minimum buffer constraint). Considering a multi-day scheduling horizon may help alleviate this issue. For instance, the scheduler may prescribe charging the EB up to 80% during the first night, reducing the amount of energy that must be charged during the second night.

Another issue that operators often neglect is the impact of the charging scheduling decisions on the aging of the batteries ; the most expensive and environmentally unfriendly component of an EBs. According to technical literature, there are two main types of *battery aging* : cycle aging and calendar aging. The former depends on the current rate and the *depth of discharge* or DoD (i.e., the charge/discharge cut-off voltages). Charging or/and discharging the batteries at high rates (e.g., using fast chargers) and draining them to their maximum DoD reduces the number of charge/discharge cycles in their lifespan (BARRÉ et al., 2013). Calendar aging depends on the batteries' average SoC and temperature during storage. Storing the batteries at high SoCs and temperatures for long periods of time also reduces the battery lifespan. PELLETIER et al., 2017 pointed out calendar aging can be improved by charging the vehicles as closely as possible to their departure times. Therefore, there is an incentive to embed this logic into the overnight charging scheduling process, even at the cost of increasing its complexity.

In this paper, we study the multi-day EB assignment and overnight recharge scheduling problem (MDEBAOSP) that can be briefly stated as follows. Given a set of vehicle blocks to be operated from a depot over several days, a set of identical EBs, and a set of available chargers at the depot whose charging function is a piecewise linear function, the MDEBAOSP consists in assigning an EB to each block and scheduling the overnight recharging operations at the depot such that the EBs never run out of energy when performing their blocks, the depot charging capacity is never exceeded, and the sum of the total charging costs and battery (calendar aging) degradation costs is minimized. The goal is to provide a decision support tool to the public transit companies that will help them to better manage their EB fleet by making decisions based on a multiple-day planning horizon. To accomplish this goal, we model the MDEBAOSP as a mixed-integer linear program (MILP) that we later leverage to build two multi-phase matheuristics. To show the interest of considering a multiple-day horizon, we introduce two other matheuristics that mimic current industrial practices and solve the problem sequentially, one day at a time. To assess all these algorithms, we report computational results obtained on a set of 264 instances generated from real-life data provided by an IT company that commercializes optimization software for public transit.

The remainder of this paper is organized as follows. Section 2.2 presents a literature review on problems related to the MDEBAOSP. Section 2.3 formally defines the MDEBAOSP and Section 2.4 formulates it as a MILP. Section 2.5 describes the solution methods proposed to solve this problem. Section 2.6 provides the results of our computational experiments. Finally, Section 2.7 concludes and discusses possible future research directions.

2.2 Literature review

The integration of EBs into an urban transit network is related to several classes of problems including, but not limited to : fleet transformation problems (FTPs), charging location problems (CLPs), charging scheduling problems (CSPs), sequence assignment problems (SAPs), and vehicle scheduling problems (VSPs). In a recent paper, DIRKS et al., 2021 extensively survey the literature on those problems and analyze the major contributions to their corresponding streams of research. For the sake of completeness, we briefly overview the main characteristics of these problems here, but we refer the reader to their excellent paper for further details. FTPs aim to create a plan spanning multiple periods (e.g., years) to replace a fleet of classical diesel-powered buses with a fleet of EBs (DIRKS et al., 2022 ; PELLETIER et al., 2019). The main decisions involve the purchase of new EBs, the retirement of old diesel-powered buses, and the purchase of the charging stations needed to power the EBs of the new fleet. The aim is to minimize the sum of operational and fleet and charger acquisition costs. As their name suggests, CLPs consist in locating charging stations across a transit network to ensure that the EBs in a fleet can operate without running out of power (Z. LIU et al., 2018 ; LOTFI et al., 2020). Usually, CLPs focus on transit systems implementing the opportunity charging strategy. Therefore, potential charger locations are typically reduced to the bus stops, the end-of-line terminals, and the hubs making up the network. The main decisions are then the number, type, and location of the chargers to be installed. Some CLP variants also consider decisions on the type and size of the batteries that should be installed in the EBs (KUNITH et al., 2017). In CLPs, the objective function typically aims to minimize the acquisition and installation cost of the charging stations (and batteries).

At an operational level, CSPs assume that the trip-to-vehicle assignments are given, and focus on scheduling charging operations between trips (SASSI-BEN SALAH & OULAMARA, 2014). Some CSP variants consider capacitated and heterogeneous charging stations (PELLETIER et al., 2018). In addition to that, some variants also include battery aging considerations (KLEIN & SCHIFFER, 2023 ; PELLETIER et al., 2018). SAPs consist in assembling sequences of trips (i.e., blocks in our jargon) and assigning each of those blocks to an EB (ROGGE et al., 2018; SASSI-BEN SALAH & OULAMARA, 2017). To ensure the operational feasibility of a block, among other things, SAPs must determine where and for how long the EB assigned to that block must charge its battery between two trips. The objective is usually to minimize energy costs. For electric vehicles, SAPs can be considered an extension of the CSPs where trip-to-vehicle assignments are additional decisions to the problem. Finally, VSPs aim to determine the minimum number of vehicles that are needed to perform a set of trips (JANOVEC & KOHÁNI, 2019; T. LIU & CEDER, 2020). They can therefore be seen as SAPs, where the number of vehicles to acquire is also a decision variable and the objective seeks to minimize not only the total cost of the energy but also that of purchasing the fleet.

As briefly discussed in Section 2.1, the VSPs take action in the previous step of the planning process, so their outputs are key inputs to our MDEBAOSP. The literature reports on several electric VSP (eVSP) variants. For instance, WEN et al., 2016 developed an adaptive large neighborhood search heuristic for an eVSP with multiple depots and a linear charging function. JANOVEC et KOHÁNI, 2019 proposed a MILP that can be solved by a commercial solver for an eVSP. Their objective was to assign a set of service trips and a set of charging events to EBs from a homogeneous fleet, operating from a single depot, creating a schedule for each vehicle and for each charger, considering partial charging, while minimizing the number of vehicles. RINALDI et al., 2020 introduce a time decomposition heuristic that solves a series of MILPs for a version of the problem with a mixed fleet (EBs and hybrid buses), operating from a single depot, while minimizing the total operational cost. ALVO et al., 2021 design a Benders decomposition algorithm for a mixed fleet (EBs and diesel buses) eVSP with a linear charging function, while minimizing first the number of diesel buses used and second their total fuel consumption. Their decomposition is structured as : (i) a master problem creating bus schedules and charger schedules, without considering charger capacity; (ii) a satellite problem that checks if feasible charger schedules can be computed for the given bus schedules. ZHANG et al., 2021 develop a branch-and-price algorithm that can handle battery degradation through cycle aging but does not allow partial charging. ZHOU et al., 2022 tackle a more complex problem that allows partial charging and considers multiple charger types. They solve their problem using a MILP, enhanced with problem-specific valid inequalities, running on a commercial solver. WU et al., 2022 propose a branch-and-price algorithm for solving a multi-depot eVSP considering a rich time-of-use electricity tarification but forcing the EBs to always charge to their full capacity and assuming constant charging times. Finally, KLEIN et SCHIFFER, 2023 design an exact branch-and-price algorithm to solve the route and recharge scheduling problem, with flexible service operations (i.e. the departure time of each vehicle is a decision of the problem). To solve large instances involving up to 500 trips, the authors devise a heuristic version of their algorithm that is based on a graph reduction technique and a diving heuristic to quickly find good primal solutions. It is worth noting that, contrary to our case, all the papers discussed above define the problem over a single-day planning horizon. To the best of our knowledge, this research is the first to integrate the overnight charging scheduling and the block assignment problems over a planning horizon of multiple days.

Another common trait in the eVSP literature is the choice of a linear function to model the battery charging process. As the name suggests, under this modeling paradigm, the amount of energy that an EB retrieves from the grid is proportional to the time it spends charging. In reality, however, the relation between charged energy and charging time is logarithmic. MONTOYA et al., 2017 showed (on an electric vehicle routing problem) that disregarding the non-linear nature of the charging function may lead to solutions that are either infeasible in the field or overly conservative (i.e., expensive or resource-consuming). They also showed that modeling the charging function using a piecewise linear function instead of a linear one leads to a more accurate representation of the charging process, but also makes the underlying optimization problem considerably harder to solve. In this research, we build on their findings and use a piecewise linear function to model the charging process.

All the papers cited in the previous paragraphs consider a planning horizon of one day, while we are interested in a multiple-day horizon. Given the size of practical multi-day eVSPs, they are typically solved in two phases : in the first phase, a series of single-day eVSPs is first solved to devise vehicle blocks to cover on each day ; in the second phase, a MDEBAOSP is solved to assign EBs to these blocks and determine the overnight recharge schedule for each night. The first-phase eVSPs can be solved using one of the algorithms mentioned above. To the best of our knowledge, the second-phase MDEBAOSP that we study in this paper is new. It can be seen as similar to the eVSP if we consider that the blocks in the MDEBAOSP play the same role as the trips in the eVSP, except that the blocks may include recharging events and, therefore, the net energy consumed along them may be positive, negative or null. On the other hand, the recharge scheduling part in the MDEBAOSP is much more complex than in the eVSP because of the specific structure of the charging operations. In the eVSP, charging operations are scattered during the entire planning horizon. In the MDEBAOSP, they are concentrated in short time windows corresponding to each night spent at the depot. This structure makes the classical algorithms to solve eVSP not suited for the MDEBAOSP. Finally, classical eVSP algorithms do not consider battery degradation and non-linear charging function.

2.3 The multi-day electric bus assignment and overnight recharge scheduling problem

In the classical workflow of a transit operator, the MDEBAOSP (an operational problem) arises after solving an eVSP (a tactical problem) to produce a set of vehicle blocks for each day in the planning horizon. These blocks may or may not include scheduled en-route charging events. Formally, the MDEBAOSP can be described as follows. Let D be the set of days in the planning horizon (numbered from 1 to $|D|$). Let B_d, $d \in D$, be the set of blocks to be operated on day d and denote by $B = \bigcup_{d \in D} B_d$ the set of all blocks. Each block $i \in B$ is defined as a sequence of bus trips and, possibly, *charging events* that ensure that the EB will have enough energy to reach the next charger or the end of the block. A bus assigned to a block i starts and ends at a depot at time h_i^S and h_i^E, respectively. Given that the charging operations within each block are predefined, block i is also associated with a net energy consumption e_i (that can be positive, negative or null), a maximum net SoC increase e_i^{maxI}, and a maximum net SoC decrease e_i^{maxD}. Note that due to the out-of-depot charging events, the SoC of the EB assigned to a given block may, at some point, be greater than its initial SoC (i.e., the SoC when the EB leaves the depot). Therefore, parameter e_i^{maxI} can be used to avoid charging batteries that are already full. Similarly, parameter e_i^{maxD} ensures that the EB has no energy shortage along the block if it leaves the depot with a SoC of at least e_i^{maxD}. Figure 2.1 illustrates the intuition behind these two parameters with a vehicle block performing 3 trips.

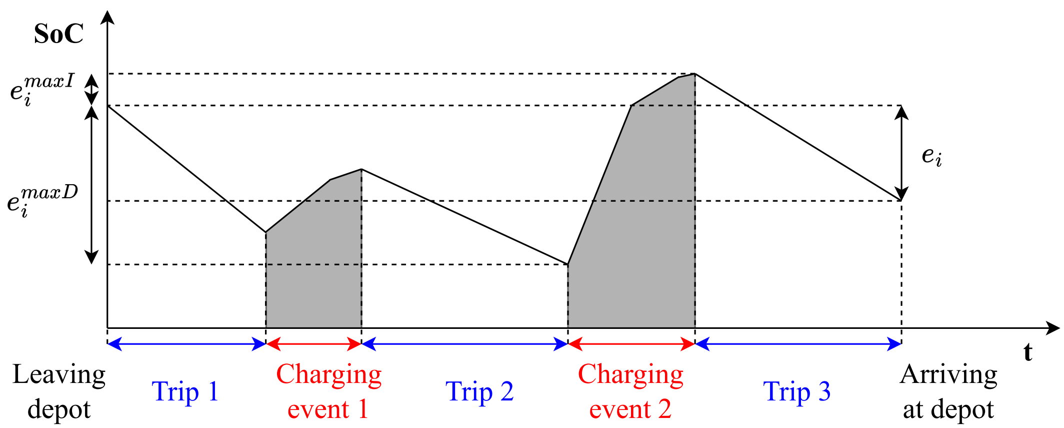

FIGURE 2.1 – Energy variation within a vehicle block i

To operate the vehicle blocks in B, the transit company uses a fleet V of identical EBs with a battery capacity of Q units. At the beginning of the horizon, EB $v \in V$ is available from time h_v^{init} with a SoC of SOC_v^{init}. Then, its SoC varies throughout the horizon according to the sequence of blocks it is assigned to and the overnight recharging operations it undergoes. At anytime, the SoC must remain between SOC^{min} and SOC^{max}. Each EB in V is assigned to at most one vehicle block per day. Given that the number of blocks to service might differ from one day to another and that the EB fleet may contain reserve EBs, some EBs may not be assigned to a block on some days. To deal with this case in our model, we create dummy blocks for each day that are added to keep the daily number of blocks constant and equal to the number of EBs. Each dummy block represents an idle

EB for a day, that has zero energy consumption, the latest possible starting time and the earliest ending time. These dummy blocks are part of the sets B_d, $d \in D$.

At the depot, there is a set C of identical chargers available to recharge (fully or partially) the EBs overnight. Therefore, at most $|C|$ EBs can recharge simultaneously. We assume that $|C| < |V|$ and that the overnight charging operations are not preemptive. The charging function f is a concave piecewise linear function that associates, for a given initial SoC, the amount of energy recharged with the charging time. We denote by P the set of linear pieces of f and associate with each piece p three values : (i) the total energy q_p that can be charged on piece p ; (ii) the time θ_p needed to charge the q_p units of energy (see Figure 2.2) ; and, (iii) the cost γ_p for charging the q_p units of energy. Note that $\sum_{p \in P} q_p$ is equal to the energy required to fully recharge a battery.

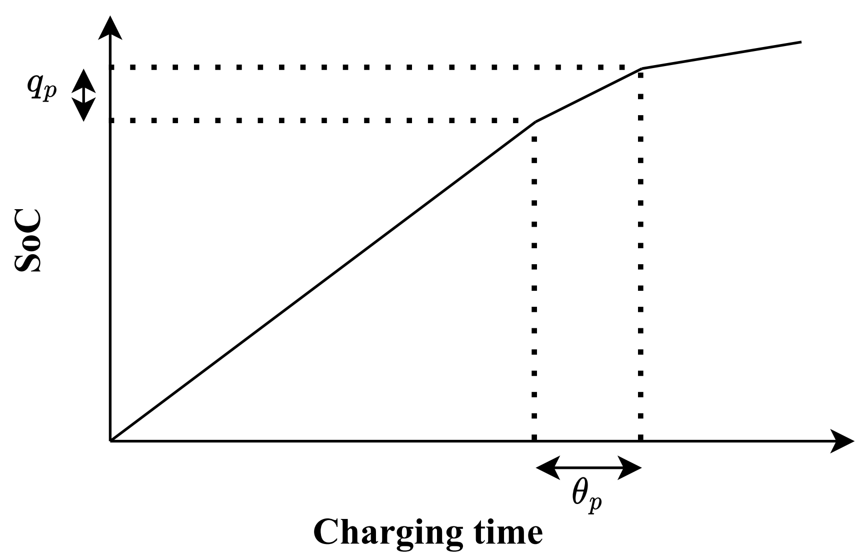

FIGURE 2.2 – Concave piecewise linear charging function f

As mentioned earlier, battery calendar aging can be improved by charging the EBs close to their departure time. The reason is that the battery degrades faster when it stores energy at high SoC levels (PELLETIER et al., 2018). To favor the generation of charging schedules that reduce calendar aging, we consider a unit *damage cost* of δ for every minute an EB spends at the depot between the end of a charging operation and the start time of its next vehicle block. Note that we do not consider cycle aging. The reasons are two-fold. First, the vehicle blocks, and their energy consumption, are given and unmodifiable. Second, the chargers are homogeneous and they deliver an invariable current rate. Therefore, in our setting, there is little room to optimize cycle aging ; but taking it into account would greatly increase the complexity of our models and methods.

The MDEBAOSP consists in assigning the EBs to the vehicle blocks and scheduling their overnight recharges such that each block is serviced by an EB, the EBs do not run out of energy, the number of available chargers is never exceeded, and the sum of the energy costs and damage costs is minimized. The notation used is summarized in Table 2.1, which also includes notation introduced in the next section.

2.4 Mixed integer programming formulation

In this section we introduce a two-commodity network flow MILP formulation for the MDEBAOSP. One commodity models the flow of the EBs through the vehicle blocks to determine the sequences of blocks assigned to the EBs over the planning horizon. The other commodity models, for each day, the flow of the chargers through the EB recharging operations to determine the recharge schedule of the EBs. The latter draws inspiration from the model proposed by FROGER et al., 2022 for an electric vehicle routing problem with capacitated charging stations.

The problem is defined on a directed graph $G = (N, A)$, where $N = B \cup \{c_d \mid d \in D\}$ is the node set and $A = A^{bus} \cup \left(\bigcup_{d \in D} A_d^{chg}\right)$ is the arc set. The EBs' flow on the subnetwork that comprises the block nodes B and the arcs in A^{bus}, represents the possible block successions for an EB. There exists an arc $(i, j) \in A^{bus}$ with $i \in B_d$ if and only if $d \neq |D|$, $j \in B_{d+1}$ and there is sufficient time between these two blocks to recharge the minimum energy to be able to perform both blocks consecutively. A feasible bus assignment solution corresponds to a set of $|V|$ disjoint paths, all starting from a node in B_1 and ending at a node in $B_{|D|}$.

To model the charger assignment on day $d \in D$, there is a subnetwork that contains the

TABLE 2.1 – Sets and parameters used in the model

Sets	
D	Set of days in the planning horizon
B	Set of vehicle blocks
B_d	Set of vehicle blocks on day d
V	Set of available EBs
C	Set of chargers
P	Set of linear pieces in the charging function
A	Set of arcs
A^{bus}	Subset of arcs for the bus assignment
A_d^{chg}	Subset of arcs for the overnight charger assignment before day d
N	Set of nodes
Parameters	
h_i^E	Ending time of vehicle block i
h_i^S	Starting time of vehicle block i
e_i	Net energy consumption along vehicle block i
e_i^{maxI}	Maximum net SoC increase along vehicle block i
e_i^{maxD}	Maximum net SoC decrease along vehicle block i
Q	Battery charging capacity
h_v^{init}	Initial available time of EB v
SOC_v^{init}	Initial SoC of EB v
SOC^{max}	Maximum SoC of the battery
SOC^{min}	Minimum SoC of the battery
f	Piecewise linear charging function
q_p	Maximum SoC difference on piece p
θ_p	Maximum charging time on piece p
γ_p	Maximum charging cost on piece p
δ	Unit damage cost spent at the depot after a charging operation
M	Large constant (time span of the planning horizon)
c_d	Charger node on day d

nodes in $B_d \cup \{c_d\}$ and the arcs in A_d^{chg}, representing the possible successions of charging operations as well as the first and last operations for each available charger. A charging operation is associated with a block in B_d and is performed on the EB to be assigned to this block. There is an arc $(i,j) \in A_d^{chg}$ if one of the following three sets of conditions is met : (i) $i = c_d$ and $j \in B_d$; (ii) $j = c_d$ and $i \in B_d$; and (iii) $i,j \in B_d$ and $i \neq j$. A feasible charger assignment for day d is obtained as a subset of at most $|C|$ circuits starting and ending at c_d and visiting exactly each node in B_d exactly once. In this case, we assume that each EB needs to be recharged every night but possibly for a duration of zero time units (which, in practice, corresponds to not recharging).

An example of a graph G defined for a MDEBAOSP instance with 3 days, 3 EBs, 3 vehicle blocks per day, and 2 chargers at the depot can be found in Figure 2.3. The set of paths made up of bold arcs represents a feasible solution where an EB is assigned to the sequence of blocks 1 – 4 – 8 (the orange EB), another to 2 – 6 – 7 (the green EB), and the last one to 3 – 5 – 9 (the yellow EB). During the night between days 1 and 2, one of the chargers recharges the orange EB, while the other one recharges the yellow and green EBs (in that order). The sequences of charging operations are then 4 and 5 – 6. During the night between days 2 and 3, the sequences of charging operations are 8, and 7 – 9. One of the chargers recharges the orange EB and the other the green and yellow EBs (in that order). It is worth noting that in this example, we assume that the three EBs are fully charged before Day 1 and, therefore, no charging operations are needed. Node c_1 and the arcs in A_1^{chg} have, thus, been omitted.

The decision variables of the proposed MILP are as follows :

— $x_{i,j}$: Binary variable equal to 1 if an EB covers block j immediately after block i and to 0 otherwise, $\forall (i, j) \in A^{bus}$.

— $y_{i,j}$: Nonnegative variable indicating the SoC of the EB after performing block i if $x_{i,j} = 1$ or set to 0 otherwise, $\forall (i, j) \in A^{bus}$.

— $\underline{q}_i$: Nonnegative variable indicating the SoC of the EB performing block i before its charging operation preceding block i, $\forall i \in B$.

— $\bar{q}_i$: Nonnegative variable indicating the SoC of the EB performing block i after its charging operation preceding block i, $\forall i \in B$.

— $\alpha_{i,v}$: Binary variable equal to 1 if EB j is assigned to block i on the first day and to 0 otherwise, $\forall i \in B_1, v \in V$.

— t_i : Nonnegative variable specifying the required charging time before performing block i, $\forall i \in B$.

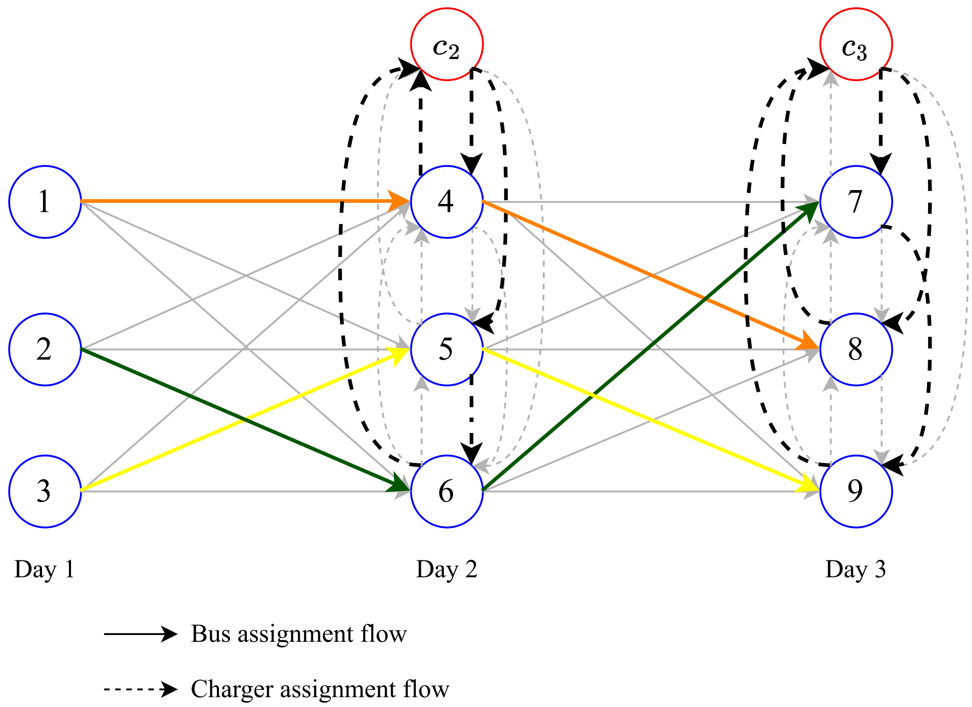

FIGURE 2.3 – Graph G representing the problem with block node set B in blue and charger node set C in red.

— a_i : Continuous variable indicating the recharge starting time before performing block i, $\forall i \in B$.

— Δ_i : Nonnegative variable indicating the waiting time between the end of the recharge and the start of block i, $\forall i \in B$.

— $\underline{\lambda}_i^p$ (resp. $\bar{\lambda}_i^p$) : Nonnegative variable indicating the fulfilled fraction of piece p of the SoC charging function when the EB performing block i arrives at (resp. leaves) the depot before (resp. after) performing block i, $\forall i \in B, p \in P$.

— $u_{i,j}$: Binary variable equal to 1 if a charger is used to charge the EB assigned to block j immediately after the EB assigned to block i and to 0 otherwise, $\forall d \in D, (i,j) \in A_d^{chg}$.

Figure 2.4 illustrates the relationships between variables and parameters associated with a block i and its preceding charging operation. If $x_{k,i} = 1$, then blocks k and i are assigned consecutively to the same EB. Block k ends at time h_k^E while block i starts at h_i^S

and ends at h_i^E. The charging operation between these two blocks starts at time a_i and lasts t_i units of time. The waiting time after the recharge is, thus, given by $\Delta_i = h_i^S - (a_i + t_i)$. From the energy point of view, variable $y_{k,i}$ indicates the SoC of the EB at the end of block k. This value is equal to the SoC $\underline{q}_i$ before starting the recharge. Then, variable $\bar{q}_i$ indicates the SoC after the recharge and depends on $\underline{q}_i$ and the recharging time t_i. Finally, e_i provides the net energy consumed when performing block i.

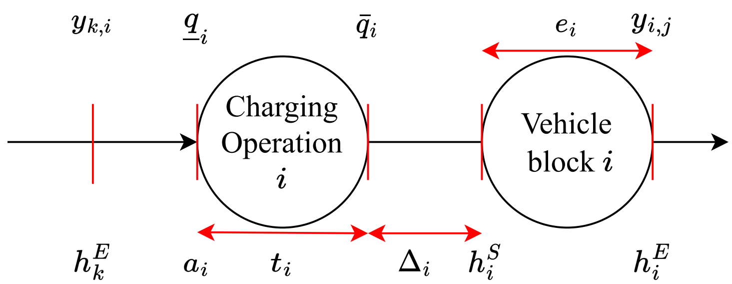

FIGURE 2.4 – Variables and parameters associated with block i and its preceding charging operation, performed after block k and before block j (energy-related variables/parameters on top; time-related ones at the bottom)

To improve readability, we introduce the proposed MILP in two steps. First, we present the model using the charging function f or, more precisely, its inverse f^{-1}, to englobe all charging decisions. Then, we discuss how to express this piecewise linear function using additional variables and constraints.

The objective function (2.1) of the MDEBAOSP minimizes the total charging costs and the calendar aging costs generated by the idle time between the end of the charging operations and the start of the blocks. Note that the $\bar{\lambda}_i^p$ and $\underline{\lambda}_i^p$ variables depend on the $\underline{q}_i$ and $\bar{q}_i$ variables and their relationship will be made explicit only in the second part of the model below.

$$\min \qquad \sum_{i \in B} \sum_{p \in P} \gamma_p (\bar{\lambda}_i^p - \underline{\lambda}_i^p) + \sum_{i \in B} \delta \Delta_i \tag{2.1}$$

This MILP includes four sets of constraints : the first set of constraints models the EB-to-block assignment; the second one tracks the SoC variations along the nodes of the network ; the third set computes the charging times and schedules the charging tasks ; and the last one models the piecewise linear charging function.

Constraints (2.2)–(2.3) ensure that each block has a successor (except those on the last day) and a predecessor (except those on the first day), creating a feasible bus assignment as a set of $|V|$ disjoint paths.

$$\sum_{j:(i,j)\in A^{bus}} x_{i,j} = 1, \qquad \forall i \in B \setminus B_{|D|} \tag{2.2}$$

$$\sum_{j:(j,i)\in A^{bus}} x_{j,i} = 1, \qquad \forall i \in B \setminus B_1 \tag{2.3}$$

Constraints (2.4) restrict variables $y_{i,j}$ to take a positive value only if there is an EB flow on arc (i,j). Constraints (2.5)–(2.6) compute the SoC between consecutive blocks. Constraints (2.7) initialize the SoC at the beginning of the time horizon. Constraints (2.8)–(2.9) assign each EB to a unique block on the first day. Constraints (2.10)–(2.11) stipulate that the SoC of the EB assigned to each block i must be within the feasible range.

$$y_{i,j} \leq SOC^{max}\, x_{i,j}, \qquad \forall (i,j) \in A^{bus} \tag{2.4}$$

$$\sum_{j:(i,j)\in A^{bus}} y_{i,j} = \bar{q}_i - e_i, \qquad \forall i \in B \setminus B_{|D|} \tag{2.5}$$

$$\underline{q}_i = \sum_{j:(j,i)\in A^{bus}} y_{j,i}, \qquad \forall i \in B \setminus B_1 \tag{2.6}$$

$$\underline{q}_i = \sum_{v\in V} \alpha_{i,v}\, SOC_v^{init}, \qquad \forall i \in B_1 \tag{2.7}$$

$$\sum_{v\in V} \alpha_{i,v} = 1, \qquad \forall i \in B_1 \tag{2.8}$$

$$\sum_{i\in B_1} \alpha_{i,v} = 1, \qquad \forall v \in V \tag{2.9}$$

$$\bar{q}_i \geq SOC^{min} + e_i^{maxD}, \qquad \forall i \in B \tag{2.10}$$

$$\bar{q}_i \leq SOC^{max} - e_i^{maxI}, \qquad \forall i \in B \tag{2.11}$$

Constraints (2.12) and (2.13) impose a lower bound on the starting time of the recharge before block i depending on its predecessor block or its initial available time, while constraints (2.14) allow to compute the waiting time after this recharge. Constraints (2.15) determine the time required to charge the EB assigned to block i from a SoC of $\underline{q}_i$ to a SoC of $\bar{q}_i$. These constraints are nonlinear and will be expressed differently below (see constraints (2.27)–(2.43)). Constraints (2.16)–(2.18) define the flow structure for the chargers on each day, while constraints (2.19) impose to schedule a charging task before each block on each day. Constraints (2.20) ensure that there is no overlap between two consecutive charging operations.

$$a_i \geq \sum_{j:(j,i)\in A^{bus}} x_{j,i}\, h_j^E, \qquad \forall i \in B \setminus B_1 \tag{2.12}$$

$$a_i \geq \sum_{v\in V} \alpha_{i,v}\, h_v^{init}, \qquad \forall i \in B_1 \tag{2.13}$$

$$a_i + t_i + \Delta_i = h_i^S, \qquad \forall i \in B \tag{2.14}$$

$$t_i = f^{-1}(\bar{q}_i) - f^{-1}(\underline{q}_i), \qquad \forall i \in B \tag{2.15}$$

$$\sum_{i\in B_d} u_{c_d,i} \leq |C|, \qquad \forall d \in D \tag{2.16}$$

$$\sum_{i\in B_d} u_{i,c_d} \leq |C|, \qquad \forall d \in D \tag{2.17}$$

$$\sum_{j\in B_d\cup\{c_d\}\setminus\{i\}} (u_{j,i} - u_{i,j}) = 0, \qquad \forall d \in D, i \in B_d \tag{2.18}$$

$$\sum_{j\in B_d\cup\{c_d\}\setminus\{i\}} u_{j,i} = 1, \qquad \forall d \in D, i \in B_d \tag{2.19}$$

$$a_i + t_i \leq a_j + M(1 - u_{i,j}), \qquad \forall d \in D, i, j \in B_d \tag{2.20}$$

Finally, constraints (2.21)-(2.26) define the domains of the decision variables.

$$x_{i,j} \in \{0,1\}, \qquad \forall (i,j) \in A^{bus} \tag{2.21}$$

$$y_{i,j} \geq 0, \qquad \forall (i,j) \in A^{bus} \tag{2.22}$$

$$\underline{q}_i, \bar{q}_i, t_i, \Delta_i \geq 0, \qquad \forall i \in B \tag{2.23}$$

$$0 \leq \underline{\lambda}_i^p, \bar{\lambda}_i^p \leq 1, \qquad \forall i \in B, p \in P \tag{2.24}$$

$$\alpha_{i,v} \in \{0,1\}, \qquad \forall i \in B_1, v \in V \tag{2.25}$$

$$u_{i,j} \in \{0,1\}, \qquad \forall d \in D, (i,j) \in A_d^{chg} \tag{2.26}$$

To model the piecewise linear charging function f, we introduce the following additional variables :

- $\underline{w}_i^p$ (resp. $\bar{w}_i^p$) : Binary variable equal to 1 if SoC $\underline{q}_i$ (resp. $\bar{q}_i$) is on piece p of the charging function f and to 0 otherwise, $\forall i \in B, p \in P$.
- $\underline{\theta}_i$ (resp. $\bar{\theta}_i$) : Nonnegative variable equal to $f^{-1}(\underline{q}_i)$ (resp. $f^{-1}(\bar{q}_i)$), $\forall i \in B$.

We also replace constraints (2.15) by the following constraints :

$$t_i = \bar{\theta}_i - \underline{\theta}_i, \qquad \forall i \in B \tag{2.27}$$

$$\sum_{p \in P} \underline{w}_i^p = 1, \qquad \forall i \in B \tag{2.28}$$

$$\underline{q}_i \geq \Big(\sum_{\substack{p' \in P: \\ p' < p}} q_{p'} \Big) \, \underline{w}_i^p, \qquad \forall i \in B, p \in P \tag{2.29}$$

$$\underline{q}_i \leq \Big(\sum_{\substack{p' \in P: \\ p' \leq p}} q_{p'} \Big) \, \underline{w}_i^p + (1 - \underline{w}_i^p) \, Q, \qquad \forall i \in B, p \in P \tag{2.30}$$

$$\underline{\lambda}_i^p \geq \sum_{\substack{p' \in P: \\ p' > p}} \underline{w}_i^{p'}, \qquad \forall i \in B, p \in P \tag{2.31}$$

$$\underline{\lambda}_i^p \leq 1 - \sum_{\substack{p' \in P: \\ p' < p}} \underline{w}_i^{p'}, \qquad \forall i \in B, p \in P \tag{2.32}$$

$$\underline{q}_i = \sum_{p \in P} q_p \, \underline{\lambda}_i^p, \qquad \forall i \in B \tag{2.33}$$

$$\underline{\theta}_i = \sum_{p \in P} \theta_p \, \underline{\lambda}_i^p, \qquad \forall i \in B \tag{2.34}$$

$$\sum_{p \in P} \bar{w}_i^p = 1, \qquad \forall i \in B \tag{2.35}$$

$$\bar{q}_i \geq \Big(\sum_{\substack{p' \in P: \\ p' < p}} q_{p'} \Big) \, \bar{w}_i^p, \qquad \forall i \in B, p \in P \tag{2.36}$$

$$\bar{q}_i \leq \Big(\sum_{\substack{p' \in P: \\ p' \leq p}} q_{p'} \Big) \, \bar{w}_i^p + (1 - \bar{w}_i^p) \, Q, \qquad \forall i \in B, p \in P \tag{2.37}$$

$$\bar{\lambda}_i^p \geq \sum_{\substack{p' \in P: \\ p' > p}} \bar{w}_i^{p'}, \qquad \forall i \in B, \; p \in P \tag{2.38}$$

$$\bar{\lambda}_i^p \leq 1 - \sum_{\substack{p' \in P: \\ p' < p}} \bar{w}_i^{p'}, \qquad \forall i \in B, p \in P \tag{2.39}$$

$$\bar{q}_i = \sum_{p \in P} q_p \, \bar{\lambda}_i^p, \qquad \forall i \in B \tag{2.40}$$

$$\bar{\theta}_i = \sum_{p \in P} \theta_p \, \bar{\lambda}_i^p, \qquad \forall i \in B \tag{2.41}$$

$$\underline{\theta}_i, \bar{\theta}_i \geq 0, \qquad \forall i \in B \tag{2.42}$$

$$\underline{w}_i^p, \bar{w}_i^p \in \{0,1\}, \qquad \forall i \in B, p \in P. \tag{2.43}$$

Constraints (2.27) are equivalent to constraints (2.15) but expressed linearly using the $\underline{\theta}_i$ and $\bar{\theta}_i$ variables. For each block $i \in B$, constraints (2.28)–(2.34) are dedicated to the computation of $\underline{\theta}_i$ as a function of $\underline{q}_i$. Indeed, constraints (2.28) impose that a single piece be selected, whereas constraints (2.29)–(2.30) ensure that $\underline{q}_i$ is part of this piece. Constraints (2.31) and (2.32) set the fulfilled fraction of a piece equal to 1 if it is before the selected piece and to 0 if it is after, respectively. Constraints (2.33) allow to compute the value of $\underline{\lambda}_i^p$ for the selected piece p given the other $\underline{\lambda}_i^{p'}$ values. Ultimately, the value of $\underline{\theta}_i$ is obtained through constraints (2.34) as a function of the $\underline{\lambda}_i^p$ variables. Constraints (2.35)–(2.41) play a similar role but they are used to compute for each block $i \in B$ the value of $\bar{\theta}_i$ in function of $\bar{q}_i$. Finally, the domains of the new variables are restricted by constraints (2.42)–(2.43).

In the following, we refer to the MILP (2.1)–(2.14), (2.16)–(2.43) as the MDEBAOSP-MILP.

2.5 Solution algorithms

The MDEBAOSP-MILP can be solved using the branch-and-cut algorithm embedded in commercial MILP solvers (see Section 2.6 for details). However, our computational results indicate that it is difficult to solve instances with a tight recharge scheduling sub-problem, i.e., instances in which the number of chargers is much lower than the number of EBs. In order to solve such instances more efficiently, we propose three matheuristics that are presented in this section.

2.5.1 Assign-then-schedule heuristic

Our tests revealed that, when solving the MDEBAOSP-MILP, the branching is mainly done on the $u_{i,j}$ variables that are responsible for the scheduling of the charging operations. In fact, minimizing the calendar aging costs is what makes the problem difficult to solve as omitting this criterion yields a large number of feasible charging schedules with the same cost. From this observation, we propose a first matheuristic that decomposes the problem into two subproblems that are solved sequentially : assigning first the EBs to the blocks, then scheduling the charging operations. Algorithm 2 provides a high-level description of the proposed Assign-then-Schedule (AtS) heuristic. In the first line the algorithm solves EB-to-block assignment problem over the whole planning horizon, minimizing only the charging costs, i.e., setting $\delta = 0$ in the MDEBSP-MILP and solving it by a MILP solver. In Line 2, we record the EB-to-block assignment and the charging operations prescribed in this solution. Each charging operation is associated with a duration and a pair of release and due times given by the EB assignment and the start and end times of the vehicle blocks. Then, assuming that the recharge scheduling problem becomes separable per day once the EB assignment and the charging operation durations are known, we solve for each day its corresponding recharge scheduling problem Line 3). This problem aims at scheduling the charging operations while minimizing the calendar aging costs. To do so, we first enumerate feasible individual charger schedules (Line 4), before formulating the problem as a set partitioning model and solving it with a MILP solver (Line 5). We discuss this model below.

The proposed set partitioning approach assumes that it is possible to enumerate all possible individual charger schedules. The latter is defined as a sequence of charging operations, and their starting times, that can be feasibly performed by a single charger. It is worth noting that in practice, fully enumerating the charging schedules is doable. Indeed, charging operations are relatively long (with respect to the length of the overnight period) and therefore each charger only performs a few charging operations per night. For day $d \in D$, denote by T_d the set of charging operations to accomplish before the start of the blocks in B_d. We include in this set only the *real* charging operations, i.e., we exclude those with a zero duration. Let H_d^R, H_d^D, and U_d be the earliest release time, the latest due time, and the minimum duration of the charging operations in T_d, respectively. Then, an upper bound on the maximum number of charging operations that a charger can process on the night preceding day d is given by : $k_d = \lfloor (H_d^D - H_d^R)/U_d \rfloor$.

Algorithme 2 : Assign-then-Schedule (AtS) heuristic

1 Solve the MDEBAOSP, minimizing only the total charging costs;
2 From the computed solution, save the EB-to-block assignment and the charging operations;
3 **foreach** *day* $d \in D$ **do**
4   Generate non-dominated feasible charger schedules compatible with the saved EB-to-block assignment and containing up to k_d charging operations to accomplish before the blocks in B_d;
5   Solve a set partitioning problem to find an optimal subset of charger schedules;
6 **end**

In Line 4, the individual charger schedules are generated by enumerating all subsets of charging operations containing at most k_d elements. For each subset, all possible permutations (sequences) of its operations are considered. For a given sequence s, a schedule is established by scheduling each operation as late as possible (to minimize the calendar aging costs) in reverse order, i.e., from the last to the first. More precisely, let $i_1, i_2, \ldots, i_n$ be a sequence of n charging operations ($n \leq k_d$), where the release time, the due time, and the duration of operation i are denoted as h_i^R, h_i^D and t_i, respectively. Then, the starting times a_{i_j}, $j = 1, \ldots, n$, of the operations are computed with the following backward recursion :

$$a_{i_n} = h_{i_n}^D - t_{i_n} \tag{2.44}$$

$$a_{i_j} = \min \{h_{i_j}^D, a_{i_{j+1}}\} - t_{i_j}, \qquad j = n-1, n-2, \ldots, 1. \tag{2.45}$$

This charger schedule is feasible if and only if $a_{i_j} \geq h_{i_j}^R$ for all $j \in \{1, 2, \ldots, n\}$. The (calendar aging) cost ℓ_s of this schedule s is given by :

$$\ell_s = \delta \sum_{j=1}^{n} [h_{i_j}^D - (a_{i_j} + t_{i_j})]. \tag{2.46}$$

Among all feasible permutations of a subset of charging operations, we keep a single one, namely, the one with the lowest cost. The others are dominated and can, thus, be discarded. An extensive pseudocode of the generation of the non-dominated feasible charger schedules is given in Appendix, Section 3.6.

The set of all non-dominated feasible charger schedules is denoted as S_d. For each schedule $s \in S_d$ and operation $i \in T_d$, we define a binary parameter r_{si} that takes value 1 if schedule s contains operation i and 0 otherwise. Furthermore, we associate a binary variable v_s with each schedule $s \in S_d$ to indicate if charger schedule s is selected or not for the recharging schedule on day d. The set partitioning model with a side constraint solved in Line 5 of Algorithm 2 is as follows :

$$\min \quad \sum_{s \in S_d} \ell_s v_s \tag{2.47}$$

subject to :

$$\sum_{s \in S_d} r_{si} v_s = 1, \qquad \forall i \in T_d \tag{2.48}$$

$$\sum_{s \in S_d} v_s \leq |C|, \tag{2.49}$$

$$v_s \in \{0,1\}, \qquad \forall s \in S_d. \tag{2.50}$$

The objective function (2.47) aims at minimizing the total calendar aging costs. The set partitioning constraints (2.48) impose that each charging operation in T_d is scheduled in one of the selected charger schedules, while constraint (2.49) ensures that the available number of chargers is not exceeded.

When the value of k_d is small, model (2.47)–(2.50) is relatively easy to solve using a commercial MILP solver. Finally, note that the charging schedule obtained for each day in the solution computed in Line 1 of Algorithm 2 provides an upper bound on the optimal value of model (2.47)–(2.50) that can be exploited by the solver.

2.5.2 Daily-assign-then-schedule heuristic

As previously mentioned, the MDEBAOSP combines two subproblems : an assignment problem of EBs to vehicle blocks and a recharge scheduling problem. Once the assignment of EBs to blocks is determined, the total quantity of energy to recharge on each EB is fixed, which makes the recharge scheduling problem simpler to solve. From this observation, we propose a second matheuristic which adds to the AtS heuristic a preliminary phase that identifies successions of blocks to be operated by the same EB. This new heuristic is called the Daily-Assign-then-Schedule (D-AtS) heuristic as it computes these block-to-block assignments one day at a time. The D-AtS heuristic is described in Algorithm 3. It consists of three main phases. The first phase (Lines 1–4) consists in solving an assignment problem for each day d in D except the first one. It computes for each block in B_{d-1} a successor block in B_d, i.e., it determines the values of the $x_{i,j}$ variables. This assignment problem is discussed in the next paragraph. Given these fixed $x_{i,j}$ variables, the second phase (Lines 5–6) assigns an EB to each sequence of blocks and finds the amount of energy to charge in each EB every night seeking to minimize the total charging costs, omitting the calendar aging costs ($\delta = 0$). Similar to AtS, in the last phase (Lines 7–10), D-AtSschedules the charging operations in order to minimize the calendar aging costs, taking into account the decisions fixed in the previous phases.

For each day $d \in D \setminus \{1\}$, the goal of the assignment problem solved in Line 2 of Algorithm 3 is to find a successor block in B_d for each block in B_{d-1} in such a way that i) the minimum energy required to operate all blocks in $B_{d-1} \cup B_d$ is minimized, and ii) the time available at the depot to carry the charging operations is maximized. This assignment problem is defined as follows. Consider a bipartite directed graph where the node set is given by $B_{d-1} \cup B_d$. The arc set, denoted $\tilde{A}_d$, contains an arc (i, j) with $i \in B_{d-1}$ and $j \in B_d$ if and only if the same EB can be assigned to both blocks i and j, i.e., if

$$h_j^S - h_i^E \geq max\{0, f^{-1}(SOC^{min} + e_j^{maxD}) - f^{-1}(SOC^{max} - e_i)\}. \tag{2.51}$$

In this expression, $SOC^{min} + e_j^{maxD}$ and $SOC^{max} - e_i$ indicate the minimum SoC of an EB at the start of block j and the maximum SoC at the end of block i, respectively. Therefore, if

Algorithme 3 : Daily-Assign-then-Schedule (D-AtS) heuristic

foreach *day* $d \in D \setminus \{1\}$ **do**
  Solve an assignment problem to match the vehicle blocks of day $d-1$ with those of day d;
  From the computed solution, save the block-to-block assignment (the $x_{i,j}$ variable values);
end
Solve the MDEBAOSP with fixed $x_{i,j}$ variables, minimizing only the total charging costs;
From the computed solution, save the EB-to-block assignment and the charging operations;
foreach *day* $d \in D$ **do**
  Generate non-dominated feasible charger schedules compatible with the saved EB-to-block assignment containing up to k_d charging operations to accomplish before the blocks in B_d;
  Solve a set partitioning problem to find an optimal subset of charger schedules;
end

$SOC^{min} + e_j^{maxD} > SOC^{max} - e_i$, then $f^{-1}(SOC^{min} + e_j^{maxD}) - f^{-1}(SOC^{max} - e_i)$ provides the minimum charging time between these two blocks. Hence, condition (2.51) ensures that block i ends before the start of block j and that there is sufficient time between these two blocks to recharge the minimum required energy. For each arc $(i,j) \in \tilde{A}_d$, we associate a cost c_{ij} that is defined as follows :

$$c_{i,j} = \begin{cases} \frac{(SOC^{min}+e_j^{maxD})-(SOC^{max}-e_i)}{h_j^S - h_i^E} & \text{if } (SOC^{min} + e_j^{maxD}) - (SOC^{max} - e_i) > 0 \\ 0 & \text{otherwise.} \end{cases} \tag{2.52}$$

Thus, this cost structure favors matching pairs of blocks that induce a small minimum amount of energy to recharge and a larger recharge time window availability.

Let us define a binary variable $z_{i,j}$ for each arc $(i,j) \in \tilde{A}_d$ that takes value 1 if block i is matched with block j. The assignment problem can be formulated as follows :

$$\min \sum_{(i,j)\in\tilde{A}_d} c_{i,j} z_{i,j} \tag{2.53}$$

subject to :

$$\sum_{i:(i,j)\in\tilde{A}_d} z_{i,j} = 1, \qquad \forall j \in B_d \tag{2.54}$$

$$\sum_{j:(i,j)\in\tilde{A}_d} z_{i,j} = 1, \qquad \forall i \in B_{d-1} \tag{2.55}$$

$$z_{i,j} \in \{0,1\}, \qquad \forall (i,j) \in \tilde{A}_d. \tag{2.56}$$

The objective function (2.53) minimizes the sum of the costs of the selected arcs. Constraints (2.54) and (2.55) ensure that each block in B_d is matched with a unique block in B_{d-1} and vice-versa. It is well known that this problem can be solved in polynomial time using, for instance, the Hungarian algorithm (KUHN, 1955).

In practice, bus trip timetables often repeat every weekday during a season (or even throughout the year). In this case, the vehicle blocks can also be identical every day. Therefore, the same assignment problem may arise for multiple pairs of consecutive days in the planning horizon and only one of them needs to be solved. The computed solution will then be repeated for each identical pair of days, yielding consistent block-to-block assignment on multiple consecutive days. This consistency is often appreciated by transit companies as it eases the overnight operations at the depot. One can note that the block-to-block assignment computed in Line 2 could yield an infeasible MDEBAOSP at Line 5 due to the lack of long-term vision. A smart mechanism to "repair" the solution would be to add standby EBs in the set B_d, represented by dummy blocks that has zero energy consumption, the latest possible starting time and the earliest ending time. The heuristic would need to be adapted accordingly in order to manage those EBs. Transport companies usually have such buses in case of breakdown or maintenance on one of their working buses so this approach is realistic.

To conclude this section, we propose a speedup technique that can be applied in the D-AtS heuristic. At the end of the first phase, when the successions between the blocks are known, we can set the values of some of the $\underline{w}_j^p$ variables. Note that $SOC^{min} + e_i^{maxD} - e_i$ is a lower bound on the SoC of the EB that performs block $i \in B_d$, $d \in D \setminus \{|D|\}$, if we assume that it began this block with a minimal SoC of $SOC^{min} + e_i^{maxD}$. Then, if block $j \in B_{d+1}$ is the chosen successor of block i (i.e., $x_{i,j} = 1$), the variables $\underline{w}_j^p$ for $p \in P$ such that $\sum_{p' \leq p} q_{p'} < SOC^{min} + e_i^{maxD} - e_i$ can be set to 0 in the model solved in Line 5 of Algorithm 3.

2.5.3 Short-sighted heuristic

The assignment of diesel buses to blocks is traditionally done on a daily basis, because the buses can be fully refueled overnight and, thus, considered equivalent. This practice is still in place in many transit companies that have already started integrating EBs into their fleets. Consequently, decisions on EB assignments and charging times are made every night to fulfill the needs of the blocks to be operated on the next day only. In this section, we introduce another matheuristic, called the short-sighted heuristic (or simply SS), replicating this decision process. The main motivation to develop this heuristic is to have a tool to evaluate the benefits of considering a multi-day planning horizon. Algorithm 4 presents the main steps of this third heuristic. For each day $d \in D$, SS solves (see Line 2) a single-day problem that assigns the EBs to the blocks in B_d and determines the charging time of each EB during the night between $d-1$ and d. This problem is described below. It is worth mentioning that, more often than not, the rules currently applied by transit companies to schedule EB overnight charging totally disregard calendar aging costs. To establish a fair comparison between SS, AtS, and D-AtS on that criterion, Lines 4–5 schedule the fixed-time charging operations prior to day d as described in Section 2.5.1. Once the block assignment and charging scheduling problems for day d are solved, SS uses the solution (see Line 7) to set the initial conditions for the next day, that is, the time at which each EB becomes available and the SoC of each EB at the beginning of the d-to-$d+1$ night. This initialization procedure is also discussed below.

The single-day problem solved in Line 2 corresponds to the MDEBAOSP tackled in Line 1 of the AtS heuristic (Algorithm 2), but restricted to a single day d (still with $\delta = 0$). We model it using the following restricted version of MDEBSP-MILP (2.1)–(2.14), (2.16)–(2.43). First, all $x_{i,j}$ and $y_{i,j}$ variables and their related constraints (2.2)–(2.6), (2.12), and (2.21)–(2.22) are discarded because this problem focuses on a single

Algorithme 4 : Short-sighted heuristic

1 **foreach** *day* $d \in D$ **do**
2 Solve a single-day EB assignment and overnight recharge scheduling problem for blocks in B_d;
3 From the computed solution, save the EB-to-block assignment and the charging operations;
4 Generate non-dominated feasible charger schedules compatible with the saved EB-to-block assignment containing up to k_d charging operations to accomplish before the blocks in B_d;
5 Solve a set partitioning problem to find an optimal subset of charger schedules;
6 **if** $d < |D|$ **then**
7 Set the initial conditions for day $d+1$;
8 **end**
9 **end**

day. Second, all sets B_1 and B are replaced by B_d and $d \in D$ can be removed as d is the single day to consider. Third, we change the notation of the parameters SOC_v^{init} and h_v^{init} to $SOC_v^{init,d}$ and $h_v^{init,d}$ to highlight that their values vary with day d. The rest of the model remains unchanged. Hence, the problem defined for each day $d \in D$ requires initial conditions for each EB $v \in V$, namely, their initial available time $h_v^{init,d}$ and SoC $SOC_v^{init,d}$. When $d = 1$, these values are provided by the input to the whole problem, i.e., $h_v^{init,d} = h_v^{init}$ and $SOC_v^{init,d} = SOC_v^{init}$ for all $v \in V$. When $d > 1$, they are collected from the solution of the previous iteration in Line 7. More precisely, for EB $v \in V$, if it was assigned to block $i \in B_{d-1}$ in this solution ($\alpha_{i,v} = 1$), then we set $h_v^{init,d} = h_i^E$ and $SOC_v^{init,d} = \bar{q}_i - e_i$ (where $\bar{q}_i$ is also taken from this solution).

Two variants are proposed regarding the design of the charging operations in the short-sighted heuristic. The first is the one described, where we look to minimize the total charging costs in Line 2. This variant is called the Minimum Short-Sighted (Min-SS). In the second variant, the EBs are charged until their battery is full, they have to leave the depot or they have to let another EB recharged. This is translated into a maximization of the total charging costs and yields a variant called the Maximum Short-Sighted (Max-SS) heuristic. This second variant replicates another widely-applied industrial practice :

charge every EB as much as possible every night as it is traditionally done with diesel buses.

2.6 Computational experiments

We implemented the proposed algorithms in C++. Our implementation uses IBM ILOG CPLEX 20.1 to solve the MILPs with a default optimality gap tolerance of 0.001%. To assess the performance of the proposed solution methods, we conducted computational experiments on instances built based on real operational data provided by our industrial partner, GIRO Inc., one of the world-leading optimization software providers for public transit companies. All computations were performed on a 64-bit computer equipped with an Intel Gold 6148 Skylake CPU (2.40 GHz), 10 gigabytes of main memory, running on CentOS Linux 7. In the remainder of this section, we first describe the instances and then we report and discuss our results and findings. All gaps reported in the results are computed as the relative difference between a reference value and an observed value using the following expression $gap = \frac{obs-ref}{ref}$.

2.6.1 Instance generation

GIRO Inc. provided us with two real-world instances coming from two European public transit operators. The first operates 43 vehicle blocks and the second 54. Both companies repeat the blocks every weekday. For each block, we received the starting time, the ending time, the net energy consumption, and the sequence of trips and out-of-depot charging events making up the block. The latter are especially relevant since they allow us to compute the e_i^{maxI} and e_i^{maxD} parameters for each block i. In both instances, there is one EB per block and the fleet is homogeneous. Therefore, we did not need to add dummy blocks to these two instances. The EBs have a battery with capacity of $Q = 363$ kWh and their SoC must remain between $SOC^{min} = 10\%$ and $SOC^{max} = 100\%$. Both instances have a nearly 1-to-1 charger-to-block ratio. Indeed, there are 42 and 52 chargers, in the first and second instances, respectively. In all our experiments we assumed that the EBs start the planning horizon with a full battery ($SOC_v^{init} = SOC^{max} - max_{i \in B_1}(e_i^{maxI})$) and that they are all available at the beginning of the planning horizon ($h_v^{init} = 0$).

We used the GIRO data to build three sets of instances. The first set referred to as *real-world set*, is made up of 4 (= 2 $\times$ 2) instances : a 3-day and a 5-day version of each of the two original instances. To name our instances, we use the following convention *B_D_C*, where *B* is the number of blocks, *D* is the number of days in the planning horizon, and *C* is the number of chargers. As it stands, the 4 instances in the real-world set are named 43_3_42, 43_5_42, 54_3_52, and 54_5_52, respectively.

To build the second and third datasets, we merged the 43 and 54 blocks from the original instances into a single set $\mathscr{S}$ that we randomly sampled to create new instances. The first new set, called *block variation set*, is made up of 160 (= 8 $\times$ 2 $\times$ 10) instances with 20, 30, 40, 50, 60, 70, 80, or 90 blocks and 3 or 5 days in the planning horizon. For each combination of a number of blocks and a number of days, we generated 10 instances. To make instances that are harder to solve and to reflect the near future in which the number of EBs in the fleets is expected to be significantly larger than the number of chargers available at the depots, we set the charger-to-block ratio to 0.5. In other words, instances in this set have 1 charger for every 2 blocks.

The third set of instances, called *charger variation set*, was built to illustrate how our algorithms can serve as a *what if* scenario analysis tool to assist operators in finding the critical number of chargers for their operations (i.e., reducing their charging infrastructure investments). This set contains 100 instances (= 2 $\times$ 5 $\times$ 10) with 60 blocks and 3 or 5 days in the planning horizon. In these instances, the number of chargers equals 20, 25, 35, 40, or 45. For each combination of a number of days and a number of chargers, we generated 10 instances. Note that the block variation set already contains instances belonging to the 60_3_30 and 60_5_30 families. Therefore, we do not need to generate them for this set. To facilitate the readability and interpretability of the results, we included the results obtained on the 60_3_30 and 60_5_30 families in the results for both sets.

As mentioned earlier, transit companies seldom consider calendar aging costs when planning their overnight charging operations. Therefore, our partner did not have data to share on this parameter. To complete our instances, we computed the calendar aging cost coefficient δ using the battery degradation cost function introduced in HOKE et al., 2014. In their function, the degradation cost is computed as a function of the battery purchase costs and the lifetime degradation resulting from the battery's charge profile. The latter is computed as a relative gap between i) the lifespan resulting from always charging the battery using the ideal charging profile (i.e., nominal lifespan) and ii) the lifespan resulting from charging the battery with a given charging profile in every charging cycle until the end of the battery's life (i.e., observed lifespan). For the sake of brevity, we defer the discussion on how we established the nominal and observed lifespans of the EBs in our instances to Appendix, Section 3.6. Considering a battery price to be USD 150,000 we obtained a calendar aging cost δ of USD 0.05 per minute. We also discuss the detail of our cost estimation in Appendix, Section 3.6.

Another parameter that GIRO did not share with us was the EBs' battery charging function f. This function is difficult to establish in close form because it depends on many different and (sometimes) difficult-to-measure factors (e.g., the power used, the degradation state of the battery, and the room temperature). For this reason, EB operators are rarely aware of the exact charging function of their vehicles and rely on approximations when planning their recharging operations. In our instances, we use the piecewise linear approximation introduced in MONTOYA et al., 2017. In particular, we use their charging function for a slow charger scaled up to match the average charging rate of the two operators' charging infrastructure provided by the industrial partner. Finally, we used the average energy cost reported in PELLETIER et al., 2018 as our charging cost γ_p.

2.6.2 Results with the MILP

In the first set of experiments we solved the 264 instances (= 4 + 160 + 100) using the MILP introduced in Section 2.4 running on CPLEX for 5 hours. Out of the 264 instances, the solver found optimal solutions for 27 instances, and feasible-but-unproven solutions for 184, and could not find a feasible solution to the remaining 53. Table 2.2 summarizes the results. The first column indicates the instance family ; the second column reports the number of feasible solutions found for each family ; the third column reports the number of optimal solutions found for each family ; the fourth column shows the average gap on the objective function between the best integer solution and the best lower bound computed by CPLEX ; the fifth column reports the average computational time ; the sixth column shows the average total charging cost ; and the seventh column shows the average total calendar aging cost. Note that the last line of the table indicates the total or average value for each column, with instance families 60_3_30 and 60_5_30 recorded only once because they belong in both block variation set and charger variation set.

As the top of this table shows, CPLEX solved the 4 real-world instances to optimality in a short computational time (20 s on average). These results are explained by the large charger-to-block ratio in these instances. Indeed, under this scenario, the scheduling subproblem becomes trivial, so the MDEBAOSP practically reduces to an EB-to-block assignment problem.

The results on the block variation set paint a different picture. Recall that in these instances, the number of blocks gradually increases while the charger-to-block ratio remains constant. CPLEX was unable to prove optimality on any of the 187 instances in the set. On the other hand, the gap is relatively low, ranging from an average of 1.49% in the 20_3_10 family to 1.91% in the 90_5_45 family. The results show that the gap remains relatively stable in instances with a 3-day planning horizon, while it increases with the number of blocks in instances with a 5-day horizon. Moreover, in the latter instance type, CPLEX faces more difficulties delivering feasible solutions (e.g., only 2 out of 10 in the 90_5_45 family). These results are plausibly explained by the much larger number of scheduling-related variables. Note (from Columns 6 and 7) that the charging costs largely dominate the calendar aging costs. Note also that the charging costs are largely driven by the (predetermined) net energy consumption of the blocks. Therefore, CPLEX is capable of establishing, very quickly, a high-quality lower bound for this component of the cost. On the contrary, the calendar aging costs depend only on the scheduling decisions. Hence, when there is a large number of scheduling-related variables, the linear relaxation is weaker and so the solver has trouble deriving good lower bounds for the calendar aging cost component. This observation also sheds some light on the extra complexity that results from considering the calendar aging criterion in the MDEBAOSP.

Finally, the results on the charging variation set confirm that the difficulty of the instances decreases with the number of chargers. CPLEX moves from finding no feasible solution on the 60_3_20 family to finding a feasible solution with a small gap of (on avg.) 0.01% to all 10 instances in the 60_5_45 family. It is worth noting that the solutions to all instances with a 3-day planning horizon and the solutions to all instances with a 5-day horizon have the same charging costs (7126 $ and 14904 $, respectively). Therefore, the difference in the gaps comes exclusively from the calendar aging costs. These results suggest that companies that do not focus on preserving the batteries of their EBs could drastically reduce their charging infrastructure investments by implementing tools such as our MILP to plan their charging operations. For example, a close comparison of the results obtained for the 60_5_45 and 60_5_35 instances shows that CPLEX was able to deliver solutions with the same charging costs using 20% fewer chargers.

In conclusion the MILP can efficiently solve the real-world instances. It is worth recalling that these instances reflect today's business scenario, where many operators own (and can use) one charger per vehicle. However, this scenario is rapidly (and unfavorably) evolving as operators keep adding EBs to their fleets. The data show that when the charger-to-block ratio tightens, the MILP starts to struggle. This is specially true when the number of blocks and days approach industrial-scale values (60 and 5 respectively). In the near future (i.e., when the EBs in the fleet will largely outnumber the chargers) heuristics that can scale better will be valuable to practitioners.

TABLE 2.2 – Computational results - MILP running on CPLEX for 5 hours

Instance family	# Feasible solutions	# Optimal solutions	Gap w.r.t. LB (%)	Computational time (s)	Charging costs ($)	Cal. aging costs ($)
43_3_42	1	1	0.00	3	4520	0.00
54_3_52	1	1	0.00	14	6866	0.04
43_5_42	1	1	0.00	8	9490	0.00
54_5_52	1	1	0.01	54	14355	0.97
20_3_10	10	0	1.49	18000	2379	37.51
30_3_15	10	0	1.54	18000	3568	56.23
40_3_20	10	0	1.75	18000	4788	85.45
50_3_25	10	0	1.70	18000	5954	103.19
60_3_30	10	0	1.65	18000	7126	119.23
70_3_35	10	0	1.61	18000	8282	135.19
80_3_40	10	0	1.60	18000	9453	153.32
90_3_45	10	0	1.64	18000	10630	177.56
20_5_10	10	0	1.64	18000	4984	84.35
30_5_15	10	0	1.67	18000	7465	127.76
40_5_20	10	0	1.85	18000	10014	188.72
50_5_25	9	0	1.76	18000	12479	223.82
60_5_30	8	0	1.79	18000	14903	271.58
70_5_35	7	0	1.87	18000	17406	332.12
80_5_40	4	0	1.84	18000	19797	370.78
90_5_45	2	0	1.91	18000	22225	432.08
60_3_20	0	0	–	–	–	–
60_3_25	7	0	2.81	18000	7152	206.90
60_3_35	10	0	0.81	18000	7126	58.41
60_3_40	10	3	0.16	17820	7126	11.17
60_3_45	10	10	0.01	1065	7126	0.61
60_5_20	0	0	–	–	–	–
60_5_25	0	0	–	–	–	–
60_5_35	10	0	0.94	18000	14904	141.45
60_5_40	10	0	0.29	18000	14904	43.46
60_5_45	10	10	0.01	12302	14904	1.72
Total / Average	211	27	1.32	16663	9335	121.15

2.6.3 Results with the assign-then-schedule and daily-assign-then-schedule heuristics

In the second set of experiments, we solved the 264 instances using the AtS heuristic introduced in Section 2.5.1. In these experiments, we set the maximum execution time for each phase of the heuristic (i.e., EB-to-block assignment & charging and Scheduling) to 1 hour. It is worth noting that the scheduling phase runs in parallel since the problem can be decomposed by day. The method found feasible solutions for 216 of the 264 instances in the testbed, and could not find a feasible solution for the remaining 48. Table 2.3 summarizes the results. The first column indicates the instance family; the second column reports the number of feasible solutions found for each family; the third column shows the average gap in the objective function with respect to the solutions delivered by the MILP; the fourth column reports the average computational time; the fifth column shows the average absolute and relative gaps for the total charging cost with respect to the MILP solutions; and the sixth column shows the average absolute and relative gaps for the total calendar aging cost with respect to the MILP solutions. Note that we do not compute the gaps when the MILP or AtS did not find a feasible solution for an instance.

As these results show, AtS solves more instances than the MILP and it is much faster. However, a close examination of the data reported in the third column shows that the MILP consistently delivers better solutions. Even if AtS found optimal solutions to the 4 real-world instances, in the remaining families the average gap with respect to the MILP solutions was 0.82% with a maximum of 1.12% on the 20_5_10 family. A plausible explanation for this behavior is that AtS lacks a mechanism to reconsider decisions made during the first phase. Once the EB-to-block and the duration of each charging operation have been decided, the scheduling problem to solve in the second phase becomes over-constrained. As it stands, it may be impossible for the method to retrieve a charging schedule leading to the optimal calendar aging cost. A quick look at the data in the fifth and sixth columns seems to confirm this intuition. As the table shows, the whole gap with respect to the MILP solutions is due to the calendar aging costs. In other words, the heuristic is capable of finding (during the first phase) a set of EB-to-block assignments and charging decisions leading to a total energy cost that matches that of the MILP solutions, but the resulting scheduling problem (even if solved to optimality) cannot lead to global solutions that also match the calendar aging costs.

In the third set of experiments we solved the 264 instances using the D-AtS heuristic introduced in Section 2.5.2. On these experiments, we did not set a time limit for the EB-to-block assignment phase. On the other hand, we set a 1-hour time limit on both the charging and scheduling phases. Similar to the AtS experiments, the scheduling phase was run in parallel taking advantage of the natural day-by-day problem decomposition.

TABLE 2.3 – Computational results - Assign-then-Schedule heuristic

Instance configuration	# Feasible solutions	Gap w.r.t. MILP (%)	Computational time (s)	Charging costs gap ($ (%))	Cal. aging costs gap ($ (%))
43_3_42	1	0.00	3	0(0)	0.00(0)
54_3_52	1	0.00	4	0(0)	0.00(0)
43_5_42	1	0.00	5	0(0)	0.00(0)
54_5_52	1	0.00	9	0(0)	0.00(0)
20_3_10	10	0.92	1	0(0)	22.00(72)
30_3_15	10	0.96	3	0(0)	34.50(66)
40_3_20	10	0.85	9	0(0)	41.61(49)
50_3_25	10	0.93	17	0(0)	56.62(55)
60_3_30	10	0.76	31	0(0)	54.90(46)
70_3_35	10	0.84	139	0(0)	70.73(53)
80_3_40	10	0.75	73	0(0)	72.26(47)
90_3_45	9	0.82	153	0(0)	88.72(50)
20_5_10	10	1.12	3	0(0)	56.65(74)
30_5_15	10	1.03	23	0(0)	78.22(63)
40_5_20	10	0.99	88	0(0)	100.79(54)
50_5_25	10	1.01	86	0(0)	128.54(58)
60_5_30	8	0.88	273	0(0)	134.38(48)
70_5_35	7	0.76	803	0(0)	134.58(41)
80_5_40	5	0.76	1451	0(0)	153.06(41)
90_5_45	4	–	1412	−(−)	−(−)
60_3_20	0	–	–	−(−)	−(−)
60_3_25	9	0.93	127	0(0)	68.58(33)
60_3_35	10	0.81	23	0(0)	58.27(103)
60_3_40	10	0.77	19	0(0)	54.65(1444)
60_3_45	10	0.35	18	0(0)	25.14(4061)
60_5_20	0	–	–	−(−)	−(−)
60_5_25	0	–	–	−(−)	−(−)
60_5_35	10	0.82	301	0(0)	122.60(92)
60_5_40	10	0.74	57	0(0)	110.46(278)
60_5_45	10	0.49	48	0(0)	73.02(4862)
Total / Average	216	0.82	151	0(0)	72.71(570)

The results, summarized in Table 2.4, show that D-AtS found feasible solutions for 255 of the 264 instances, and could not find a feasible solution for the remaining 9. This table contains the same columns as Table 2.3, plus the fourth column providing the gap with respect to the solutions delivered by AtS. Here again, we do not compute the gaps when the MILP, AtS or D-AtS did not find a feasible solution for an instance.

As the results show, D-AtS solves more instances than both the MILP and AtS. Furthermore, a quick inspection of Columns 4 and 5 reveals that, in general, D-AtS performs better than AtS (with an average improvement of 0.15%) and slightly closes the gap with the MILP (with an average gap of 0.66%). Similar to the results observed in the AtS experiments, the gap between the D-AtS and MILP solutions comes entirely from the calendar aging costs. However, that gap is smaller than that reported by AtS (Avg. of 452% vs 570%). This improvement is probably explained by the strategy employed by D-AtS to build EB-to-block assignments. Indeed, D-AtS assigns EBs to blocks trying to minimize the charging costs but also trying to maximize the time that the EBs spend at the depot. Therefore, the scheduling problem that D-AtS solves in the third phase has wider time windows. Needless to say, the latter allows the heuristic to find schedules with better calendar aging costs. It is worth noting that D-AtS's EB-to-block assignment strategy can, at least in theory, lead to an infeasible scheduling problem. However, we did not observe this situation in any of our experiments. In terms of computational performance, D-AtS also outperformed AtS. The explanation is that D-AtS fixes the $x_{i,j}$ variables in the EB-to-block assignment phase (Lines 1- 4). The latter implicitly decides the energy consumption of each EB in the fleet along the planning horizon and provides a lower bound on each EB's SoC at the beginning and the end of each charging operation. Fixing the $x_{i,j}$ variables also helps to bound some of the $u_{i,j}$ variables, because of the time constraints generated by the sequence of vehicle blocks. Another element that contributes to D-AtS's computational performance is the low time complexity of the Hungarian algorithm used in the EB-to-block assignment phase.

2.6.4 Results with the short-sighted heuristics

In the fourth set of experiments, we solved the 264 instances running the Min-SS heuristic for up to 1 hour. The results are summarized in Table 2.5, which reports the same statistics as Table 2.4 except for an additional column (Column 5) that shows the average gap in the objective function with respect to the D-AtS solutions.

As Column 2 shows, Min-SS only found feasible solutions for 206 out of the 264 instances; the lowest count among the methods tested up to this point. Min-SS did not find solutions for the remaining 58 instances due to feasibility issues. Not enough energy

TABLE 2.4 – Computational results - Daily-Assign-then-Schedule heuristic

Instance family	# Feasible solutions	Gap w.r.t. MILP (%)	Gap w.r.t. AtS (%)	Computational time (s)	Charging costs gap ($ (%))	Cal. aging costs gap ($ (%))
43_3_42	1	0.05	0.05	2	2(0)	0.00(0)
54_3_52	1	0.00	0.00	2	0(0)	0.00(0)
43_5_42	1	0.02	0.02	2	2(0)	0.00(0)
54_5_52	1	0.00	0.00	3	0(0)	0.00(0)
20_3_10	10	0.97	0.06	0	0(0)	23.31(76)
30_3_15	10	0.66	−0.30	1	0(0)	23.68(46)
40_3_20	10	0.59	−0.26	2	0(0)	28.65(34)
50_3_25	10	0.65	−0.28	3	0(0)	39.03(39)
60_3_30	10	0.63	−0.12	5	0(0)	45.67(39)
70_3_35	10	0.78	−0.06	7	1(0)	64.39(48)
80_3_40	10	0.70	−0.06	15	1(0)	65.68(43)
90_3_45	10	0.69	−0.12	24	2(0)	73.21(41)
20_5_10	10	1.11	−0.01	0	0(0)	56.19(76)
30_5_15	10	0.76	−0.27	1	0(0)	57.66(47)
40_5_20	10	0.72	−0.26	3	0(0)	73.34(39)
50_5_25	10	0.80	−0.22	6	0(0)	100.78(46)
60_5_30	10	0.65	−0.20	10	0(0)	98.83(37)
70_5_35	10	0.61	−0.13	15	1(0)	106.93(33)
80_5_40	10	0.57	−0.15	29	2(0)	112.14(31)
90_5_45	10	0.59	0.02	36	2(0)	132.13(31)
60_3_20	10	–	–	338	−(−)	−(−)
60_3_25	10	0.70	−0.22	55	0(0)	51.09(25)
60_3_35	10	0.66	−0.15	4	0(0)	46.96(83)
60_3_40	10	0.63	−0.14	5	0(0)	44.44(1363)
60_3_45	10	0.30	−0.05	4	0(0)	21.35(3505)
60_5_20	1	–	–	2806	−(−)	−(−)
60_5_25	10	–	–	87	−(−)	−(−)
60_5_35	10	0.61	−0.20	8	0(0)	91.41(70)
60_5_40	10	0.57	−0.17	8	0(0)	85.38(220)
60_5_45	10	0.36	−0.13	7	0(0)	53.96(3632)
Total / Average	255	0.66	−0.15	37	0(0)	59.05(452)

was charged into some EBs during the early days of the planning horizon and the method could not create a feasible block-to-bus assignment at some point. In further experimentations, we were able to find feasible solutions for the remaining 58 instances by adding a few reserve EBs (i.e., increasing the size of the fleet). This result highlights the benefits of considering the multi-day planning horizon rather than following the legacy industrial practice of solving consecutive single-day problems. In terms of solution quality, the results suggest that, when it finds a feasible solution, Min-SS is competitive with D-AtS. While Min-SS delivers a slightly better average performance (with a gap of -0.05%), it does not dominate D-AtS across all instance families. This good performance may be explained by Min-SS's capacity to optimally solve the daily (small) MILPs.

TABLE 2.5 – Computational results - Minimum short-sighted heuristic

Instance family	# Feasible solutions	Gap w.r.t. MILP (%)	Gap w.r.t. AtS (%)	Gap w.r.t. D-AtS (%)	Computational time (s)	Charging costs gap ($ (%))	Cal. aging costs gap ($ (%))
43_3_42	0	–	–	–	–	−(−)	−(−)
54_3_52	1	0.00	0.00	0.00	2	0(0)	0.00(0)
43_5_42	0	–	–	–	–	−(−)	−(−)
54_5_52	1	0.00	0.00	0.00	3	0(0)	0.00(0)
20_3_10	8	0.71	−0.23	−0.30	0	0(0)	17.06(59)
30_3_15	8	0.63	−0.29	−0.02	1	0(0)	23.05(42)
40_3_20	9	0.64	−0.20	0.05	2	0(0)	31.47(37)
50_3_25	8	0.69	−0.24	0.01	5	0(0)	42.10(41)
60_3_30	8	0.68	−0.09	0.00	8	0(0)	49.36(42)
70_3_35	9	0.68	−0.16	−0.10	16	0(0)	57.29(43)
80_3_40	10	0.66	−0.09	−0.03	31	0(0)	63.79(42)
90_3_45	10	0.65	−0.18	−0.04	46	0(0)	70.53(40)
20_5_10	8	0.75	−0.38	−0.39	1	0(0)	37.73(51)
30_5_15	8	0.64	−0.36	−0.12	2	0(0)	49.29(40)
40_5_20	9	0.62	−0.34	−0.08	5	0(0)	63.97(33)
50_5_25	8	0.76	−0.23	−0.06	8	0(0)	97.27(43)
60_5_30	8	0.63	−0.23	−0.04	14	0(0)	96.26(36)
70_5_35	9	0.52	−0.24	−0.12	27	0(0)	92.44(28)
80_5_40	10	0.51	−0.25	−0.09	59	0(0)	103.69(28)
90_5_45	10	0.44	−0.18	−0.15	82	0(0)	98.93(23)
60_3_20	0	–	–	–	–	−(−)	−(−)
60_3_25	8	0.95	0.01	0.16	65	0(0)	70.12(34)
60_3_35	8	0.61	−0.24	−0.08	7	0(0)	44.18(78)
60_3_40	8	0.67	−0.09	0.03	8	0(0)	48.07(1652)
60_3_45	8	0.34	−0.02	0.02	6	0(0)	24.22(4051)
60_5_20	0	–	–	–	–	−(−)	−(−)
60_5_25	8	–	–	0.17	104	−(−)	−(−)
60_5_35	8	0.61	−0.20	−0.01	13	0(0)	92.61(70)
60_5_40	8	0.60	−0.11	0.02	13	0(0)	90.57(221)
60_5_45	8	0.41	−0.10	0.03	10	0(0)	62.04(4138)
Total / Average	206	0.63	−0.19	−0.05	23	0(0)	58.21(496)

In the fifth, and last, set of experiments, we solved the 264 instances running Max-SS for up to 1 hour. Table 2.6 summarizes the results under the light of the same metrics used in Table 2.5. As the table shows, Max-SS hit a new low in terms of feasible solutions with only 146 out of the 264 instances. Min-SS did not find solutions for the remaining 118 instances because it reaches the time limit. This result is even more notorious in the 5-day instances where the heuristic could only retrieve feasible solutions for 26% of the benchmarks (38 out of 142). Recall that Max-SS's main objective is to reproduce the widespread industrial practice of charging the EBs as much as possible every night. For this reason, the problems solved in the scheduling phase typically include jobs (i.e., charging operations) with long processing times that are nearly impossible to fit together due to the charger capacity constraints. This charging policy has a second undesirable effect : in terms of solution quality, Max-SS also delivers the worst performance among the tested methods. The average gap with respect to the MILP solutions is 10.15%, and this figure is 9.31% and 9.44% with respect to AtS and D-AtS. A close look at Column 6 shows that Max-SS yields significant gaps in terms of the charging costs (the dominant term in the objective function) with respect to the MILP (Avg. of 7%). These results are not surprising, since, contrary to the other approaches, Max-SS explicitly seeks to charge more energy than is really needed to cover the blocks. These results tip again the scales in favor of considering a multi-period horizon rather than solving sequential daily problems.

TABLE 2.6 – Computational results - Maximum short-sighted heuristic

Instance family	# Feasible solutions	Gap w.r.t. MILP (%)	Gap w.r.t. AtS (%)	Gap w.r.t. D-AtS (%)	Computational time (s)	Charging costs gap ($ (%))	Cal. aging costs gap ($ (%))
43_3_42	1	9.05	9.05	8.99	4	409(9)	0.00(0)
54_3_52	1	9.24	9.24	9.24	5	624(9)	10.99(25033)
43_5_42	1	4.30	4.30	4.28	6	408(4)	0.00(0)
54_5_52	1	4.50	4.50	4.50	10	624(4)	21.77(2240)
20_3_10	10	12.27	11.25	11.19	2188	217(9)	77.48(250)
30_3_15	10	12.24	11.17	11.50	3600	318(9)	124.40(236)
40_3_20	10	11.95	11.00	11.29	3600	420(9)	162.06(192)
50_3_25	10	11.53	10.49	10.80	3600	502(8)	196.61(192)
60_3_30	8	11.48	10.64	10.79	3600	598(8)	235.21(196)
70_3_35	10	11.26	10.34	10.41	3600	675(8)	273.08(203)
80_3_40	9	11.14	10.3	10.38	3600	769(8)	300.71(196)
90_3_45	5	10.55	9.95	10.06	3600	823(8)	317.55(179)
20_5_10	4	7.67	6.33	6.45	144	224(5)	159.06(216)
30_5_15	2	5.70	4.73	5.03	3600	237(3)	201.34(161)
40_5_20	1	7.49	6.35	6.8	3600	425(4)	352.66(180)
50_5_25	0	–	–	–	–	–(–)	–(–)
60_5_30	0	–	–	–	–	–(–)	–(–)
70_5_35	0	–	–	–	–	–(–)	–(–)
80_5_40	0	–	–	–	–	–(–)	–(–)
90_5_45	0	–	–	–	–	–(–)	–(–)
60_3_20	0	–	–	–	–	–(–)	–(–)
60_3_25	4	7.19	6.84	7.12	3600	353(5)	171.78(82)
60_3_35	10	12.06	11.16	11.33	1145	642(9)	224.25(394)
60_3_40	10	11.63	10.78	10.93	166	642(9)	187.67(5434)
60_3_45	10	10.72	10.33	10.38	48	642(9)	121.54(20125)
60_5_20	0	–	–	–	–	–(–)	–(–)
60_5_25	0	–	–	–	–	–(–)	–(–)
60_5_35	9	7.04	6.17	6.39	2000	638(4)	423.81(314)
60_5_40	10	6.68	5.90	6.07	312	642(4)	356.20(891)
60_5_45	10	5.92	5.40	5.54	70	642(4)	240.08(16107)
Total / Average	146	10.15	9.31	9.47	2095	552(7)	218.00(3306)

2.7 Conclusion

In this paper, we introduced the MDEBAOSP and formulated it as a MILP that can be solved using a commercial solver. To obtain faster computational times, we also developed two matheuristics called Assign-then-Schedule and Daily-Assign-then-Schedule, both having complementary advantages. To evaluate our algorithms, we used a set of 264 instances generated from data of an EB operator. First, the MILP solver is able to find near-optimal solutions, with an average optimality gap of 1.32%, but it is time and resourceconsuming, reaching the provided time limit for most instances. The Assign-then-Schedule heuristic offers a good compromise between solution quality and computational performance, with a small average gap of 0.82% w.r.t. MILP approach and an average computation time of 151 s. Finally, the Daily-Assign-then-Schedule heuristic provides good solutions in short computational times, with a small average gap of 0.66% w.r.t. MILP approach and an average computation time of 37 s. We showed the benefits of the proposed methods by comparing them to widely-used industrial policies, in which the problem is solved sequentially, one day at a time. We implemented these policies via two versions of a short-sighted heuristic, namely, the Minimum Short-Sighted and Maximum Short-Sighted heuristics. The results provided by the Minimum Short-Sighted method show the value of considering a multi-day planning horizon, by finding feasible solutions for only 206 instances against 255 for the Daily-Assign-then-Schedule heuristic. The results of the Maximum Short-Sighted method also showed the negative impact of using the trivial policy of charging the EBs as much as possible every night, inducing an average charging costs gap of 7% w.r.t MILP approach and an average calendar aging costs gap of more than 3000%.

As a first research perspective, we can propose additionals method to solve the problem. For instance, MDEBAOSP can be seen as an extension of the CSP. Thus, by using the assignment step of the D-AtS as an initial step, the charging scheduling algorithm from KLEIN et SCHIFFER, 2023 can then be applied since it considers battery aging. An interesting research perspective is to extend the problem to consider a target ending SoC, higher than the minimum SoC, at the end of the time period. This feature would be useful in cases in which transit agencies want to build cyclic planning, but the time between cycles (e.g., the weekend) is not long enough to charge all the EBs to their full capacity. Another research direction could be to extend the problem to consider the more strategic objective of minimizing the number of chargers. A final interesting research avenue would be to consider a more fine-grained EB operation and also schedule out-of-depot recharges. The latter could be achieved by dividing blocks into smaller atomic units (i.e., sub-blocks) and letting the models and methods decide if, where, and for how long, each EB should charge between two sub-blocks. By having access to the blocks content, the additional decisions could have an impact on the battery cycle aging. Then, all aspects of battery aging could be included in the problem.

Acknowledgments

We thank the personnel of GIRO Inc. for fruitful discussions and for providing real-world datasets. We gratefully acknowledge the financial support of GIRO Inc. and the Natural Sciences and Engineering Research Council of Canada under the grant RDCPJ 520349-17. This research was also partially funded by HEC Montreal through the research professorship on Clean Transportation Analytics. This research was also enabled in part by the support provided by Calcul Québec (www.calculquebec.ca) and Digital Research Alliance of Canada (www.alliancecan.ca).

References

ALVO, M., ANGULO, G., & KLAPP, M. A. (2021). An exact solution approach for an electric bus dispatch problem. *Transportation Research Part E : Logistics and Transportation Review*, *156*, 102528.

BARRÉ, A., DEGUILHEM, B., GROLLEAU, S., GÉRARD, M., SUARD, F., & RIU, D. (2013). A review on lithium-ion battery ageing mechanisms and estimations for automotive applications. *Journal of Power Sources*, *241*, 680-689.

BLOOMBERG NEW ENERGY FINANCE. (2018). *Electric buses in cities : Driving towards cleaner air and lower CO2* (Report) (Visité en Mars 2024). on the behalf of : Financing Sustainable Cities Initiative, C40 Cities, World Resources Institute, Citi Foundation. https://data.bloomberglp.com/professional/sites/24/2018/05/Electric-Buses-in-Cities-Report-BNEF-C40-Citi.pdf

BUNTE, S., & KLIEWER, N. (2009). An overview on vehicle scheduling models. *Public Transport*, *1*(4), 299-317.

CAUGHILL, P. (2018). Report Shows Half of Public Buses Will be Electric by 2025. *Futurism*. https://futurism.com/new-report-majority-public-buses-electric-2025

DIRKS, N., SCHIFFER, M., & WALTHER, G. (2022). On the integration of battery electric buses into urban bus networks. *Transportation Research Part C : Emerging Technologies*, *139*, 103628.

DIRKS, N., WAGNER, D., SCHIFFER, M., & WALTHER, G. (2021). A Concise Guide on the Integration of Battery Electric Buses into Urban Bus Networks. *arXiv preprints arXiv :2104.10752v1*.

FROGER, A., JABALI, O., MENDOZA, J. E., & LAPORTE, G. (2022). The Electric Vehicle Routing Problem with Capacitated Charging Stations. *Transportation Science*, *56*, 460-482.

HEAP, B. R. (1963). Permutations by Interchanges. *The Computer Journal*, *6*(3), 293-298.

HOKE, A., BRISSETTE, A., SMITH, K., PRATT, A., & MAKSIMOVIC, D. (2014). Accounting for Lithium-Ion Battery Degradation in Electric Vehicle Charging Optimization. *IEEE Journal of Emerging and Selected Topics in Power Electronics*, *2*(3), 691-700.

INSEE RÉFÉRENCES. (2019). *Changement climatique et effet de serre* (Report). Insee. https://www.insee.fr/fr/statistiques/3676581

IPCC. (2014). *Climate Change 2014 : AR5 Synthesis Report* (rapp. tech.).

JANOVEC, M., & KOHÁNI, M. (2019). Exact approach to the electric bus fleet scheduling. *Transportation Research Procedia*, *40*, 1380-1387.

KLEIN, P. S., & SCHIFFER, M. (2023). Electric vehicle charge scheduling with flexible service operations. *57*(6), 1605-1626.

KLIEWER, N., MELLOULI, T., & SUHL, L. (2006). A time–space network based exact optimization model for multi-depot bus scheduling. *European Journal of Operational Research*, *175*(3), 1616-1627.

KUHN, H. W. (1955). The Hungarian method for the assignment problem. *Naval Research Logistics Quarterly*, *2*(1-2), 83-97.

KUNITH, A., MENDELEVITCH, R., & GOEHLICH, D. (2017). Electrification of a city bus network—An optimization model for cost-effective placing of charging infrastructure and battery sizing of fast-charging electric bus systems. *International Journal of Sustainable Transportation*, *11*(10), 707-720.

LIU, T., & CEDER, A. (2020). Battery-electric transit vehicle scheduling with optimal number of stationary chargers. *Transportation Research Part C : Emerging Technologies*, *114*, 118-139.

LIU, Z., SONG, Z., & HE, Y. (2018). Planning of Fast-Charging Stations for a Battery Electric Bus System under Energy Consumption Uncertainty. *Transportation Research Record*, *2672*(8), 96-107.

LÖBEL, A. (1999). Solving Large-Scale Multiple-Depot Vehicle Scheduling Problems. *Computer-Aided Transit Scheduling*.

LOTFI, M., PEREIRA, P., PATERAKIS, N. G., GABBAR, H. A., & CATALÃO, J. P. S. (2020). Optimal Design of Electric Bus Transport Systems With Minimal Total Ownership Cost. *IEEE Access*, *8*.

LUNZ, B., YAN, Z., GERSCHLER, J. B., & SAUER, D. U. (2012). Influence of plug-in hybrid electric vehicle charging strategies on charging and battery degradation costs. *Energy Policy*, *46*, 511-519.

MONTOYA, A., GUÉRET, C., MENDOZA, J. E., & VILLEGAS, J. G. (2017). The electric vehicle routing problem with nonlinear charging function. *Transportation Research Part B : Methodological*, *103*, 87-110.

PELLETIER, S., JABALI, O., & LAPORTE, G. (2018). Charge scheduling for electric freight vehicles. *Transportation Research Part B : Methodological*, *115*, 246-269.

PELLETIER, S., JABALI, O., LAPORTE, G., & VENERONI, M. (2017). Battery degradation and behaviour for electric vehicles : Review and numerical analyses of several models. *Transportation Research Part B : Methodological*, *103*, 158-187.

PELLETIER, S., JABALI, O., MENDOZA, J. E., & LAPORTE, G. (2019). The electric bus fleet transition problem. *Transportation Research Part C-Emerging Technologies*, *109*, 174-193.

RINALDI, M., PICARELLI, E., D'ARIANO, A., & VITI, F. (2020). Mixed-fleet single-terminal bus scheduling problem : Modelling, solution scheme and potential applications. *Omega*, *96*, 102070.

ROGGE, M., van der HURK, E., LARSEN, A., & SAUER, D. U. (2018). Electric bus fleet size and mix problem with optimization of charging infrastructure. *Applied Energy*, *211*, 282-295.

SASSI-BEN SALAH, O., & OULAMARA, A. (2014). Simultaneous electric vehicles scheduling and optimal charging in the business context : case study. *5th IET Hybrid and Electric Vehicles Conference (HEVC 2014)*, 1-6.

SASSI-BEN SALAH, O., & OULAMARA, A. (2017). Electric vehicle scheduling and optimal charging problem : complexity, exact and heuristic approaches. *International Journal of Production Research*, *55*(2), 519-535.

UNFCCC. (2016). *Report of the Conference of the Parties on its twenty-first session, held in Paris from 30 November to 13 December 2015. Part one : Proceedings* (rapp. tech.).

WANG, Y., HUANG, Y., XU, J., & BARCLAY, N. (2017). Optimal recharging scheduling for urban electric buses : A case study in Davis. *Transportation Research Part E : Logistics and Transportation Review*, *100*, 115-132.

WEN, M., LINDE, E., ROPKE, S., MIRCHANDANI, P., & LARSEN, A. (2016). An adaptive large neighborhood search heuristic for the Electric Vehicle Scheduling Problem. *Computers & Operations Research*, *76*, 73-83.

WU, W., LIN, Y., LIU, R., & JIN, W. (2022). The multi-depot electric vehicle scheduling problem with power grid characteristics. *Transportation Research Part B : Methodological*, *155*, 322-347.

XYLIA, M., LEDUC, S., PATRIZIO, P., KRAXNER, F., & SILVEIRA, S. (2017). Locating charging infrastructure for electric buses in Stockholm. *Transportation Research Part C : Emerging Technologies*, *78*, 183-200.

ZHANG, L., WANG, S., & QU, X. (2021). Optimal electric bus fleet scheduling considering battery degradation and non-linear charging profile. *Transportation Research Part E : Logistics and Transportation Review*, *154*, 102445.

ZHOU, Y., MENG, Q., & ONG, G. P. (2022). Electric Bus Charging Scheduling for a Single Public Transport Route Considering Nonlinear Charging Profile and Battery Degradation Effect. *Transportation Research Part B : Methodological*, *159*, 49-75.

Chapitre 3

A matheuristic for a multi-day electric bus assignment and recharge scheduling problem

Résumé

La proportion de bus électriques dans les flottes de transport public augmente en réponse aux émissions de gaz à effet de serre dans le secteur du transport public. En raison de contraintes d'espace et de budget, il est souvent impossible de recharger l'ensemble du parc de bus électriques pendant la nuit. Une solution potentielle consiste à équilibrer les opérations de recharge entre la nuit au dépôt ainsi que la journée pendant leur fonctionnement normal. Il est donc nécessaire de concevoir des techniques d'optimisation qui permettent de recharger les véhicules à la fois pendant la nuit et en cours de route. Dans cette étude, nous considérons un problème d'affectation et de programmation de la recharge des bus électriques sur plusieurs jours qui peut être brièvement énoncé comme suit. Étant donné un ensemble de blocs de véhicules (séquences de trajets de bus programmés qui devraient être effectués par le même bus un jour donné), un ensemble de bus électriques et un ensemble de chargeurs, l'objectif est d'affecter un bus électrique à chaque bloc sur plusieurs jours et d'ordonnancer les événements de recharge pendant la nuit et en route. Des chargeurs sont installés au dépôt et aux arrêts suffisamment longs. Chaque chargeur a sa propre fonction de charge qui est linéaire par morceaux. Les décisions sont prises en veillant à ce que les bus ne manquent jamais d'énergie pour effectuer les blocs qui leur sont assignés, que la capacité des chargeurs à n'importe quel endroit ne soit jamais dépassée et que la somme des coûts de charge totaux et des dommages à long terme causés à la batterie soit minimisée. Nous modélisons d'abord ce problème sous la forme d'un programme linéaire en nombres entiers (MILP) qui peut être résolu à l'aide d'un solveur commercial. Ensuite, pour obtenir des temps de calcul plus rapides, nous développons une matheuristique basée sur le MILP, dans laquelle certaines parties des décisions sont reconsidérées à chaque itération de la méthode. Pour évaluer tous ces algorithmes, nous utilisons un ensemble de 72 instances générées à partir des données d'un opérateur de bus.

Abstract

The proportion of electric buses (EBs) in public transit fleets is increasing in response to greenhouse gas emissions in the public transit sector. Due to space and budget constraints, more often than not, it is sometimes unfeasible to charge the entire EB fleet overnight. A potential solution lies in balancing the charging operations between the overnight time at the depot and the driving daytime during their regular operation. Thus, there is a need to devise optimization techniques that help to recharge using both overnight and en-route charging. In this study, we consider a multi-day electric bus assignment and recharge scheduling problem that can be briefly stated as follows. Given a set of vehicle blocks (sequences of timetabled bus trips that should be operated by the same bus on a given day), a set of EBs and a set of chargers, the objective is to assign an EB to each block over multiple days and to schedule both overnight and en-route charging events. Chargers are installed at the depot and at sufficiently long stops. Each charger has its own charging function that is piecewise linear. The decisions are made to ensure that the EBs never

run out of energy performing their assigned blocks, the charging capacity at any location should not be exceeded, and the sum of the total charging costs and long run damages to the battery are minimized. We first model this problem as a mixed integer linear program (MILP) that can be solved with a commercial solver. Then, to yield faster computational times, we develop a matheuristic based on the MILP, in which parts of the decisions are reconsidered at each iteration of the method. To evaluate all these algorithms, we use a set of 72 instances generated from data of an EB operator.

3.1 Introduction

In 2014, the Intergovernmental Panel on Climate Change (IPCC) issued a series of recommendations to mitigate global warming, one of which is the extensive electrification of transportation networks (IPCC, 2014). The goal is to curb the increase in greenhouse gas emissions, as the transport sector alone accounts for 15% of global emissions (IPCC, 2023). The overarching objective of these measures is to prevent a 5°C rise in global temperatures by 2100, which could result in severe consequences such as water scarcity, soil degradation, and an influx of climate refugees.

Given that the transportation sector is a major source of these greenhouse gases, one leverage that governments can use to reduce these emissions is the electrification of public transit domain, particularly urban buses. The implementation of electric-powered vehicles in the public transit sector presents various strategic, tactical, and operational challenges to overcome. Diesel-powered buses still account for a large proportion of the current public transit bus fleets, and replacing them with electric buses (EBs) is not straightforward. EBs typically have a significantly restricted driving range, requiring frequent recharging events either between trips or even en-route, contingent upon factors such as the technology used, the length of the bus line, and the charging time available. To address these technological limitations, transit authorities need to install charging infrastructure along the line, as well as at terminals located at the end of the lines, and depots. There are two primary strategies for charging EBs : en-route charging (Y. WANG et al., 2017 ; XYLIA et al., 2017) and overnight charging (HOUBBADI et al., 2019 ; VENDÉ, DESAULNIERS, KERGOSIEN & MENDOZA, 2023). When using the en-route charging strategy, EBs are charged while performing their regular operation, typically at end-of-line terminals or sufficiently long-term stops, such as at transfer points between lines. This method demands a substantial initial investment in charging infrastructure, including fast chargers, high-tension power lines, and high-voltage transformers, as buses need multiple and rapid battery recharges throughout the day. However, given that EBs can charge frequently, small batteries can be used, helping to reduce the upfront costs associated with fleet purchases. Overnight charging implements the opposite strategy. EBs are charged only at depots, mainly during the night. To implement this strategy, EBs require a longer driving range. Therefore, they must be equipped with larger-capacity batteries, which are more expensive. Moreover, batteries with a sufficient capacity to operate for an entire day without recharging are still uncommon. To overcome this problem, transit companies must ensure that they have several buses to cover each line of the network, enabling drivers to quickly change buses when their batteries are low. The additional number of buses increases the upfront cost of the fleet. Finally, the overnight charging strategy implies charging only during the night ; therefore, a large number of charging events must occur simultaneously, involving an expensive charging infrastructure.

This issue of managing EBs, including their recharging operations, over a transit network relates to a class of problems known as the electric vehicle scheduling problems (eVSP). These problems consist in assembling sequences of trips, also called blocks, and assigning each of those blocks to an EB (SASSI-BEN SALAH & OULAMARA, 2017). To ensure the feasibility of a solution, among other things, eVSPs must determine where and for how long the EBs must charge their batteries between two trips. The objective may be to minimize the energy costs (ROGGE et al., 2018), or to minimize the number of vehicles that are needed to perform a set of trips (JANOVEC & KOHÁNI, 2019 ; T. LIU & CEDER, 2020).

The literature reports on several eVSP variants. JANOVEC et KOHÁNI, 2019 propose a variant in which they assign a set of trips and a set of charging events to EBs from a homogeneous fleet, while minimizing the number of used vehicles. They formulated the problem with a mixed-integer linear program (MILP) that can be solved by a commercial solver. RINALDI et al., 2020 introduce a time decomposition heuristic that solves a series of MILPs for a version of the problem with a mixed fleet composed of EBs and hybrid buses, minimizing the total operational cost. YAO et al., 2020 present a multiple vehicle type version of the problem, each type having its own driving range and charger. They propose a genetic algorithm to solve the problem. ALVO et al., 2021 design a Benders decomposition algorithm for an eVSP with a mixed fleet composed of EBs and diesel buses and a linear charging function. Their objective is to minimize first the number of diesel buses used and then their total fuel consumption. Their decomposition is structured as follows : i) a master problem determines bus schedules and charger schedules, without considering charger capacity ; ii) a sub-problem problem that checks if feasible charger schedules can be computed from the bus schedules calculated in the previous step. ZHANG et al., 2021 develop a branch-and-price algorithm that can handle battery degradation due to cycle aging but does not allow partial charging. ZHOU et al., 2022 deal with a more complex problem that considers multiple charger types. They solve their problem using a MILP enhanced with problem-specific valid inequalities. WU et al., 2022 propose a branch-and-price algorithm for solving a multi-depot eVSP considering a time-of-use electricity pricing but forcing the EBs to always charge to their full capacity and assuming constant charging times. KLEIN et SCHIFFER, 2023 design an exact branch-and-price algorithm to solve the route and recharge scheduling problem with flexible service operations (meaning that the departure time for each vehicle is a decision variable). To solve large instances involving up to 500 trips, the authors devise a heuristic version of their algorithm that is based on a graph reduction technique and a diving heuristic to quickly find good primal solutions. AVISHAN et al., 2023 present a stochastic variant of the eVSP, with travel time and energy consumption uncertainty. Their objective is to find the minimum number of EBs to cover a set of trips. The problem is solved using an evolutionary matheuristic in which subsets of trips are generated based on their start time. Those subsets of trips are then merged in order to create a set of feasible candidate schedules, describing the set of trips assigned to an EB. Finally, a set covering problem is solved to select the best schedules minimizing the total costs (EB purchasing costs and charging costs). Finally, de VOS et al., 2023 develop a branch-and-price algorithm to solve the multi-depot eVSP, considering capacitated charging stations and partial charging. The linear relaxation is computed using two possible heuristics : truncated price-and-branch and truncated column generation.

The papers surveyed above focus on a one-day planning horizon, whereas our interest lies in an extended multi-day horizon. Given the size of multi-day eVSPs in practice, they are usually solved with a multi-phase approach. First, timetabled trip sequences are computed for each day within the planning horizon (e.g., a week) by solving an eVSP. Then, each night, EBs are assigned to vehicle blocks scheduled to operate from their depot the next day, taking into account their current state of charge (SoC). Finally, each EB is recharged overnight with just enough energy to fulfill its assigned block. While this day-by-day process is straightforward to comprehend and implement, VENDÉ, DESAULNIERS, KERGOSIEN et MENDOZA, 2023 demonstrate its potential unsuitability in practical scenarios. Our current research extends their work, in which they solve a multi-day EB assignment and overnight recharge scheduling problem (MDEBAOSP) that can be briefly stated as follows. The problem considers a set of vehicle blocks (sequences of timetabled trips performed by the same bus on a given day) to be operated over several days, a set of identical EBs, and a set of chargers available at the depot (whose charging function is piecewise linear). The MDEBAOSP consists in assigning an EB to each block and to schedule the overnight recharging operations at the depot. The assignment and schedule must ensure that the EBs never run out of energy when performing their blocks and that the depot charging capacity is never exceeded. They considered two objectives : minimizing the total charging costs and the battery degradation costs due to calendar aging. Although our study share some features with this work, some differences arise. First, in VENDÉ, DESAULNIERS, KERGOSIEN et MENDOZA, 2023 the vehicle blocks are considered as unbreakable. In our research, blocks are decomposed into sub-blocks for which charging events occurring between sub-blocks can be added. This translates into a greater number of charging and scheduling decisions. Second, the type of long-term battery degradation considered is different. The technical literature highlights two types of battery aging : cycle aging and calendar aging. Cycle aging depends on factors such as the current rate, and the depth of discharge or DoD (i.e., the charge/discharge cut-off voltages). Charging or/and discharging the batteries at high rates (e.g., using fast chargers) and draining them to their maximum DoD reduces the number of charge/discharge cycles in their lifespan (BARRÉ et al., 2013). Calendar aging is influenced by the average state of charge (SoC) and the temperature to which batteries are exposed during storage. Prolonged storage at elevated SoCs and temperatures has the effect of diminishing the overall lifespan of the batteries (PELLETIER et al., 2017). VENDÉ, DESAULNIERS, KERGOSIEN et MENDOZA, 2023 only considers calendar aging because only the overnight charging was optimized. In our research, we seek to favor cycle aging, which is influenced by the charging rate applied. Therefore, we prioritize the on charging overnight at the depot using low charging rate chargers instead of charging events occurring en-route at a higher charging rate. Therefore, the goal is to reduce the frequency of charging en-route events to minimize their long-term impact on the battery's health. Finally, VENDÉ, DESAULNIERS, KERGOSIEN et MENDOZA, 2023 consider a multi-day planning horizon with an initial and final SoC that can be different. This suggests that there is a potential break in operations (e.g., on a Sunday), during which most of the fleet would remain at the depot and have sufficient time for full charging. Finally, in our research, we consider a cyclic schedule in which the SoC of the battery at the end of the last day must be equal to the SoC of the battery at the beginning of the first day of the planning horizon, which makes the problem more realistic.

Despite considering a multi-day planning horizon, it is sometimes very difficult to find a feasible solution for the overnight recharging problem, due to a lack of chargers or an excessive number of EBs requiring charging. To address this challenge, several transit companies have implemented a mix of overnight and en-route charging strategies (WEI et al., 2018). This mix of charging strategies is complex to handle and typically occurs in three steps. First, EBs leave the depot with a fully charged battery. Then, charging events are inserted within EBs blocks if they run out of energy in order to perform the end of the block. Finally, EBs are recharged overnight at the depot. In this study, we focused on transit systems that use a mix of both overnight and en-route charging strategies, and we manage the charging decision regarding both strategies.

In this paper, we study the multi-day EB assignment and recharge scheduling problem (MDEBARSP), which can be summarized as follows. Given a set of vehicle blocks (sequences of timetabled bus trips that should be operated by the same bus on a given day), a set of EBs, and a set of chargers, the objective of the MDEBARSP is to assign an EB to each block over a multi-day planning horizon and to schedule both overnight and en-route recharging events. Chargers are installed at the depot, and at sufficiently long stops. Each charger has its own charging function, which is by piecewise linear. Decisions are made to ensure that the EBs never run out of energy while performing their assigned blocks, that the charging capacity at any location and any time is not exceeded, and that the sum of the total charging costs and long-run damages to the battery is minimized. We formulate the MDEBARSP as a MILP and develop a matheuristic to solve this problem. In the proposed approach, the problem is decomposed into inter-block decisions and intra-block decisions. Inter-block decisions involve assigning EBs to blocks and sequencing overnight charging events performed at the depot. Intra-block decisions determine which en-route charging events can be removed and the duration of all charging events. During each iteration of the method, the portion of the solution corresponding to inter-block decisions is questioned and then modified according to the intra-block decisions, and vice versa in the next iteration. To evaluate the performance of our algorithm, we present computational results obtained on a set of 72 instances generated using data provided by an IT company that commercializes optimization software for public transit. The goal is to show the interest of considering a mix of overnight and en-route charging strategies.

The remainder of this paper is organized as follow. Section 3.2 formally defines the MDEBARSP and Section 3.3 formulates it as a MILP. Section 3.4 describes the proposed solution method to solve this problem. Section 3.5 provides the results of our computational experiments. Finally, Section 3.6 concludes and discusses possible future research directions.

3.2 The multi-day electric bus assignment and recharge scheduling problem

In the classical workflow of a transit operator, the MDEBARSP (an operational problem) arises after solving an eVSP (a tactical problem) to produce a set of vehicle blocks for each day in the planning horizon. These blocks may or may not include scheduled en-route charging events. Formally, the MDEBARSP can be described as follows. Let D be the set of days in the planning horizon (numbered from 1 to $|D|$). Let B_d, $d \in D$, be the set of blocks to be operated on day d from a given depot and denote by $B = \bigcup_{d \in D} B_d$ the set of all blocks. Each block $i \in B$ is defined by a sequence of bus trips called sub-blocks. Let B^i, $i \in B$ be the set of sub-blocks of vehicle block i. Let L be the set of locations, where chargers are installed, and $B_{d,l}$, $d \in D$ and $l \in L$, the set of sub-blocks performed on day d and starting at location l. A bus assigned to a block i starts and ends the k^{th} sub-block of the block at time $h^S_{i,k}$ and $h^E_{i,k}$, and at location $l^S_{i,k}$ and $l^E_{i,k}$, respectively. Given that the performed routes within each block are predefined, k^{th} sub-block of block i is also associated with a net energy consumption $e_{i,k}$ (that can be positive, negative, or null). A bus assigned to a block i starts and ends at a depot l_0.

To operate the vehicle blocks in B, we assume that the transit company employs a fleet V of identical EBs with a battery capacity of Q. The SoC of each EB varies throughout the horizon according to the sequence of blocks it is assigned to, and the overnight and en-route recharging events it undergoes. At any time, the SoC must remain between SOC^{min} and SOC^{max}. Each EB in V is assigned to at most one vehicle block per day. Given that the number of blocks to operate might differ from one day to another and that the EB fleet may include reserve EBs, some EBs may not be assigned to a block on some days. To avoid this case in our model, we create dummy blocks for each day that are added to keep the daily number of blocks constant and equal to the number of EBs. Each dummy block represents an idle EB for a day. It contains a single sub-block, that has zero energy consumption, the latest possible starting time, the earliest ending time, and the starting and ending locations set as the depot. These dummy blocks are part of the sets B_d, $d \in D$, and their sub-blocks are part of the sets B_{d,l_0}, $d \in D$.

At each charging location $l \in L$, there is a set C_l of identical chargers. We denote $C = \bigcup_{l \in L} C_l$ the set of all chargers. Chargers installed at the depot, belonging to set C_{l_0}, are used overnight whereas chargers installed on the network, belonging to set C_l, $l \in L \backslash \{l_0\}$, are used en-route during the day. At most $|C_l|$ EBs can recharge simultaneously at each charging location l. We assume that $|C_l| < |V|$ and that the charging events are not preemptive. The charging function f_l is a concave piecewise linear function that associates the amount of energy recharged by a charger installed at charging location l, $l \in L$, with the charging time, given an initial SoC. We denote by P_l the set of linear pieces of f_l and associate with each piece p the time $\theta_{l,p}$ needed to fulfill the segment, the energy recharged $q_{l,p}$ and the charging cost $\gamma_{l,p}$ for charging these q_p units of energy (see Figure 3.1). Note that $\sum_{p \in P_l} q_{l,p}$ is equal to the energy required to fully recharge an empty battery.

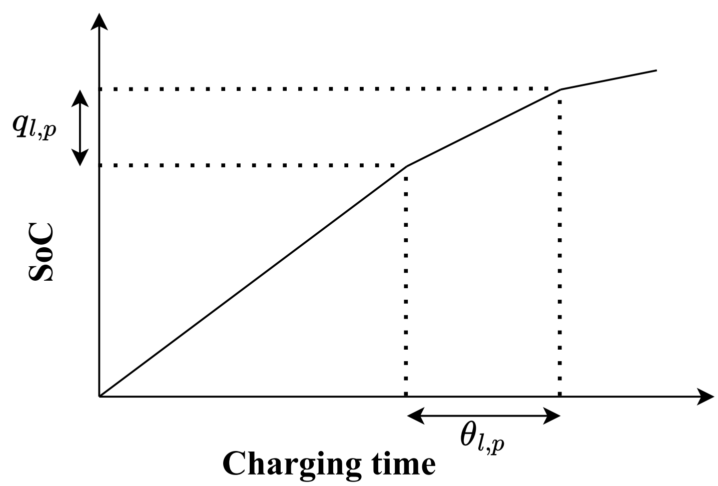

FIGURE 3.1 – Concave piecewise linear charging function f_l

Batteries possess a given number of charging cycles which they can undergo during their lifespan. Moreover, the higher the charging rate used to recharge a battery, the more its lifespan decreases over time. Therefore, in order to favor the reduction of battery degradation and limit the reduction of battery lifespan, a unit damage cost of ρ_l is charged for each charging event performed at charging location l, $l \in L$, depending on the charging rate of the installed chargers at that location. By minimizing this total damage cost for each charging event, the objective is to reduce the number of charging events and prioritize charging events at locations where chargers with lower charging rates are installed.

The MDEBARSP consists in assigning the EBs to the vehicle blocks and scheduling their recharges, both overnight and en-route, such that each block is serviced by an EB, the EBs do not run out of energy, the number of available chargers at each charging location is never exceeded, and the sum of the energy costs and the long-term damage costs is minimized. The notation used is summarized in Table 3.1, which also includes notation introduced in the next section.

3.3 Mixed integer programming formulation

In this section, we introduce a two-commodity network flow MILP formulation for the MDEBARSP. One commodity models the flow of the EBs through the vehicle blocks to determine the sequences of blocks assigned to the EBs over the planning horizon. The other commodity models, for each day and each charging location, the flow of the chargers through the EB recharging events to determine the recharge schedule of the EBs. Our model builds upon that of VENDÉ, DESAULNIERS, KERGOSIEN et MENDOZA, 2023 for a multi-day EB assignment and overnight recharge scheduling problem.

The problem is defined on a directed graph $G = (N, A)$, where $N = \bigcup_{\substack{d \in D \\ l \in L}} \left(B_{d,l} \cup \{c_{d,l}\}\right)$ is the node set and $A = A^{bus} \cup \left(\bigcup_{\substack{d \in D \\ l \in L}} A^{chg}_{d,l}\right)$ is the arc set. The arcs subset A^{bus} represents the possible block successions for an EB. There exists an arc $(i, j) \in A^{bus}$ if one of the following two sets of conditions is met : i) $d \neq |D|$, $i \in B_d$ and $j \in B_{d+1}$; ii) $d = |D|$, $i \in B_d$ and $j \in B_1$. Thus, the EBs flow on the subnetwork that comprises the block nodes B and the arcs in A^{bus}. A feasible bus assignment solution corresponds to a set of $|V|$ disjoint paths, all starting from a node in B_1, ending at a node in B_1, and visiting exactly one node in each set B_d, $d \in D \backslash \{1\}$. The arcs subset $A^{chg}_{d,l}$ represents the possible

TABLE 3.1 – Sets and parameters used in the model

Sets	
D	Set of days in the planning horizon
L	Set of charging locations
B	Set of vehicle blocks
B_d	Set of vehicle blocks on day d
B^i	Set of sub-blocks of block i
$B_{d,l}$	Set of sub-blocks on day d starting at charging location l
V	Set of available EBs
C	Set of chargers
C_l	Set of chargers at charging location l
P_l	Set of linear pieces in the charging function at charging location l
A	Set of arcs
A^{bus}	Subset of arcs for the bus assignment
$A^{chg}_{d,l}$	Subset of arcs for the charger assignment before day d at charging location l
N	Set of nodes
Parameters	
$h^E_{i,k}$	Ending time of k^{th} sub-block of block i
$h^S_{i,k}$	Starting time of k^{th} sub-block of block i
$l^E_{i,k}$	Ending location of k^{th} sub-block of block i
$l^S_{i,k}$	Starting location of k^{th} sub-block of block i
$e_{i,k}$	Energy consumption along k^{th} sub-block of block i
l_0	Depot
Q	Battery charging capacity
SOC^{max}	Maximum SoC of the battery
SOC^{min}	Minimum SoC of the battery
f_l	Piecewise linear charging function at charging location l
$q_{l,p}$	Maximum SoC difference on piece p at charging location l
$\theta_{l,p}$	Maximum charging time on piece p at charging location l
$\gamma_{l,p}$	Maximum charging cost on piece p at charging location l
ρ_l	Unit damage cost spent for each charging event performed at charging location l
M	Large constant (time span of the planning horizon)
$c_{d,l}$	Charger node at charging location l on day d

successions of charging events and also includes arcs connecting the sequence with the chargers installed at location l, at the beginning and the end of the charging sequence. A charging event is associated with a sub-block in $B_{d,l}$ and is performed on the EB to be assigned to the block of this sub-block. To each set $B_{d,l}$ is associated a node $c_{d,l}$ representing the chargers installed at location l. There is an arc $(i,j) \in A^{chg}_{d,l}$ if one of the following three sets of conditions is met : i) $i = c_{d,l}$ and $j \in B_{d,l}$; ii) $j = c_{d,l}$ and $i \in B_{d,l}$; and iii) $i, j \in B_{d,l}$ and $i \neq j$. Thus, to model the charger assignment on day $d \in D$ at charging location $l \in L$, there is a subnetwork that contains the nodes in $B_{d,l} \cup \{c_{d,l}\}$ and the arcs in $A^{chg}_{d,l}$. A feasible charger sequence for day d at charging location l is obtained as a subset of at most $|C_l|$ circuits starting and ending at $c_{d,l}$ and visiting exactly each node in $B_{d,l}$ exactly once. In this case, we assume that each EB needs to be recharged every night and between every sub-blocks but possibly for a duration of zero units of time (which, in practice, corresponds to not recharging).

Figure 3.2 shows an example of graph G defined for the MDEBARSP with 3 days, 2 EBs, 2 vehicle blocks per day, the first one consisting of 3 sub-blocks and the second one of 2 sub-blocks, one charger at the depot (O) for overnight charging, and one charger on the network (E) for en-route charging. The block b for day a is denoted (a,b). The set of paths represents a feasible solution where the blue EB is assigned to the sequence of blocks $(1,1)$ – $(2,2)$ – $(3,2)$ – $(1,1)$, and the red EB to $(1,2)$ – $(2,1)$ – $(3,1)$ – $(1,2)$. The arcs composing these paths belong to A^{bus}. The sub-blocks are denoted by (a,b,c), a and b have the same meaning as the blocks notation, and c denotes the sub-block. Given that each sub-block is associated to a unique charging event, (a,b,c) denotes a sub-block and its preceding charging event. During the night before day one, between days three and one, the overnight charger (O) recharges the blue EB first then the red EB, resulting in the following charging event sequence on charger O : $(1,1,X)$ – $(1,2,A)$. During day one, the en-route charger (E) recharges the blue EB twice and then the red EB once, resulting in the following charging event sequence on charger E : $(1,1,Y)$ – $(1,1,Z)$ – $(1,2,B)$. During the night between days one and two, charger O recharges the red and blue EBs in that order, resulting in the following charging event sequence on charger O : $(2,1,X)$ – $(2,2,A)$. During day two, charger E recharges the blue EB, followed by the red EB, and then the blue EB again, resulting in the following charging event sequence on charger E : $(2,1,Y)$ – $(2,2,B)$ – $(2,1,Z)$. During the night between days two and three, charger O recharges the blue and red EBs in that order, resulting in the following charging event sequence on charger O : $(3,2,A)-(3,1,X)$. During day three, charger E recharges the blue EB once and then the red EB twice, resulting in the following charging event sequence on charger E : $(3,2,B)-(3,1,Y)-(3,1,Z)$. The arcs composing these charging sequences belong to $A^{chg}_{d,l}, \forall d \in D, l \in L$. Note that arcs that are not in the solution have been omitted.

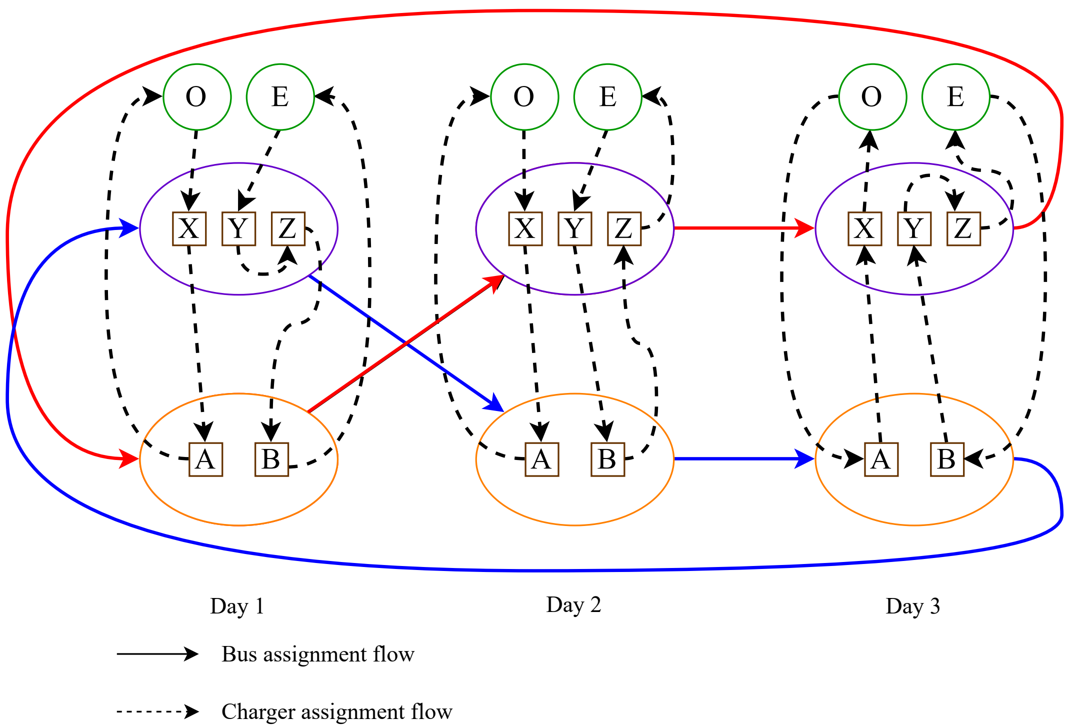

FIGURE 3.2 – Graph G representing the problem with block 1 of each day in purple and block 2 in orange, sub-block set $\bigcup_{i \in B} B^i$ in brown and charger node set C in green

The decision variables in the proposed MILP are as follows :

— $x_{i,j}$: Binary variable equal to 1 whether an EB covers block j immediately after block i, 0 otherwise, $\forall (i,j) \in A^{bus}$.

— $y_{i,j}$: Nonnegative variable indicating the SoC of the EB after completing block i if $x_{i,j} = 1$, 0 otherwise, $\forall (i,j) \in A^{bus}$.

— $\underline{q}_{i,k}$: Nonnegative variable indicating the SoC of the EB performing block i right before starting the charging event preceding the k^{th} sub-block of block i, $\forall i \in B, k \in$

B^i.

— $\bar{q}_{i,k}$: Nonnegative variable indicating the SoC of the EB performing block i right after ending the charging event preceding the k^{th} sub-block of block i, $\forall i \in B, k \in B^i$.

— $t_{i,k}$: Nonnegative variable specifying the required charging time of the charging event preceding the k^{th} sub-block of block i, $\forall i \in B, k \in B^i$.

— $a_{i,k}$: Continuous variable indicating the starting time of the charging event preceding the k^{th} sub-block of block i, $\forall i \in B, k \in B^i$.

— $r_{i,k}$: Binary variable equal to 1 whether a charging event takes place for the EB performing block i right before the k^{th} sub-block of block i, and 0 otherwise, $\forall i \in B, k \in B^i$.

— $\underline{\lambda}^p_{i,k}$ (resp. $\bar{\lambda}^p_{i,k}$) : Nonnegative variable indicating the fulfilled fraction of piece p of the SoC charging function when the EB performing block i arrives at (resp. leaves) the charging location right for the the charging event preceding the k^{th} sub-block of block i, $\forall i \in B, k \in B^i, p \in P$.

— $u^{j,m}_{i,k}$: Binary variable equal to 1 whether a charger is used to charge the EB assigned to block j immediately after the EB assigned to block i, respectively right before the m^{th} sub-block of block j and the k^{th} sub-block of block i, and 0 otherwise, $\forall d \in D, (i,j) \in A^{chg}_{d,l}, k \in B^i, m \in B^j$.

Figure 3.3 illustrates the relationships between variables and parameters associated with a sub-block k of block i and its preceding charging event. We consider two cases : either sub-block k is the first of its block, then it would be preceded by an overnight charging event (a); or sub-block k is not the first of its block (so $k = 1$), then it would be preceded by an en-route charging event (b). In the first case, if $x_{j,i} = 1$, then blocks j and i are assigned consecutively to the same EB, allowing it to be available for charging at time $h^E_{j,|B^j|}$ before performing the first sub-block of block i. In the second case, sub-blocks $k-1$ and k are assigned consecutively to the same EB, allowing it to be available for charging at time $h^E_{i,k-1}$ before performing the sub-block k of block i. After the charging event, the assigned EB should start the sub-block k at $h^S_{i,k}$ and should finish at $h^E_{i,k}$. The charging event between these two sub-blocks, whether they belong to the same block or not, starts at time $a_{i,k}$ and lasts $t_{i,k}$ units of time. From the energy point of view, variable $y_{j,i}$ indicates the SoC of the EB at the end of block j. This value is equal to the SoC $\underline{q}_{i,1}$ before starting the recharge. If the consecutive sub-blocks belong to the same block, $\underline{q}_{i,k}$ would be equal to $\bar{q}_{i,k-1} - e_{i,k-1}$ that indicates the SoC of the EB after operating sub-block $k-1$ with the associated energy consumption. Then, variable $\bar{q}_{i,k}$ indicates the SoC after the recharge and depends on $\underline{q}_{i,k}$ and the recharging time $t_{i,k}$. Finally, $e_{i,k}$ provides the net energy consumed when performing sub-block k of block i.

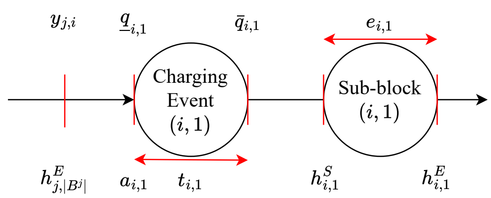

(a) Overnight charging event

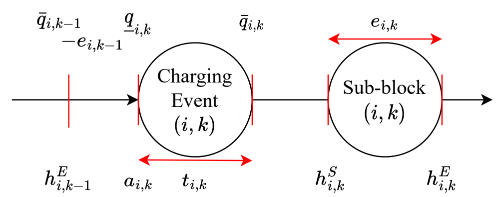

(b) En-route charging event

FIGURE 3.3 – Variables and parameters associated with a sub-block k of block i and its preceding charging event (energy-related variables/parameters on top; time-related ones at the bottom).

To improve readability, we introduce the proposed MILP in two steps. First, we present the model using the charging functions f_l or, more precisely, their inverse f_l^{-1}, to englobe all charging decisions. Then, we discuss how to express these piecewise linear functions using additional variables and constraints.

The objective function (3.1) minimizes the total charging costs and the battery degradation costs incurred by the presence of a charging event. Note that the $\bar{\lambda}^p_{i,k}$ and $\underline{\lambda}^p_{i,k}$ variables depend on the $\underline{q}_{i,k}$ and $\bar{q}_{i,k}$ variables, and their relationship will be made explicit only in the second part of the model below.

$$\min \quad \sum_{i \in B} \sum_{k \in B^i} \Big(\sum_{p \in P_{l^S_{i,k}}} [\gamma_{p,l^S_{i,k}} (\bar{\lambda}^p_{i,k} - \underline{\lambda}^p_{i,k})] + \rho_{l^S_{i,k}} r_{i,k} \Big) \tag{3.1}$$

This MILP includes four sets of constraints : the first set of constraints models the EB-to-block assignment; the second one tracks the SoC variations along the nodes of the network; the third set computes the charging times and schedules the charging events; and the last one models the piecewise linear charging functions.

Constraints (3.2)–(3.3) ensure that each block has a successor and a predecessor, creating a feasible bus assignment as a set of $|V|$ disjoint paths.

$$\sum_{j:(i,j)\in A^{bus}} x_{i,j} = 1, \qquad \forall i \in B \tag{3.2}$$

$$\sum_{j:(j,i)\in A^{bus}} x_{j,i} = 1, \qquad \forall i \in B \tag{3.3}$$

Constraints (3.4) restrict variables $y_{i,j}$ to take a positive value only if there is an EB flow on arc (i,j). Constraints (3.5)–(3.7) compute the SoC between consecutive sub-blocks. Constraints (3.8)–(3.9) stipulate that the SoC of the EB assigned to each sub-block k from block i must be within a feasible range.

$$y_{i,j} \leq SOC^{max}\, x_{i,j}, \qquad \forall (i,j) \in A^{bus} \tag{3.4}$$

$$\sum_{j:(i,j)\in A} y_{i,j} = \bar{q}_{i,|B^i|} - e_{i,|B^i|}, \qquad \forall i \in B \tag{3.5}$$

$$\underline{q}_{i,1} = \sum_{j:(j,i)\in A^{bus}} y_{j,i}, \qquad \forall i \in B \tag{3.6}$$

$$\bar{q}_{i,k} - e_{i,k} = \underline{q}_{i,k+1}, \qquad \forall i \in B, k, k+1 \in B^i \tag{3.7}$$

$$\bar{q}_{i,k} \geq e_{i,k} + SOC^{min}, \qquad \forall i \in B, k \in B^i \tag{3.8}$$

$$\bar{q}_{i,k} \leq SOC^{max}, \qquad \forall i \in B, k \in B^i \tag{3.9}$$

Constraints (3.10)–(3.12) impose a lower bound on the starting time of the recharge before sub-block k from block i depending on its predecessor sub-block, whereas constraints (3.13) ensure recharge ends before the starting time of the sub-block. Constraints (3.14) determine the time required to charge the EB assigned to sub-block k from block i from a SoC of $\underline{q}_{i,k}$ to a SoC of $\bar{q}_{i,k}$. These constraints are nonlinear and will be expressed differently below (see constraints (3.26)–(3.43)). Constraints (3.15) bound the charging time with the presence of a charging event. Constraints (3.16)–(3.18) define the flow structure for the chargers on each day at each charging location, whereas constraints (3.19) impose to schedule a charging event before each sub-block on each day at each charging location. Constraints (3.20) ensure that there is no overlap between two consecutive charging events.

$$a_{i,1} \geq \sum_{j:(j,i)\in A^{bus}} x_{j,i}\, h^E_{j,|B^j|}, \qquad \forall i \in B \backslash B_1 \tag{3.10}$$

$$a_{i,1} \geq \sum_{j:(j,i)\in A^{bus}} x_{j,i}\, h^E_{j,|B^j|} - |D|\, M, \qquad \forall i \in B_1 \tag{3.11}$$

$$a_{i,k} \geq h^E_{i,k-1}, \qquad \forall i \in B, k-1, k \in B^i \tag{3.12}$$

$$a_{i,k} + t_{i,k} \leq h^S_{i,k}, \qquad \forall i \in B, k \in B^i \tag{3.13}$$

$$t_{i,k} = f^{-1}_{l^S_{i,k}}(\bar{q}_{i,k}) - f^{-1}_{l^S_{i,k}}(\underline{q}_{i,k}), \qquad \forall i \in B, k \in B^i \tag{3.14}$$

$$t_{i,k} \leq r_{i,k} \sum_{p \in P_{l^S_{i,k}}} \theta_{p,l^S_{i,k}}, \qquad \forall i \in B, k \in B^i \tag{3.15}$$

$$\sum_{(i,k)\in B_{d,l}} u^{i,k}_{c_{d,l},1} \leq |C_l|, \qquad \forall d \in D, l \in L \tag{3.16}$$

$$\sum_{(i,k)\in B_{d,l}} u^{c_{d,l},1}_{i,k} \leq |C_l|, \qquad \forall d \in D, l \in L \tag{3.17}$$

$$\sum_{(j,m)\in B_{d,l}\cup\{(c_{d,l},1)\}\backslash\{(i,k)\}} (u^{i,k}_{j,m} - u^{j,m}_{i,k}) = 0, \qquad \forall d \in D, l \in L, (i,k) \in B_{d,l} \tag{3.18}$$

$$\sum_{(j,m)\in B_{d,l}\cup\{(c_{d,l},1)\}\backslash\{(i,k)\}} u^{j,m}_{i,k} = 1, \qquad \forall d \in D, l \in L, (i,k) \in B_{d,l} \tag{3.19}$$

$$a_{i,k} + t_{i,k} \leq a_{j,m} + M(1 - u^{j,m}_{i,k}), \qquad \forall d \in D, l \in L, (i,k), (j,m) \in B_{d,l} \tag{3.20}$$

Finally, constraints (3.21)-(3.25) define the domains of the decision variables.

$$x_{i,j} \in \{0,1\}, \qquad \forall (i,j) \in A^{bus} \tag{3.21}$$

$$y_{i,j} \geq 0, \qquad \forall (i,j) \in A^{bus} \tag{3.22}$$

$$r_{i,k} \in \{0,1\}, \qquad \forall i \in B, k \in B^i \tag{3.23}$$

$$\underline{q}_{i,k}, \bar{q}_{i,k}, t_{i,k} \geq 0, \qquad \forall i \in B, k \in B^i \tag{3.24}$$

$$u^{j,m}_{i,k} \in \{0,1\}, \qquad \forall d \in D, l \in L, (i,k), (j,m) \in B_{d,l} \tag{3.25}$$

To model the piecewise linear charging function f_l, we introduce the following additional variables :

— $\underline{w}_{i,k}^p$ (resp. $\bar{w}_{i,k}^p$) : Binary variable equal to 1 whether SoC $\underline{q}_{i,k}$ (resp. $\bar{q}_{i,k}$) is on piece p of the charging function $f_{l_{i,k}^S}$ and to 0 otherwise, $\forall i \in B, k \in B^i, p \in P_{l_{i,k}^S}$.

— $\underline{\theta}_{i,k}$ (resp. $\bar{\theta}_{i,k}$) : Nonnegative variable equal to $f_{l_{i,k}^S}^{-1}(\underline{q}_{i,k})$ (resp. $f_{l_{i,k}^S}^{-1}(\bar{q}_{i,k})$), $\forall i \in B, k \in B^i$.

We also replace constraints (3.14) by the following constraints :

$$t_{i,k} = \bar{\theta}_{i,k} - \underline{\theta}_{i,k}, \qquad \forall i \in B, k \in B^i \tag{3.26}$$

$$\sum_{p \in P_{l_{i,k}^S}} \underline{w}_{i,k}^p = 1, \qquad \forall i \in B, k \in B^i \tag{3.27}$$

$$\underline{q}_{i,k} \geq \Big(\sum_{\substack{p' \in P_{l_{i,k}^S} : \\ p' < p}} q_{p',l_{i,k}^S} \Big)\, \underline{w}_{i,k}^p, \qquad \forall i \in B, k \in B^i, p \in P_{l_{i,k}^S} \tag{3.28}$$

$$\underline{q}_{i,k} \leq \Big(\sum_{\substack{p' \in P_{l_{i,k}^S} : \\ p' \leq p}} q_{p',l_{i,k}^S} \Big)\, \underline{w}_{i,k}^p + (1 - \underline{w}_{i,k}^p)\, Q, \qquad \forall i \in B, k \in B^i, p \in P_{l_{i,k}^S} \tag{3.29}$$

$$\underline{\lambda}_{i,k}^p \geq \sum_{\substack{p' \in P_{l_{i,k}^S} : \\ p' > p}} \underline{w}_{i,k}^{p'}, \qquad \forall i \in B, k \in B^i, p \in P_{l_{i,k}^S} \tag{3.30}$$

$$\underline{\lambda}_{i,k}^p \leq 1 - \sum_{\substack{p' \in P_{l_{i,k}^S} : \\ p' < p}} \underline{w}_{i,k}^{p'}, \qquad \forall i \in B, k \in B^i, p \in P_{l_{i,k}^S} \tag{3.31}$$

$$\underline{q}_{i,k} = \sum_{p \in P_{l_{i,k}^S}} q_{p,l_{i,k}^S} \cdot \underline{\lambda}_{i,k}^p, \qquad \forall i \in B, k \in B^i \tag{3.32}$$

$$\underline{\theta}_{i,k} = \sum_{p \in P_{l_{i,k}^S}} \theta_{p,l_{i,k}^S} \cdot \underline{\lambda}_{i,k}^p, \qquad \forall i \in B, k \in B^i \tag{3.33}$$

$$\sum_{p \in P_{l_{i,k}^S}} \bar{w}_{i,k}^p = 1, \qquad \forall i \in B, k \in B^i \tag{3.34}$$

$$\bar{q}_{i,k} \geq \Big(\sum_{\substack{p' \in P_{l_{i,k}^S} : \\ p' < p}} q_{p',l_{i,k}^S} \Big)\, \bar{w}_{i,k}^p, \qquad \forall i \in B, k \in B^i, p \in P_{l_{i,k}^S} \tag{3.35}$$

$$\bar{q}_{i,k} \leq \Big(\sum_{\substack{p' \in P_{l^S_{i,k}}: \\ p' \leq p}} q_{p', l^S_{i,k}} \Big) \bar{w}^p_{i,k} + (1 - \bar{w}^p_{i,k})\, Q, \qquad \forall i \in B, k \in B^i, p \in P_{l^S_{i,k}} \tag{3.36}$$

$$\bar{\lambda}^p_{i,k} \geq \sum_{\substack{p' \in P_{l^S_{i,k}}: \\ p' > p}} \bar{w}^{p'}_{i,k}, \qquad \forall i \in B, k \in B^i, p \in P_{l^S_{i,k}} \tag{3.37}$$

$$\bar{\lambda}^p_{i,k} \leq 1 - \sum_{\substack{p' \in P_{l^S_{i,k}}: \\ p' < p}} \bar{w}^{p'}_{i,k}, \qquad \forall i \in B, k \in B^i, p \in P_{l^S_{i,k}} \tag{3.38}$$

$$\bar{q}_{i,k} = \sum_{p \in P_{l^S_{i,k}}} q_{p, l^S_{i,k}} \cdot \bar{\lambda}^p_{i,k}, \qquad \forall i \in B, k \in B^i \tag{3.39}$$

$$\bar{\theta}_{i,k} = \sum_{p \in P_{l^S_{i,k}}} \theta_{p, l^S_{i,k}} \cdot \bar{\lambda}^p_{i,k}, \qquad \forall i \in B, k \in B^i \tag{3.40}$$

$$\underline{\theta}_{i,k}, \bar{\theta}_{i,k} \geq 0, \qquad \forall i \in B, k \in B^i \tag{3.41}$$

$$0 \leq \underline{\lambda}^p_{i,k}, \bar{\lambda}^p_{i,k} \leq 1, \qquad \forall i \in B, k \in B^i, p \in P_{l^S_{i,k}} \tag{3.42}$$

$$\underline{w}^p_{i,k}, \bar{w}^p_{i,k} \in \{0,1\}, \qquad \forall i \in B, k \in B^i, p \in P_{l^S_{i,k}} \tag{3.43}$$

Constraints (3.26) are equivalent to constraints (3.14) but expressed linearly using the $\underline{\theta}_{i,k}$ and $\bar{\theta}_{i,k}$ variables. For each sub-block $k \in B^i$ from block $i \in B$, constraints (3.27)–(3.33) are dedicated to the computation of $\underline{\theta}_{i,k}$ in function of $\underline{q}_{i,k}$. Indeed, constraints (3.27) impose that a single piece be selected, whereas constraints (3.28)–(3.29) ensure that $\underline{q}_{i,k}$ is part of this piece. Constraints (3.30) and (3.31) set the fulfilled fraction of a piece equal to 1 if it is before the selected piece and to 0 if it is after, respectively. Constraints (3.32) allow to compute the value of $\underline{\lambda}^p_{i,k}$ for the selected piece p given the other $\underline{\lambda}^{p'}_{i,k}$ values. Ultimately, the value of $\underline{\theta}_{i,k}$ is obtained through constraints (3.33) as a function of the $\underline{\lambda}^p_{i,k}$ variables. Constraints (3.34)–(3.40) play a similar role, but they are used to compute for each sub-block $k \in B^i$ from block $i \in B$ the value of $\bar{\theta}_{i,k}$ in function of $\bar{q}_{i,k}$. Finally, the domains of the new variables are restricted by constraints (3.41)–(3.43).

In the following, we refer to the MILP (3.1)–(3.13), (3.15)–(3.43) as the MDEBARSP-MILP.

3.4 An iterative two-phase matheuristic

The MDEBARSP-MILP can be solved using the branch-and-cut algorithm embedded in commercial MILP solver (see Section 3.5 for details). However, our computational results indicated that even moderately-sized instances are difficult to solve to optimality. In order to find better solutions for such instances, we propose an iterative two-phase matheuristic described below.

The iterative two-phase matheuristic (ITPM) consists of two main stages on each iteration, as the name suggests. The first stage focuses exclusively on decisions related to the presence of charging events between sub-blocks, and sequencing en-route charging events. This set of decisions is called *intra-block decisions*. This stage also determines the required charging time of overnight and en-route charging events. The second stage focuses on decisions regarding the EB-to-block assignment and the sequence of overnight charging events, later referenced as *inter-block decisions*. The main loop is started and be restarted by an initialization method, which sets inter-block decisions. Algorithm 5 provides a high-level description of the proposed iterative two-phase matheuristic.

Algorithme 5 : Iterative two-phase matheuristic (ITPM)

```
Initialize inter-block decisions ;
while time limit is not exceeded do
    Improve intra-block and charging time decisions given inter-block decisions :
      EB-to-block assignment and sequences of overnight charging events ;
    if feasible integer solution is found then
        Improve inter-block decisions given intra-block and charging time
          decisions, and EB availability time ;
    else
        Reinitialize inter-block decisions with random ;
    end
end
```

3.4.1 Intra-block and charging time decisions stage

The first stage of the iteration, Line 3, uses a set of inter-block decisions, for its decision-making process. Given a fixed set of EB-to-block assignments and a fixed sequence for overnight charging events for each charger installed at the depot, the first stage of the iteration's method determines : whether a charging event takes place for an EB before performing a sub-block $r_{i,k}$; the required charging time for every charging event $t_{i,k}$, for both overnight and en-route ; and the sequence of en-route charging events for each en-route charger, represented by $u_{i,k}^{j,m}$ variables. The decision-making process takes into consideration constraints EB availability time, sub-block consumption, charger capacity, and EB's SoC. These intra-block and charging time decisions are made by solving a mathematical model, noted INTRA-MILP, corresponding to objective function (3.1) and constraints (3.4)–(3.13), (3.15)–(3.43), with $x_{i,j}$, and $u_{i,k}^{j,m}$ variables fixed at values given by the inter-block decisions. Note that not all $u_{i,k}^{j,m}$ are set by the inter-block decisions, bot only the ones corresponding to overnight charging events. To prevent this stage from consuming all the allocated computation time for the method, a computation time limit is imposed.

3.4.2 Inter-block decisions stage

The intra-block and charging time decisions are subsequently passed on to the second stage. Line 5 uses the intra-block decisions given by the previous stage of the method and looks for a new set of EB-to-block assignments and a new sequence for the overnight charging events. In order to make decisions in this stage, a MILP is solved and this MILP is equivalent to the MDEBARSP-MILP, with fixed $t_{i,k}$, $r_{i,k}$, and $u_{i,k}^{j,m}$ fixed variables fixed at values given by the intra-block decisions. Note that not all are set by the intra-block decisions, but only the ones corresponding to en-route charging events. However, the objective function to evaluate a solution is not the same as the MDEBARSP-MILP. The problem solved during this stage aims to maximize the total sum of overnight charging event durations (3.44).

$$\max \quad \sum_{i \in B} t_{i,1} \tag{3.44}$$

The resulting MILP, noted INTER-MILP, consists of objective function (3.44) and constraints (3.2)–(3.13), (3.15)–(3.43). The model determines the EB-to-block assignments and the charging sequences at the depot during each night in order to maximize the total overnight charging time. Thus, the intra-block decision stage could use these sequences to create longer charging events at night, when charging costs are lower. If EBs charge sufficiently at night, this would help to eliminate some of the en-route charging events between sub-blocks, leading to lower costs in the objective function (3.1).

Given that the intra-block decisions are an input of the model, there are no additional decisions to make regarding the content of the blocks and those blocks are considered as unbreakable objects. The problem solved during this stage is similar to the MDEBAOSP (VENDÉ, DESAULNIERS, KERGOSIEN & MENDOZA, 2023), which assigns a set of blocks, considered as unbreakable objects, to EBs and schedules their overnight charging events. The differences between both problems are the objective function and the cyclic aspect of the planning horizon, which are not considered in VENDÉ, DESAULNIERS, KERGOSIEN et MENDOZA, 2023. In order to take into account the SoC variation of the EB performing the blocks and anticipate discharges occurring during the day, some preprocessing of the information provided by the intra-block decision stage is necessary. The net energy consumption e_i for each block $i \in B$, uses the consumption of the sub-blocks that make them up, as well as the en-route charging events and is computed as $e_i = \bar{q}^*_{i,1} - (\bar{q}^*_{i,|B^i|} - e_{i,|B^i|})$. The maximum decrease of energy e_i^{maxD} for each block $i \in B$, uses the SoC of the EBs after each en-route charging event during block i and is computed as $e_i^{maxD} = \max_{k \in B^i} \bar{q}^*_{i,1} - (\bar{q}^*_{i,k} - e_{i,k})$. The maximum increase of energy e_i^{maxI} for each block $i \in B$, uses the SoC of the EBs after each en-route charging event during block i and is computed as $e_i^{maxI} = \max_{k \in B^i} \bar{q}^*_{i,k} - \bar{q}^*_{i,1}$. $\bar{q}^*_{i,k}$ indicates the SoC of the EB performing k^{th} sub-block of block i after its preceding charging event as computed during the intra-block decision stage. By using the MDEBAOSP model instead of the INTER-MILP, we would eliminate some continuous variables, some constraints, and some arcs from the graph describing the problem, which make it easier to solve.

The INTER-MILP is solved using a commercial solver. In order to help the solver, we determine an upper and a lower bound of the value of the objective function of the INTER-MILP (3.44). Those bounds are derived from the feasible solution computed in the previous stage. The lower bound is equal to the total charging duration of EBs overnight provided by the solution found at the previous intra-block stage. It is computed as $LB = \sum_{i \in B} t^*_{l,1}$, where $t^*_{i,1}$ is the required charging time before performing the first sub-block of block i, $i \in B$. The upper bound is determined as the minimum of two values : the total time available to use all the chargers installed at the depot, computed as $chargers\_time = \sum_{d \in D} |B_d| \big(\max_{i \in B_d} h^S_{i,1} - \min_{i \in B_{d-1}} h^E_{i,|B^i|} \big)$; and an overestimate of the time needed to fully charge all EBs, computed as $EBs\_time = |B| \big(f^{-1}_{l_0}(SOC^{max}) - f^{-1}_{l_0}(SOC^{min}) \big)$. Thus, the upper bound is computed as $UB = \min(chargers\_time, EBs\_time)$. To prevent this stage from consuming all the allocated execution time for the method, a computation time limit imposed. Given that it can be difficult to close the optimality gap for the INTER-MILP, an optimality gap of 5% to reach is provided to the solver.

One could note that the matheuristics proposed by VENDÉ, DESAULNIERS, KERGOSIEN et MENDOZA, 2023 are not applicable for solving this version of the EB assignment and overnight charging problem because of the major differences between the MDEBAOSP and the INTER-MILP. These matheuristics are based on a problem decomposition approach, where the EB-to-block assignment is computed separately from long-term damages to the battery optimization. In the daily-assign-then schedule method, the EB-to-block assignment was performed by considering only the block to come and not the entire sequence of blocks. This method can be effective if an initial day and a final day are considered. However, in the MDEBARSP, the planning horizon is cyclic, which eliminates the notion of an initial or final day. This cyclic nature of the problem introduces challenges in finding feasible assignments. In the assign-then schedule method, the charging events were rescheduled in order to prevent long-term damages to the battery and only calendar aging was considered. Given that the type of long-term damages to the battery being addressed in the MDEBARSP is different, the method is unsuitable for our problem.

3.4.3 Initialization stage

In order to quickly enter into the ITPM's main loop, some initial inter-block decisions must be made. Line 1 looks for an initial EB-to-block assignment and a sequence for overnight charging events. This stage unfolds in two steps. First, an initial sequence for charging events is computed for each charger. For each pair of day $d \in D$ and charging location $l \in L$, the charging events associated to day d and location l are sorted by either increasing starting time of the associated block for an overnight charging event, i.e. $(i,1) < (j,1) \Leftrightarrow h^S_{i,1} < h^S_{j,1}, i,j \in B_d$; or by increasing ending time of the associated previous sub-block for an en-route charging event, i.e. $(i,k) < (j,m) \Leftrightarrow h^E_{i,k-1} < h^E_{j,m-1}, \forall (i,k),(j,m) \in B_{d,l}, l \in L \backslash \{l_0\}$. Then, to schedule the charging events on chargers, we assign the charging events one by one in the order defined above, to the first available charger. The first available charger is defined as the charging whose starting time of sub-block associated with the last assigned charging event is the smallest. A pseudocode of the charging sequence initialization procedure is given in Section 29. This procedure need to be called for each day $d \in D$ and charging location $l \in L$. After the charging sequences are established, a mathematical model corresponding to constraint s(3.1)–(3.13), (3.15), (3.20)–(3.43) including the fixed $u^{j,m}_{i,k}$ variables is solved by a solver that stops at the first feasible solution found. From this feasible solution, an initial EB-to-block assignment and a sequence for overnight charging events can be extracted.

3.4.4 Reinitialization stage

During the algorithm's main loop, the intra-block decisions stage (Line 3) cannot find a feasible solution from the EB-to-block assignments and the sequences for overnight charging events determined during the inter-block decision stage (Line 5) in some cases. During this stage, maximizing the total sum of overnight charging events' durations may lead to the creation of a set of charging events with unbalanced durations, some of which are very small to allow the creation of larger events. Although the durations of the overnight charging events are not transmitted to the intra-block decisions stage, they are used to determine the EB-to-block assignments. This results in sequences of blocks with potentially little time for overnight charging for some blocks. The associated EBs leave the depot with limited SoC and may fail to reach the first installed en-route charger. Consequently, no feasible solution with these EB-to-block assignments and these sequences for overnight charging events can be found. In order to continue the iterative process with a new feasible solution, a randomized version of the initialization method, performed at Line 1, is called at Line 7 performs a randomized version of the initialization method. After the charging events have been sorted, we randomly select a single charging event from the first K charging events, and we assign it to the first available charger, until there are no events left to be assigned. A mathematical solver is then called to solve the MDEBARSP-MILP, with the variables $u_{i,j}$ fixed, however the solver stops at the first feasible solution found. This randomized method produces new sequences of charging events and thus a new set of EB-to-block assignments that can be explored by the algorithm. One could note that if $K = 1$, this method would produce the exact same result as the initialization method.

3.5 Computational experiments

We implemented the proposed algorithms in C++. Our implementation uses IBM ILOG CPLEX 20.1 to solve the MILPs with a default optimality gap tolerance of 0.001%. To evaluate the effectiveness of our proposed solution methods, we conducted computational experiments on instances generated from operational data provided by our industrial partner, GIRO Inc., one of the world-leading optimization software companies for public transit companies. All computations were carried out on a 64-bit computer with an Intel Gold 6148 Skylake CPU (2.40 GHz), 10 gigabytes of main memory, and CentOS Linux 7 operating system. In the following section, we first provide a description of the instances and subsequently present and discuss our results and findings. The reported gaps in the results are calculated as the relative difference between a reference value and an observed value using the following formula : $gap = \frac{obs-ref}{ref}$.

3.5.1 Instance generation

GIRO Inc. provided us with several real-world instances coming from three European public transit operators. These instances describe the set of blocks performed during a single day, with their sub-blocks and all their related information. For each of the three companies, the set of blocks is repeated every day. For each sub-block of a block, the instance indicates the starting time, ending time, starting location, ending location and energy consumption along the sub-block. In all instances, there is one EB per block and the fleet is homogeneous. Therefore, we did not need to add dummy blocks to these instances. The EBs have a battery with capacity of $Q = 290$ kWh and their SoC must remain between $SOC^{min} = 10\%$ and $SOC^{max} = 100\%$.

In order to generate instances from these three public transit networks, we used a parameter, called target SoC threshold, that influences the division of blocks into a set of sub-blocks by inserting en-route charging opportunities during the day. When a target SoC threshold is reached by the EB performing the block, the current sub-block is terminated to allow the EB to set a course for a charger. Thus, the higher the SoC target, the greater the charging opportunities. Assuming that an EB starts its block with a full battery, instances have been generated according to three possible SoC targets : 30% SoC (low charging opportunities), 50% SoC (middle charging opportunities), and 70% SoC (high charging opportunities). Additionally, each instance is generated with a version where the duration between sub-blocks, dedicated to charging, is longer. Although the lines covered by all the buses remain unchanged, the blocks and their composition differ. With these configurations, the generated instances contain between 38 and 41 blocks per day.

Our industrial partner shared with us a lot of information regarding bus trips, but only a few regarding the charging infrastructure. A parameter that they did not share with us was the EBs' battery charging function f. This function is difficult to establish in close form because it depends on many different and (sometimes) difficult to measure factors (e.g., the power used, the degradation state of the battery, and the room temperature). Consequently, EB operators have limited knowledge about the precise charging function of their vehicles and often rely on approximations when planning recharging events. In our instances, we adopted the piecewise linear approximation proposed by MONTOYA et al., 2017 to estimate the charging function. Specifically, we adjusted their charging function to match the average charging rate of the three operators' charging infrastructure, provided by the industrial partner, for both the overnight (slow) chargers and en-route (fast) chargers. Finally, we used the energy costs reported in PELLETIER et al., 2018 as our charging cost $\gamma_{l,p}$, by considering low energy costs for $\gamma_{l_0,p}, p \in P_{l_0}$ because the associated charging events are usually operated at night during off-peak hours, and high energy costs otherwise. We also generated instances where energy costs are constants for all chargers, set as low energy costs.

Transit companies rarely consider battery aging costs when planning their overnight charging events. Therefore, our partner did not have data to share on this parameter. To complete our instances, we computed the unit damage cost spent for each charging event performed, which depends on the charging rate of the used charger and so on the charging location. This cost is computed as a function of the purchasing cost of the battery and the time required to fully recharge the battery (ECHEVERRI GUZMAN, 2020). A higher charging rate induces shorter charging durations and, therefore, higher unit damage costs for each charging event performed. Considering a battery price of USD 150,000 we obtained a unit damage cost ρ_l of USD 26.4 for overnight charging events at the depot and USD 38.5 for en-route charging events on the network.

To make instances that are harder to solve and to reflect the near future in which the number of EBs in the fleets is expected to be significantly larger than the number of chargers available at the depot, we set the number of chargers as $c_{d,l_0} = \lceil \frac{\max_{d \in D} |B_d|}{5} \rfloor \cdot \frac{5}{2} + 5$ for the depot l_0 and $c_{d,l} = \lceil \frac{\max_{d \in D} |B_d|}{5} \rfloor \cdot \frac{1}{2} + 2$ for $l \in L \backslash \{l_0\}$, $\forall d \in D$. Each instance is generated with a 3 or 5 days in the planning horizon. Thus, the set of instances contains 72 instances (= $3 \times 3 \times 2 \times 2 \times 2$). In the following, we may refer to a configuration as an instance family using the following convention *cost_nbDays_opportunity*, where *cost* indicates whether the charging costs are location dependent (L) or constant (C), *nbDays* is the number of days in the planning horizon, and *opportunity* indicates the charging opportunity (among low, middle and high).

3.5.2 Results with the MILP

In the first set of experiments, we solved the 72 instances using the MILP introduced in Section 3.3 running on CPLEX for 3 hours. Out of the 72 instances, the solver found optimal solutions for 35 instances, and feasible-but-unproven solutions for the remaining 37. Table 3.2 summarizes the results. The first column indicates the instance family ; the second column reports the number of feasible solutions found for each configuration ; the third column reports the number of optimal solutions found for each configuration ; the fourth column shows the average gap on the objective function between the best integer solution and the best lower bound computed by CPLEX ; and the fifth column reports the average computational time.

TABLE 3.2 – Computational results - MILP (computational time limit of 3h)

Instance family	# Solved	# Optimal	Gap w.r.t. LB	Computational time (s)
L_3_low	6/6	2	1.2	7390
L_3_middle	6/6	2	2.1	7268
L_3_high	6/6	2	3.3	7297
L_5_low	6/6	2	1.4	7488
L_5_middle	6/6	1	2.2	7333
L_5_high	6/6	2	7.1	7597
Total / Average	36/36	11	2.9	7396
C_3_low	6/6	6	0.0	396
C_3_middle	6/6	5	0.4	2458
C_3_high	6/6	2	5.1	7329
C_5_low	6/6	5	0.0	2563
C_5_middle	6/6	4	0.5	4227
C_5_high	6/6	2	8.3	8048
Total / Average	36/36	24	2.4	4170

In the upper section of the table, instances where charging costs depend on location struggle with the challenge of finding optimal solutions. Fewer than a third of such instances are optimally solved. This results in large computational times. On average, instances with location dependent costs are either successfully solved within 10 minutes for the few optimally solved cases, or they reach the maximum computational time of three hours. The solver seeks a cost-optimal balance between charging at high rates for en-route charging and charging at minimal costs for overnight charging. Thus, many solutions may show proximity in their objective values while diverging significantly in the decisions made, making the instances challenging to solve optimally. Note that, the gap is relatively small at 2.9% on average (including 11 instances with a gap of 0.0%). Therefore, the MILP approach is not inherently deficient ; rather, it struggles with the challenge of closing the optimality gap.

The bottom half of the table shows different results. Instances become easier to solve when charging costs remain constant. A greater number of instances are optimally solved in this scenario. Given that charging costs are constants, it is more efficient to charge at locations where charging rates are higher, considering the objective function. There is no need to find a balance between cost and effectiveness. Thus, this results in shorter computational times and lower gaps with respect to the LB. Instances with location dependent charging costs with small gaps tend to be solved to optimality when the costs become constant. Those previously small gaps are then set to 0, contributing to lower average optimality gaps. A side effect of the constant charging costs is the charging strategy induced. The en-route charging is supposed to support the overnight charging. However, given that EBs charge at locations where charging rates are higher, the overnight charging acquires the role of support charging in this condition, which is an unexpected side effect.

3.5.3 Results with the iterative two-phase matheuristic

In the second set of experiments, we solved the 72 instances using the iterative two-phase matheuristic introduced in Section 3.4 with a total time limit of 15 minutes. We set a 3 minutes computation time limit for an iteration of the intra-block decision stage, a 5 minutes computation time limit for an iteration of the inter-block decision stage, and $K = 3$ as the selection span in the initialization method. The method found feasible solutions for all of 72 instances. Table 3.3 summarizes the results. The first column indicates the instance family ; the second column reports the number of feasible solutions found for each configuration ; the third column shows the average gap in the objective function with respect to the solutions found by the MILP ; the fourth column presents the average gap in the objective function with respect to the solutions found by the initialization stage (Line 1) ; the fifth column indicates the number of iterations performed by the method ; the sixth column reports the average computational time ; the seventh column shows the average total computational time spent to provide an initial EB-to-block assignment and a charging sequence for overnight charging (Line 1 and 7) ; the eighth column indicates the average computational time spent by the intra-block decision stage (Line 3) ; and the ninth columns shows the average computational time spent by the inter-block decision stage (Line 5). Note that we do not compute the gaps when one of both methods (MILP resolution or ITPM) did not find a feasible solution for an instance.

TABLE 3.3 – Computational results - ITPM (computational time limit of 15min)

Instance family	# Solved	Gap w.r.t. MILP (%)	Gap w.r.t. init. step (%)	# Iterations	Computational time (s)	Line 1 + 7 time (s)	Line 3 time (s)	Line 5 time (s)
L_3_low	6/6	1.2	−22.5	84	900	15	156	727
L_3_middle	6/6	1.1	−24.1	103	900	21	422	456
L_3_high	6/6	1.7	−32.8	75	900	13	675	211
L_5_low	6/6	1.5	−18.7	37	900	39	155	703
L_5_middle	6/6	1.7	−24.9	37	900	33	400	465
L_5_high	6/6	−2.2	−32.4	25	900	31	600	268
Total / Average	36/36	0.8	−25.9	60	900	25	401	472
C_3_low	6/6	0.5	−10.8	41	900	15	118	766
C_3_middle	6/6	0.7	−16.5	31	900	14	278	607
C_3_high	6/6	−1.2	−35	16	900	11	440	449
C_5_low	6/6	0.9	−7.1	17	900	17	175	706
C_5_middle	6/6	1.5	−22.6	12	900	20	304	576
C_5_high	6/6	−4.4	−35.1	8	900	17	392	490
Total / Average	36/36	−0.4	−21.2	21	900	16	284	599

The results show that ITPM finds feasible solutions for all 72 instances, consuming the allocated the 15 minutes of computation time. Moreover, the method provides good solutions. The average gap with respect to the MILP is 0.2%. Therefore, the objective values of the solution found by the ITPM are very close to those of the MILP, however, the method consumes much less computing time : 15 minutes versus 3 hours. As that seventh columns shows, the algorithm finds an initial solution quickly (either at the start or the restart) given that it only needs less than 30 seconds in average. Then, the method focuses on improving these initial solutions for the majority of the time. However, we can still observe some differences depending on whether the charging costs are location-dependent or constant. Although gaps with respect to the MILP are low (lower than 2%), gaps for instances with constant charging costs are negative. For those instances, the MILP found an optimal solution for 24 out of 36 instances and significant gaps for the remaining ones. The method managed to significantly tighten the gap for the remaining instances, which is far from optimal, showing that instances with constant charging costs are easier to solve. Whereas the fact that the computational times dedicated to optimize an initial solution are close among all instances, we observe a significant difference between the balance between the total computational times spent on the intra-block decision stage and the inter-block decision stage, for constant charging cost instances and location-dependent charging costs instances. For constant charging cost instances, the inter-block decision stage systematically consumes more computation time. When the cost of recharging does not depend on the charging location, there is no advantage to use overnight charging, at low charging rates. Then, most of the charging takes place during the en-route charging events. The bounds induced as a result of the intra-block decision stage (particularly the lower bound) are not tight enough and thus do not provide relevant information for the subsequent step. Therefore, inter-block decision stage struggles to achieve its stopping condition (optimality gap less than 5%). As a result, each iteration takes longer, leading to fewer iterations during the same computation time (21 for constant charging cost instances and 60 for location-dependent costs instances). Finally, the results show the interest of removing some charging events. The total costs are reduced by 23.5% in average between the initial solution computed during the initialization stage and the best solution found by the method.

3.6 Conclusion

In this paper, we introduced the MDEBARSP and formulated it as a MILP that can be solved using a commercial solver. To enhance computational efficiency, we proposed a matheuristic named iterative two-phase matheuristic. To evaluate our algorithm, we used a set of 72 instances derived from operational data of an EB operator. First, the MILP solver is able to find optimal solutions for half of instances and feasible solutions for the remaining instances, with a significant average optimality gap of 2.7%. Despite its effectiveness, the approach demands a significant amount of computational time, reaching the provided time limit of 3 hours for half of instances. The, the iterative two-phase matheuristic provides good solutions in short computational times, with a small average gap of 0.2% w.r.t. MILP approach and an average computational time of 15 min. It also shows a reduction of total costs of 23.5% by removing unnecessary en-route charging events.

As a first research perspective, we can propose considering of battery degradation impact over time. The lifespan of batteries diminishes over time under charging and discharging cycles. Each EB with its own trips, its battery lifespan changes in a specific way for each EB. Consequently, despite the initial uniformity of the EB fleet, their individual battery capacities evolve uniquely, resulting in a heterogeneous fleet. Another research direction could be to extend the problem by considering the more strategic objective of minimizing the number of chargers for both overnight and en-route charging. This would add a kind of technology selection decision to the problem. A final interesting research avenue would be to consider a more fine-grained EB operation and the dynamic rearrangement of sub-blocks. For instance, swapping sub-blocks between two EBs performing charging events at the same location and time could optimize certain objective functions or help further charging scheduling. Thus, it would transform the problem into an EB-to-subblock assignment problem.

Acknowledgement

We thank the personnel of GIRO Inc. for fruitful discussions and for providing real-world datasets. This research was also enabled in part by the support provided by Calcul Québec (www.calculquebec.ca) and Digital Research Alliance of Canada (www.alliancecan.ca).

References

ALVO, M., ANGULO, G., & KLAPP, M. A. (2021). An exact solution approach for an electric bus dispatch problem. *Transportation Research Part E : Logistics and Transportation Review*, *156*, 102528.

AVISHAN, F., YANIKOGLU, I., & ALWESABI, Y. (2023). Electric bus fleet scheduling under travel time and energy consumption uncertainty. *Transportation Research Part C : Emerging Technologies*, *156*, 104357.

BARRÉ, A., DEGUILHEM, B., GROLLEAU, S., GÉRARD, M., SUARD, F., & RIU, D. (2013). A review on lithium-ion battery ageing mechanisms and estimations for automotive applications. *Journal of Power Sources*, *241*, 680-689.

de VOS, M. H., von LIESHOUT, R. N., & DOLLEVOET, T. (2023). Electric Vehicle Scheduling in Public Transit with Capacitated Charging Stations. *Transportation Science*.

ECHEVERRI GUZMAN, L. C. (2020). *The Multi-period Electric Vehicle Routing problem : model and solution approaches* [thèse de doct., Université de Tours].

GOEHLICH, D., SPANGENBERG, F., & KUNITH, A. (2013). Stochastic total cost of ownership forecasting for innovative urban transport systems. *2013 IEEE International Conference on Industrial Engineering and Engineering Management*.

HOUBBADI, A., TRIGUI, R., PELISSIER, S., REDONDO-IGLESIAS, E., & BOUTON, T. (2019). Optimal Scheduling to Manage an Electric Bus Fleet Overnight Charging. *Energies*, *12*(14).

IPCC. (2014). *Climate Change 2014 : AR5 Synthesis Report* (rapp. tech.).

IPCC. (2023). *Climate Change 2023 : AR6 Synthesis Report* (rapp. tech.).

JANOVEC, M., & KOHÁNI, M. (2019). Exact approach to the electric bus fleet scheduling. *Transportation Research Procedia*, *40*, 1380-1387.

KLEIN, P. S., & SCHIFFER, M. (2023). Electric vehicle charge scheduling with flexible service operations. *57*(6), 1605-1626.

LIU, T., & CEDER, A. (2020). Battery-electric transit vehicle scheduling with optimal number of stationary chargers. *Transportation Research Part C : Emerging Technologies*, *114*, 118-139.

MONTOYA, A., GUÉRET, C., MENDOZA, J. E., & VILLEGAS, J. G. (2017). The electric vehicle routing problem with nonlinear charging function. *Transportation Research Part B : Methodological*, *103*, 87-110.

PELLETIER, S., JABALI, O., & LAPORTE, G. (2018). Charge scheduling for electric freight vehicles. *Transportation Research Part B : Methodological*, *115*, 246-269.

PELLETIER, S., JABALI, O., LAPORTE, G., & VENERONI, M. (2017). Battery degradation and behaviour for electric vehicles : Review and numerical analyses of several models. *Transportation Research Part B : Methodological*, *103*, 158-187.

RINALDI, M., PICARELLI, E., D'ARIANO, A., & VITI, F. (2020). Mixed-fleet single-terminal bus scheduling problem : Modelling, solution scheme and potential applications. *Omega*, *96*, 102070.

ROGGE, M., van der HURK, E., LARSEN, A., & SAUER, D. U. (2018). Electric bus fleet size and mix problem with optimization of charging infrastructure. *Applied Energy*, *211*, 282-295.

SASSI-BEN SALAH, O., & OULAMARA, A. (2017). Electric vehicle scheduling and optimal charging problem : complexity, exact and heuristic approaches. *International Journal of Production Research*, *55*(2), 519-535.

VENDÉ, P., DESAULNIERS, G., KERGOSIEN, Y., & MENDOZA, J. E. (2023). Matheuristics for a multi-day electric bus assignment and overnight recharge scheduling problem. *Transportation Research Part C : Emerging Technologies*, *156*, 104360.

WANG, Y., HUANG, Y., XU, J., & BARCLAY, N. (2017). Optimal recharging scheduling for urban electric buses : A case study in Davis. *Transportation Research Part E : Logistics and Transportation Review*, *100*, 115-132.

WEI, R., LIU, X., OU, Y., & KIAVASH FAYYAZ, S. (2018). Optimizing the spatio-temporal deployment of battery electric bus system. *Journal of Transport Geography*, *68*, 160-168.

WU, W., LIN, Y., LIU, R., & JIN, W. (2022). The multi-depot electric vehicle scheduling problem with power grid characteristics. *Transportation Research Part B : Methodological*, *155*, 322-347.

XYLIA, M., LEDUC, S., PATRIZIO, P., KRAXNER, F., & SILVEIRA, S. (2017). Locating charging infrastructure for electric buses in Stockholm. *Transportation Research Part C : Emerging Technologies*, *78*, 183-200.

YAO, E., LIU, T., LU, T., & YANG, Y. (2020). Optimization of electric vehicle scheduling with multiple vehicle types in public transport. *Sustainable Cities and Society*, *52*, 101862.

ZHANG, L., WANG, S., & QU, X. (2021). Optimal electric bus fleet scheduling considering battery degradation and non-linear charging profile. *Transportation Research Part E : Logistics and Transportation Review*, *154*, 102445.

ZHOU, Y., MENG, Q., & ONG, G. P. (2022). Electric Bus Charging Scheduling for a Single Public Transport Route Considering Nonlinear Charging Profile and Battery Degradation Effect. *Transportation Research Part B : Methodological*, *159*, 49-75.

Conclusion générale

L'intégration de bus électriques dans les réseaux de transport en commun représente une solution pour limiter les émissions de gaz à effet de serre. Cependant, la mise en place d'une flotte de bus électriques soulève des questions d'organisation et de dimensionnement, notamment sur les aspects d'infrastructures pour la recharge des batteries des bus. Cette thèse vise à répondre à certaines de ces questions en étudiant et résolvant les problématiques liées aux différentes stratégies de recharge (nocturne ou en route) et de localisation et dimensionnement des chargeurs. Cette thèse a abordé trois problématiques liées à ces différentes stratégies de recharge.

La recharge en route permet d'augmenter la distance pouvant être parcourue et de diminuer la fréquence de retour au dépôt. Cependant, seul un nombre limité de chargeurs peut être installé sur le réseau pour des raisons budgétaires, ce qui entraîne un partage des stations de recharge et l'utilisation de bus hybrides. Le premier chapitre présente un problème d'emplacement de chargeurs dans un réseau de transport public. À partir d'un ensemble de lignes caractérisées par une séquence d'arrêts desservis par des bus hybrides à des fréquences données, le problème consiste à trouver l'emplacement des stations de recharge qui peuvent être partagées par plusieurs lignes, combien en installer, et comment les utiliser pour garantir le même niveau de service et s'assurer qu'il existe bien un ordonnancement de recharge réalisable sur chacune des stations. Nous avons considéré deux fonctions objectifs : la maximisation de la distance parcourue en utilisant le mode électrique et la minimisation des coûts d'installation. Nous avons proposé un programme linéaire en nombres entiers (PLNE) et une méthode basée sur un algorithme de type branch-and-check pour résoudre efficacement le problème. Dans cette méthode de type branch-and-check, le problème est séparé en une relaxation du problème original et un problème de faisabilité. Le problème relaxé cherche à déterminer le nombre et l'emplacement des chargeurs ainsi que les durées des recharges des bus de chaque ligne, sans vérifier la contrainte de ressource, c'est à dire s'il existe un éventuel chevauchement des tâches de rechargement. Un problème de faisabilité est résolu à chaque fois qu'une solution est trouvée pour le problème relaxé. Dans ces problèmes de faisabilité, nous nous assurons qu'un ordonnancement réalisable pour toutes les tâches de rechargement existe. En plus d'expériences numériques montrant l'efficacité de la méthode proposée, nous proposons des perspectives managériales en présentant les bénéfices opérationnels et économiques d'utiliser des chargeurs partagés. Pour ce faire, nous avons comparé deux scénarios, dans le premier les chargeurs peuvent être partagés entre plusieurs lignes et dans le deuxième, les chargeurs sont dédiés à une seule ligne. Ensuite, nous avons montré le compromis entre l'augmentation du budget et la réalisation d'une plus grande électrification en analysant le coût d'installation de chargeurs en fonction du pourcentage de trajets à réaliser en mode électrique. L'un des principaux résultats montre que, pour utiliser uniquement le mode électrique, il faudrait augmenter le budget dédié à l'installation d'au moins 50%.

Les autorités organisatrices des transports en commun augmentent constamment la proportion de bus électriques dans leurs flottes. En raison de contraintes budgétaires, d'espace et de puissance électrique disponible, le nombre de chargeurs au dépôt est limité par rapport au nombre de bus électriques. Se pose ainsi une problématique de gestion et de planification de la recharge nocturne au dépôt. Dans le deuxième chapitre, nous considérons un problème d'affectation de bus électriques et d'ordonnancement de la recharge nocturne sur plusieurs jours, qui peut être défini de la manière suivante. Le problème considère un ensemble de blocs véhicules (suites programmées de trajets effectués par le même bus sur une journée) devant être effectués sur plusieurs jours, un ensemble de bus électriques identiques, et un ensemble de chargeurs disponibles au dépôt. L'objectif est d'affecter un bus électrique à chaque bloc et de planifier la recharge nocturne au dépôt en s'assurant que les bus ne soient jamais à court d'énergie et que la capacité de recharge au dépôt ne soit jamais dépassée. L'objectif est de minimiser le coût total de recharge tout en préservant la durée de vie de la batterie à long terme. Ce problème est modélisé sous la forme d'un PLNE et résolu à l'aide d'un solveur commercial. Afin d'obtenir des temps de calcul plus courts, nous avons développé deux matheuristiques. Dans une première matheuristique assign-then-schedule, la méthode décide de l'affectation des bus à des blocs et des durées de recharge pendant la nuit dans une première étape. Ensuite, elle ordonnance ces tâches de rechargement de manière à respecter la capacité des chargeurs, les heures de disponibilité des bus, et à minimiser la dégradation de la durée de vie de la batterie à long terme. Dans une seconde matheuristique daily-assign-then-schedule, une étape préliminaire est ajoutée à la méthode précédente. Cette étape affecte des bus à des blocs, de manière à ce que la suite de blocs effectués par un même bus entre deux jours consécutifs se répète sur l'horizon de planification. Afin de montrer l'intérêt de considérer un horizon de plusieurs jours, nous présentons deux autres matheuristiques appelées short-sighted, simulant les pratiques industrielles actuelles et résolvant le problème séquentiellement, un jour à la fois. Dans une première matheuristique minimum short-sighted, la méthode charge un bus de la quantité minimale d'énergie nécessaire pour effectuer le bloc de la journée suivante. En comparant les résultats de cette méthode et de daily-assign-then-schedule, nous remarquons qu'il est parfois impossible de trouver des solutions réalisables si on considère un jour après l'autre, montrant l'intérêt de considérer directement un horizon de planification de plusieurs jours. Dans une seconde matheuristique maximum short-sighted, la méthode charge un bus jusqu'à ce qu'il doive partir ou qu'un autre bus ait besoin du chargeur. Avec cette méthode, nous remarquons que les coûts, et en particulier les coûts liés à la dégradation de la durée de vie de la batterie à long terme, augmentent significativement comparé aux résultats de la méthode daily-assign-then-schedule.

Dans le dernier chapitre, nous considérons une extension du problème étudié dans le deuxième chapitre. Cette extension remet en question les activités journalières effectuées par les bus en introduisant des événements de recharge en route effectués pendant la journée. Étant donné que les infrastructures de recharge au dépôt sont limitées, nous cherchons à réduire les opérations de recharge pendant la nuit en rechargeant également les bus pendant la journée. Ainsi, nous avons étudié un nouveau problème d'affectation de bus électriques et d'ordonnancement de la recharge sur plusieurs jours. Les blocs véhicules sont désormais considérés comme des suites sécables de trajets effectués par le même bus sur une journée. Entre ces différents trajets, les bus peuvent effectuer des opérations de recharge sur des chargeurs installés sur le réseau de transport. En plus des décisions prises dans le problème original, nous ordonnançons les opérations de recharge en route, en nous assurant que les bus disposent de suffisamment d'énergie pour effectuer tous leurs trajets, tout en préservant la durée de vie de la batterie à long terme. Pour résoudre ce problème, nous l'avons modélisé sous la forme d'un PLNE et nous avons développé une matheuristique. À partir d'une solution initiale, la méthode va remettre en question les décisions concernant la recharge en route sans modifier celles liées à la recharge nocturne. Ensuite dans une deuxième phase, la méthode cherche à améliorer les décisions liées à la recharge nocturne sans modifier les décisions liées à la recharge en route. La méthode réitère ce processus jusqu'à ne plus pouvoir améliorer la solution courante. Les expérimentations numériques ont permis de démontrer l'intérêt d'utiliser une combinaison de ces deux stratégies de recharge mais aussi celui de limiter le nombre d'événements de recharge. À cette fin, nous avons comparé les coûts associés à des solutions dans lesquelles les bus se rechargent à chaque opportunité disponible avec celles où le nombre d'événements de recharge en route est optimisé.

Les problématiques liées à l'électrification du transport public sont complexes et de nombreuses perspectives de recherche peuvent être considérées à partir de ces problèmes étudiés dans cette thèse.

Le problème d'emplacement de chargeur relève essentiellement d'un niveau stratégique, avec des décisions qui ont des implications à long terme et ne sont pas sujettes à des révisions régulières. Par conséquent, il pourrait être bénéfique d'intégrer d'autres décisions stratégiques et de considérer l'ensemble de ces décisions simultanément. Par exemple, on peut envisager d'inclure le choix des technologies (type de chargeur, de bus ou de batterie) comme une composante du problème, ce qui permettrait d'introduire des coûts associés à l'acquisition de ces différentes technologies. Étant donné que l'installation de chargeur est un processus coûteux qui ne pourrait pas être effectué en une seule fois par une compagnie de transport, une seconde perspective serait d'aborder le problème avec une approche itérative. Chaque itération prendrait en compte la présence des chargeurs déjà installés lors des itérations précédentes comme des données du problème. Cette approche progressive permettrait d'électrifier graduellement le réseau de transport jusqu'à l'obtention d'un réseau de transport entièrement électrique. Une autre perspective de recherche pourrait consister à remettre en question les trajets d'une proportion des lignes de bus existantes. Cette réévaluation permettrait de placer des chargeurs en dehors des lignes existantes, favorisant ainsi un partage accru des chargeurs entre les lignes. Notons qu'en fixant cette proportion de changement à 100%, il serait possible de redessiner entièrement les lignes de bus, les adaptant spécifiquement aux chargeurs installés et permettant ainsi de réduire les coûts.

Le problème d'affectation des bus et de recharge relève davantage de l'opérationnel, où les infrastructures de recharge sont considérées comme des données du problème. Il existe des perspectives de recherche visant à améliorer la gestion des ressources du réseau de transport. La première ressource à considérer est le bus lui-même, en particulier sa batterie. Identifier et quantifier toutes les sources de dégradation de la durée de vie d'une batterie permettrait d'intégrer ces aspects de manière plus systématique dans les problèmes étudiés. Jusqu'à présent, chaque problème aborde un aspect spécifique de la dégradation, mais une approche intégrant toutes les sources de dégradation en même temps pourrait être bénéfique, même si elles sont souvent concurrentielles. Par exemple, vider la batterie à sa profondeur de décharge maximale (différence d'état de charge entre le début et la fin de la recharge) réduit le nombre de cycles de recharge que peut supporter une batterie. Ceci induit de recharger très fréquemment afin de limiter les variations de l'état de charge. Cependant, les batteries ont un nombre de cycles de recharge limité, ce qui implique d'attendre le plus possible avant de recharger et donc une grande profondeur de décharge. L'objectif serait de trouver un compromis optimal pour minimiser toutes les sources de dégradation et prolonger la durée de vie des batteries. De plus, la durée de vie des batteries des bus évolue en fonction des différentes sources de dégradations auxquelles elle est exposée. Ainsi, même après une période assez courte, une flotte de bus initialement homogène devient hétérogène, avec des capacités de batterie uniques à chaque bus. Une seconde perspective de recherche sur ce problème opérationnel serait de considérer une nouvelle ressource : les chauffeurs de bus. Dans les problèmes de transport public, l'aspect de gestion des ressources humaines est souvent négligé. Étant donné que les chauffeurs sont affectés à des bus, si les itinéraires des bus présentent des demandes hétérogènes, les chauffeurs peuvent être confrontés à des charges de travail inégales. Il serait donc pertinent d'intégrer une notion d'équité dans la répartition de la charge de travail des chauffeurs, en fonction des parcours des bus.

Tous ces problèmes de transport reposent sur une logistique bien orchestrée. Les tâches de rechargement peuvent être planifiées efficacement car les horaires d'arrivée et de départ des bus, ainsi que leur consommation pendant leur trajet, sont précisément connus. Cependant, les bus ne sont pas les seuls acteurs dans le réseau de transport. Ils partagent la route avec d'autres véhicules, ce qui peut introduire des incertitudes dans les données des problèmes. En effet, des événements imprévus tels qu'un trafic dense ou un accident peuvent entraîner des retards dans les horaires des bus, affectant ainsi leur arrivée prévue à la station de recharge. Ces retards peuvent à leur tour perturber les horaires des autres bus, remettant en question les décisions prises par des algorithmes. Dans ce contexte, il pourrait être judicieux de considérer des versions stochastiques de ces problèmes de recharge de véhicules qui pourraient être à l'aide de méthodes d'optimisation robuste. Il est également important de noter que ces variations de temps de trajet peuvent aussi avoir un impact non négligeable sur la consommation électrique. Ainsi, en plus de l'incertitude concernant les horaires de disponibilité des chargeurs, nous devons également prendre en compte l'incertitude liée à cette consommation.

Enfin, une dernière perspective de recherche essentielle concerne le calcul précis de la consommation des véhicules électriques. Actuellement, les autorités organisatrices des transports en commun ont tendance à surestimer significativement les consommations pour garantir que les bus ne se retrouvent pas à court d'énergie pendant leurs trajets. Cette surestimation est ensuite transmise aux modèles d'aide à la décision, entraînant ainsi des coûts de recharge plus élevés que nécessaire. Cette pratique contribue également à accélérer la dégradation des batteries, augmentant ainsi les coûts de maintenance à long terme de la flotte de véhicules. Pour éviter cette surestimation, il serait nécessaire d'obtenir des modèles capables de fournir des estimations précises de la consommation électrique. La consommation d'un véhicule électrique dépend de plusieurs facteurs tels que la distance parcourue, le poids total en charge, la température et la pente au sol. Le poids et la température sont des paramètres variables qui peuvent changer d'un jour à l'autre, voire au cours d'une même journée. Par exemple, un bus transportant un grand nombre de passagers consommera davantage qu'un bus vide. De même, les températures peuvent varier en fonction des saisons ou des conditions climatiques. Une estimation plus précise de la consommation des véhicules électriques permettrait de mieux anticiper les besoins en recharge et de réduire les coûts associés. Cela nécessiterait une prise en compte plus fine de tous les paramètres influençant la consommation, ce qui contribuerait à une planification plus efficace et durable des transports publics.

Bibliographie

ALVO, M., ANGULO, G., & KLAPP, M. A. (2021). An exact solution approach for an electric bus dispatch problem. *Transportation Research Part E : Logistics and Transportation Review*, *156*, 102528.

AN, K., JING, W., & KIM, I. (2020). Battery-swapping facility planning for electric buses with local charging systems. *International Journal of Sustainable Transportation*, *14*(7), 489-502.

ARORA, J. S. (2017). Chapter 18 - Multi-objective Optimum Design Concepts and Methods. In *Introduction to Optimum Design (Fourth Edition)*. Academic Press.

AVISHAN, F., YANIKOGLU, I., & ALWESABI, Y. (2023). Electric bus fleet scheduling under travel time and energy consumption uncertainty. *Transportation Research Part C : Emerging Technologies*, *156*, 104357.

AYAD, A., EL-TAWEEL, N. A., & FARAG, H. E. Z. (2021). Optimal Design of Battery Swapping-Based Electrified Public Bus Transit Systems. *IEEE Transactions on Transportation Electrification*, *7*(4), 2390-2401.

BARRÉ, A., DEGUILHEM, B., GROLLEAU, S., GÉRARD, M., SUARD, F., & RIU, D. (2013). A review on lithium-ion battery ageing mechanisms and estimations for automotive applications. *Journal of Power Sources*, *241*, 680-689.

BLOOMBERG NEW ENERGY FINANCE. (2018). *Electric buses in cities : Driving towards cleaner air and lower CO2* (Report) (Visité en Mars 2024). on the behalf of : Financing Sustainable Cities Initiative, C40 Cities, World Resources Institute, Citi Foundation. https://data.bloomberglp.com/professional/sites/24/2018/05/Electric-Buses-in-Cities-Report-BNEF-C40-Citi.pdf

BUNTE, S., & KLIEWER, N. (2009). An overview on vehicle scheduling models. *Public Transport*, *1*(4), 299-317.

CAUGHILL, P. (2018). Report Shows Half of Public Buses Will be Electric by 2025. *Futurism*. https://futurism.com/new-report-majority-public-buses-electric-2025

de VOS, M. H., von LIESHOUT, R. N., & DOLLEVOET, T. (2023). Electric Vehicle Scheduling in Public Transit with Capacitated Charging Stations. *Transportation Science*.

DIRKS, N., SCHIFFER, M., & WALTHER, G. (2022). On the integration of battery electric buses into urban bus networks. *Transportation Research Part C : Emerging Technologies*, *139*, 103628.

DIRKS, N., WAGNER, D., SCHIFFER, M., & WALTHER, G. (2021). A Concise Guide on the Integration of Battery Electric Buses into Urban Bus Networks. *arXiv preprints arXiv :2104.10752v1*.

ECHEVERRI GUZMAN, L. C. (2020). *The Multi-period Electric Vehicle Routing problem : model and solution approaches* [thèse de doct., Université de Tours].

FRADE, I., RIBEIRO, A., GONÇALVES, G., & ANTUNES, A. P. (2011). Optimal Location of Charging Stations for Electric Vehicles in a Neighborhood in Lisbon, Portugal. *Transportation Research Record*, *2252*(1), 91-98.

FROGER, A., JABALI, O., MENDOZA, J. E., & LAPORTE, G. (2022). The Electric Vehicle Routing Problem with Capacitated Charging Stations. *Transportation Science*, *56*, 460-482.

GAIROLA, P., & NEZAMUDDIN, N. (2022). Design of Battery Electric Bus System Considering Waiting Time Limitations. *Transportation Research Record*.

GOEHLICH, D., SPANGENBERG, F., & KUNITH, A. (2013). Stochastic total cost of ownership forecasting for innovative urban transport systems. *2013 IEEE International Conference on Industrial Engineering and Engineering Management*.

GUPTA, U. I., LEE, D., & LEUNG, J. Y. (1979). An Optimal Solution for the Channel-Assignment Problem. *IEEE Transactions on Computers*, *C-28*(11), 807-810.

HE, S. Y., KUO, Y.-H., & WU, D. (2016). Incorporating institutional and spatial factors in the selection of the optimal locations of public electric vehicle charging facilities : A case study of Beijing, China. *Transportation Research Part C : Emerging Technologies*, *67*, 131-148.

HEAP, B. R. (1963). Permutations by Interchanges. *The Computer Journal*, *6*(3), 293-298.

HOKE, A., BRISSETTE, A., SMITH, K., PRATT, A., & MAKSIMOVIC, D. (2014). Accounting for Lithium-Ion Battery Degradation in Electric Vehicle Charging Optimization. *IEEE Journal of Emerging and Selected Topics in Power Electronics*, *2*(3), 691-700.

HOUBBADI, A., TRIGUI, R., PELISSIER, S., REDONDO-IGLESIAS, E., & BOUTON, T. (2019). Optimal Scheduling to Manage an Electric Bus Fleet Overnight Charging. *Energies*, *12*(14).

INSEE RÉFÉRENCES. (2019). *Changement climatique et effet de serre* (Report). Insee. https://www.insee.fr/fr/statistiques/3676581

IPCC. (2014). *Climate Change 2014 : AR5 Synthesis Report* (rapp. tech.).

IPCC. (2023). *Climate Change 2023 : AR6 Synthesis Report* (rapp. tech.).

IPCC. (2024). *About the IPCC* [Visité en Mars 2024]. https://www.ipcc.ch/about/

JANOVEC, M., & KOHÁNI, M. (2019). Exact approach to the electric bus fleet scheduling. *Transportation Research Procedia*, *40*, 1380-1387.

KCHAOU-BOUJELBEN, M. (2021). Charging station location problem : A comprehensive review on models and solution approaches. *Transportation Research Part C : Emerging Technologies*, *132*, 103376.

KLEIN, P. S., & SCHIFFER, M. (2023). Electric vehicle charge scheduling with flexible service operations. *57*(6), 1605-1626.

KLIEWER, N., MELLOULI, T., & SUHL, L. (2006). A time–space network based exact optimization model for multi-depot bus scheduling. *European Journal of Operational Research*, *175*(3), 1616-1627.

KUHN, H. W. (1955). The Hungarian method for the assignment problem. *Naval Research Logistics Quarterly*, *2*(1-2), 83-97.

KUNITH, A., MENDELEVITCH, R., & GOEHLICH, D. (2017). Electrification of a city bus network—An optimization model for cost-effective placing of charging infrastructure and battery sizing of fast-charging electric bus systems. *International Journal of Sustainable Transportation*, *11*(10), 707-720.

LIU, T., & CEDER, A. (2020). Battery-electric transit vehicle scheduling with optimal number of stationary chargers. *Transportation Research Part C : Emerging Technologies*, *114*, 118-139.

LIU, Z., SONG, Z., & HE, Y. (2018). Planning of Fast-Charging Stations for a Battery Electric Bus System under Energy Consumption Uncertainty. *Transportation Research Record*, *2672*(8), 96-107.

LÖBEL, A. (1999). Solving Large-Scale Multiple-Depot Vehicle Scheduling Problems. *Computer-Aided Transit Scheduling*.

LOTFI, M., PEREIRA, P., PATERAKIS, N. G., GABBAR, H. A., & CATALÃO, J. P. S. (2020). Optimal Design of Electric Bus Transport Systems With Minimal Total Ownership Cost. *IEEE Access*, *8*.

LUNZ, B., YAN, Z., GERSCHLER, J. B., & SAUER, D. U. (2012). Influence of plug-in hybrid electric vehicle charging strategies on charging and battery degradation costs. *Energy Policy*, *46*, 511-519.

MAJHI, R. C., RANJITKAR, P., SHENG, M., COVIC, G. A., & WILSON, D. J. (2021). A systematic review of charging infrastructure location problem for electric vehicles. *Transport Reviews*, *41*(4), 432-455.

MINISTÈRE DE LA TANSITION ÉCOLOGIQUE. (2020). Réseau urbain Fil Bleu - Jeu de données [Data about the theoretical transport offer of Fil Bleu network, Tours, France]. https://transport.data.gouv.fr/datasets/horaires-theoriques-du-reseau-fil-bleu-tours-metropole-gtfs

MONTOYA, A., GUÉRET, C., MENDOZA, J. E., & VILLEGAS, J. G. (2017). The electric vehicle routing problem with nonlinear charging function. *Transportation Research Part B : Methodological*, *103*, 87-110.

PELLETIER, S., JABALI, O., & LAPORTE, G. (2018). Charge scheduling for electric freight vehicles. *Transportation Research Part B : Methodological*, *115*, 246-269.

PELLETIER, S., JABALI, O., LAPORTE, G., & VENERONI, M. (2017). Battery degradation and behaviour for electric vehicles : Review and numerical analyses of several models. *Transportation Research Part B : Methodological*, *103*, 158-187.

PELLETIER, S., JABALI, O., MENDOZA, J. E., & LAPORTE, G. (2019). The electric bus fleet transition problem. *Transportation Research Part C-Emerging Technologies*, *109*, 174-193.

QUINTANA, C. L., CLIMENT, L., & ARBELAEZ, A. (2022). Iterated Local Search for the eBuses Charging Location Problem. In G. RUDOLPH, A. V. KONONOVA, H. AGUIRRE, P. KERSCHKE, G. OCHOA & T. TUŠAR (Éd.), *Parallel Problem Solving from Nature – PPSN XVII*. Springer International Publishing.

RATP. (2023). *Un parc de bus plus écologique avec bus2025* [Visité en Mars 2024]. https://www.ratp.fr/groupe-ratp/programmebus2025

RINALDI, M., PICARELLI, E., D'ARIANO, A., & VITI, F. (2020). Mixed-fleet single-terminal bus scheduling problem : Modelling, solution scheme and potential applications. *Omega*, *96*, 102070.

ROGGE, M., van der HURK, E., LARSEN, A., & SAUER, D. U. (2018). Electric bus fleet size and mix problem with optimization of charging infrastructure. *Applied Energy*, *211*, 282-295.

SASSI-BEN SALAH, O., & OULAMARA, A. (2014). Simultaneous electric vehicles scheduling and optimal charging in the business context : case study. *5th IET Hybrid and Electric Vehicles Conference (HEVC 2014)*, 1-6.

SASSI-BEN SALAH, O., & OULAMARA, A. (2017). Electric vehicle scheduling and optimal charging problem : complexity, exact and heuristic approaches. *International Journal of Production Research*, *55*(2), 519-535.

SHEN, Z.-J. M., FENG, B., MAO, C., & RAN, L. (2019). Optimization models for electric vehicle service operations : A literature review. *Transportation Research Part B : Methodological*, *128*, 462-477.

SOLTANPOUR, A., GHAMAMI, M., NICKNAM, M., GANJI, M., & TIAN, W. (2022). Charging Infrastructure and Schedule Planning for a Public Transit Network with a Mixed Fleet of Electric and Diesel Buses. *Transportation Research Record*.

SUSTAINABLE BUS. (2023). *Electric bus, main fleets and projects around the world* [Visité en Mars 2024]. https://www.sustainable-bus.com/electric-bus/electric-bus-public-transport/

THORSTEINSSON, E. S. (2001). Branch-and-check : A hybrid framework integrating mixed integer programming and constraint logic programming. *International Conference on Principles and Practice of Constraint Programming*.

TOPAL, O. (2023). A novel on the retrofit from CNG buses to electric buses for rubber-tyred wheeled public transportation systems. *Proceedings of the Institution of Mechanical Engineers, Part D : Journal of Automobile Engineering*, *237*(7), 1738-1750.

UN. (1992). *United Nations Conference on Environment and Development, Rio de Janeiro, Brazil, 3-14 June 1992* [Visité en Mars 2024]. https://www.un.org/en/conferences/environment/rio1992

UN. (2024). *Conferences | Environment and sustainable development* [Visité en Mars 2024]. https://www.un.org/en/conferences/environment/index

UNFCCC. (2016). *Report of the Conference of the Parties on its twenty-first session, held in Paris from 30 November to 13 December 2015. Part one : Proceedings* (rapp. tech.).

UNFCCC. (2024). *Conference of the Parties (COP)* [Visité en Mars 2024]. https://unfccc.int/process/bodies/supreme-bodies/conference-of-the-parties-cop

VENDÉ, P., DESAULNIERS, G., GENDREAU, M., KERGOSIEN, Y., & MENDOZA, J. E. (2023). Matheuristique pour un problème d'ordonnancement d'opérations de recharge de bus électriques sur plusieurs jours. *ROADEF 2023*.

VENDÉ, P., DESAULNIERS, G., GENDREAU, M., KERGOSIEN, Y., & MENDOZA, J. E. (2024a). A matheuristic for a multi-day electric bus assignment and recharge scheduling problem. *EURO 2024*.

VENDÉ, P., DESAULNIERS, G., GENDREAU, M., KERGOSIEN, Y., & MENDOZA, J. E. (2024b). Matheuristique pour un problème d'ordonnancement d'opérations de recharge de bus électriques sur plusieurs jours. *ROADEF 2024*.

VENDÉ, P., DESAULNIERS, G., KERGOSIEN, Y., & MENDOZA, J. E. (2022a). Matheuristics for a multi-day electric bus assignment and overnight recharge scheduling problem. *VeRoLog 2022*.

VENDÉ, P., DESAULNIERS, G., KERGOSIEN, Y., & MENDOZA, J. E. (2022b). Matheuristiques pour un problème d'ordonnancement d'opérations de recharge nocturne de bus électriques sur plusieurs jours. *ROADEF 2022*.

VENDÉ, P., DESAULNIERS, G., KERGOSIEN, Y., & MENDOZA, J. E. (2023). Matheuristics for a multi-day electric bus assignment and overnight recharge scheduling problem. *Transportation Research Part C : Emerging Technologies*, *156*, 104360.

VENDÉ, P., MENDOZA, J. E., & KERGOSIEN, Y. (2021). Problème d'emplacement de bornes de recharge dans les réseaux de transport avec bus hybrides. *ROADEF 2021*.

WANG, X., YUEN, C., HASSAN, N. U., AN, N., & WU, W. (2017). Electric Vehicle Charging Station Placement for Urban Public Bus Systems. *IEEE Transactions on Intelligent Transportation Systems*, *18*(1), 128-139.

WANG, Y., LIAO, F., & LU, C. (2022). Integrated optimization of charger deployment and fleet scheduling for battery electric buses. *Transportation Research Part D : Transport and Environment*, *109*, 103382.

WANG, Y., HUANG, Y., XU, J., & BARCLAY, N. (2017). Optimal recharging scheduling for urban electric buses : A case study in Davis. *Transportation Research Part E : Logistics and Transportation Review*, *100*, 115-132.

WEI, R., LIU, X., OU, Y., & KIAVASH FAYYAZ, S. (2018). Optimizing the spatio-temporal deployment of battery electric bus system. *Journal of Transport Geography*, *68*, 160-168.

WEN, M., LINDE, E., ROPKE, S., MIRCHANDANI, P., & LARSEN, A. (2016). An adaptive large neighborhood search heuristic for the Electric Vehicle Scheduling Problem. *Computers & Operations Research*, *76*, 73-83.

WU, W., LIN, Y., LIU, R., & JIN, W. (2022). The multi-depot electric vehicle scheduling problem with power grid characteristics. *Transportation Research Part B : Methodological*, *155*, 322-347.

XYLIA, M., LEDUC, S., PATRIZIO, P., KRAXNER, F., & SILVEIRA, S. (2017). Locating charging infrastructure for electric buses in Stockholm. *Transportation Research Part C : Emerging Technologies*, *78*, 183-200.

YAO, E., LIU, T., LU, T., & YANG, Y. (2020). Optimization of electric vehicle scheduling with multiple vehicle types in public transport. *Sustainable Cities and Society*, *52*, 101862.

YE, Z., YU, N., WEI, R., & LIU, X. C. (2022). Decarbonizing regional multi-model transportation system with shared electric charging hubs. *Transportation Research Part C : Emerging Technologies*, *144*, 103881.

ZHANG, L., WANG, S., & QU, X. (2021). Optimal electric bus fleet scheduling considering battery degradation and non-linear charging profile. *Transportation Research Part E : Logistics and Transportation Review*, *154*, 102445.

ZHOU, Y., MENG, Q., & ONG, G. P. (2022). Electric Bus Charging Scheduling for a Single Public Transport Route Considering Nonlinear Charging Profile and Battery Degradation Effect. *Transportation Research Part B : Methodological*, *159*, 49-75.

Annexe A – Deploying fast-charging infrastructure on urban transit networks

Branch-and-check-based heuristic results - Second Run

Table A.1 outlines the results for HBC's second run. The first two columns categorize the instances by family. Subsequent columns present the average objective values of the best solution found (Avg. Investment), as well as the average gap with the MILP (Avg. MILP gap) and BC (Avg. BC gap). These gaps are calculated for instances meeting two conditions : 1) both methods find the same objective values after the first run, and 2) both methods provide a feasible solution after the second run. The last four columns retain the same meaning as the corresponding columns in Table 1.8. It is worth noting that the number of feasible solutions remains identical to that in the first run.

Table A.1, shows that HBC discovers 191 solutions with objective function values similar to those obtained by the MILP resolution and the BC method for comparable instances. In the case of other instances, the objective function values of the three methods appear to be closely aligned ; however, comparing them is challenging because each solution does not correspond to the same weighted electric distance value. The computation time of HBC in the second run was shorter than that in the first run. Despite this, a small number of calls to the subproblem with low computation times were still observed, for

$\lvert L \rvert$	Service frequency	Avg. investement ($\times$1000 \$)	Avg. MILP gap (%)	Avg. BC gap (%)	Avg. CPU time (s)	# Time limit exceeded	Avg. # Call S.P.	Avg. S.P. CPU time (s)
3	Low	868.2	0.0	0.0	8.8	0	3.3	3.3
	Average	868.2	0.0	0.0	14.9	0	2.6	3.0
	High	868.2	0.0	0.0	12.8	0	2.8	2.9
4	Low	1102.4	8.3	0.0	43.2	0	3.1	3.0
	Average	1102.4	0.0	0.0	30.1	0	3.4	3.0
	High	1102.4	0.0	0.0	45.2	0	3.6	3.1
5	Low	1023.3	0.0	0.0	86.3	0	2.3	3.0
	Average	995.4	0.0	0.0	100.1	1	247.1	33.5
	High	997.7	0.0	0.0	47.0	0	2.2	30.0
6	Low	916.7	0.0	0.0	198.4	2	2.0	27.5
	Average	912.8	–	0.0	146.6	1	2.2	25.4
	High	944.7	–	–	388.9	4	1015.3	93.7
7	Low	942.1	1.5	1.2	426.6	6	1.8	86.4
	Average	937.6	2.3	–	451.1	6	365.1	104.9
	High	951.6	2.2	5.7	458.5	6	1.1	99.1
8	Low	1023.0	3.2	2.0	452.6	7	1.3	92.7
	Average	1011.1	–	2.0	324.9	4	31.8	89.0
	High	1020.6	–	–	386.8	3	36.5	86.5
9	Low	1068.8	–	−0.9	280.5	4	1.0	81.8
	Average	986.0	–	–	324.9	3	1.3	78.8
	High	1148.5	–	–	421.3	2	1.7	77.6
Total - Average		986.0	1.3	0.3	205.8	49	77.6	1.7

TABLE A.1 – HBC results - Second run (investment)

the same reason as in the previous run.

A MILP model to solve the non-shared charger location problem in hybrid electric bus networks

The variables of the problem are as follows :

— $x_{l,i}$: Positive integer decision variable indicating the number of chargers installed at Stop i of Line l.

— $y_{l,i,i'}$: Binary decision variable indicating whether the segment connecting stops $i \in V_l$ and $i' \in V_l$ on Line $l \in L$ is driven in electric mode.

— $q_{l,i}$: Positive decision variable indicating the SoC when HBs servicing Line $l \in L$ arrive at stop $i \in V_l$.

— $t_{l,i}$: Positive integer decision variable indicating the charging time of an HB operating on Line $l \in L$ at Stop $i \in V_l$.

The non-shared charger location problem in HB networks can be formulated using the following MILP model.

$$\max \quad \sum_{l \in L} \sum_{(i,i') \in A_l} \frac{d_{i,i'}}{f_l} \cdot y_{l,i,i'} \tag{A.45}$$

Subject to :

$$\sum_{i \in V} \sum_{l \in L} cost_i \cdot x_{l,i} \leq B \tag{A.46}$$

$$t_{l,i} \leq f_l \cdot x_{l,i} \qquad \forall l \in L,\ \forall i \in V_l \tag{A.47}$$

$$t_{l,i} \leq w_{l,i} \qquad \forall l \in L,\ \forall i \in V_l \tag{A.48}$$

$$q_{l,i} + t_{l,i} \cdot R - e_{i,i'} \cdot y_{l,i,i'} = q_{l,i'} \qquad \forall l \in L,\ \forall (i,i') \in A_l \tag{A.49}$$

$$q_{l,i} + t_{l,i} \cdot R \leq Q \qquad \forall l \in L,\ \forall i \in V_l \tag{A.50}$$

$$q_{l,st_l} \leq q_{l,lt_l} \qquad \forall l \in L \tag{A.51}$$

$$x_{l,i} \in \mathbb{N}_0 \qquad \forall i \in V, \forall l \in L \tag{A.52}$$

$$q_{l,i} \geq 0 \qquad \forall l \in L,\ \forall i \in V_l \tag{A.53}$$

$$y_{l,i,i'} \in \{0,1\} \qquad \forall l \in L,\ \forall (i,i') \in A_l \tag{A.54}$$

$$t_{l,i} \in \mathbb{N}_0 \qquad \forall l \in L,\ \forall i \in V_l \tag{A.55}$$

Objective function (A.45) maximizes the total weighted electric distance. Constraints (A.46) ensure that the total budget for charger installation is adhered to. Constraints (A.47) limits the charging time according to the number of chargers. Constraints (A.48) ensure that the maximum stop duration at each stop is satisfied. Constraints (A.49) compute the SoC on the bus line between two stops based on the charging time of the first stop and whether the electric mode is used. Constraints (A.50) ensure that the SoC never exceeds the battery capacity. Constraints (A.51) implies that an HB ends its line with a higher SoC than at the beginning, such that no extra charging time is required to travel the line again. Constraints (A.52)–(A.55) define the domains of the decision variables.

Annexe B – Matheuristics for a multi-day electric bus assignment and overnight recharge scheduling problem

Calendar aging

The cost of a battery degradation due to calendar aging is defined in function of a battery lifetime reduction and the purchase cost of the battery. We denote c_{bd} the cost of battery degradation due to a charge cycle. From HOKE et al., 2014, it is defined as $c_{bd} = c_{bat} \frac{\Delta L}{L}$, where c_{bat} is the purchase cost of the battery and $\frac{\Delta L}{L}$ is the battery lifetime reduction due to the charge cycle being evaluated. The battery lifetime reduction depends on the total battery lifetime (L) and the lifetime degradation (ΔL). The battery lifetime reduction is computed as follows :

$$\frac{\Delta L}{L} = \frac{L_{ideal} - L_{observed}}{L_{ideal}}$$

where $L_{observed}$ and L_{ideal} are the battery lifetimes based on an observed scenario and an ideal scenario, respectively. The observed scenario is determined using a MILP that minimizes only the total charging cost. The ideal scenario considers the implementation of the solution obtained in the observed scenario in a setting where there is an unlimited number of chargers. As it stands, all the charging operations can be performed right before the corresponding EB leaves the depot to cover its next block, to the EBs never store energy at high SoCs. Needless to say, in this ideal scenario, there is no battery degradation due to calendar aging. From (LUNZ et al., 2012) and given a scenario $o \in \{observed, ideal\}$, the battery lifetimes L_o can be estimated as follows :

$$\begin{aligned} L_o =& \rho_o^{driving}\, c(SOC_o^{driving}) + \rho_o^{before}\, c(SOC_o^{before}) \\ &+ \rho_o^{charging}\, c(SOC_o^{charging}) + \rho_o^{after}\, c(SOC_o^{after}) \end{aligned}$$

where ρ_o^s is the time proportion that the EB spends in status $s \in \{driving, before, charging, after\}$ (with $\sum_s \rho_o^s = 1$), SOC_o^s is the average state of charge in status s and $c(SOC_o^s)$ is the capacity lifetime in SoC SOC_o^s. The 4 possible statuses are : $driving$ when the bus is driving, $before$ when the bus is idle before its charging operation, $charging$ when the bus is charging, and $after$ when the bus is idle after its charging operation. The capacity lifetime values are extrapolated from data in LUNZ et al., 2012. Using an exponential regression to match our battery capacity (363 kWh) and an average temperature of 22 degrees Celsius, we obtain $c(x) = 18.438\, e^{-0.014x}$.

The average values of ρ_o^s and SOC_o^s considering that an entire charging cycle lasts one day (1440 minutes), are computed from all 264 instances. For the observed scenario, buses spend an average of 863 minutes per day on the road with an average SoC of 57.5% and 577 minutes at the depot, i.e. 370 minutes before the charging operation, 137 minutes of charging and 70 minutes after the charging operation. The average SoC during these three phases is 20%, 57.5% and 95%, respectively. We thus obtain :

$$\begin{aligned} L_{observed} &= \frac{863}{1440}\, c(0.575) + \frac{370}{1440}\, c(0.20) + \frac{137}{1440}\, c(0.575) + \frac{70}{1440}\, c(0.95) \\ &= 18.31958754\ years \end{aligned}$$

For the ideal scenario, buses spend an average of 863 minutes per day on the road with an average SoC of 57.5% and 577 minutes at the depot, i.e. 440 minutes before the charging operation and 137 minutes of charging, with an average SoC of 20% and 95%, respectively. We thus obtain :

$$L_{observed} = \frac{863}{1440}\, c(0.575) + \frac{440}{1440}\, c(0.20) + \frac{137}{1440}\, c(0.575)$$

$$= 18.31025189\ years$$

Then, considering a battery price of USD 150,000 (BLOOMBERG NEW ENERGY FINANCE, 2018), the cost of a battery degradation per charge cycle can be computed as follows :

$$\begin{aligned} c_{bd} &= 150,000\ \frac{18.31958754 - 18.31025189}{18.31958754} \\ &= 76.43990691/cycle \end{aligned}$$

Finally, an entire cycle (charging and discharge) takes one day (1440 minutes), so the cost of battery degradation per minute is $\delta = \frac{76.43990691}{1440} \approx 0.05\$/min$.

Generation of non-dominated feasible charger schedules

Algorithme 6 : Generation of non-dominated feasible charger schedules

```
Input : $T_d := \{i_1, i_2, \dots, i_n\}$ : Set of charging operations of day $d$
$k_d \longleftarrow \left\lfloor \frac{H_d^D - H_d^R}{U_d} \right\rfloor$;
current_schedules_set ⟵ $\{\{i_1\}, \{i_2\}, \dots, \{i_n\}\}$;
$S_d \longleftarrow \emptyset$;
while current_schedules_set $\neq \emptyset$ do
    current_schedule ⟵ current_schedules_set.pop();
    $S_d$.push(current_schedule);
    if current_schedule.size() $< k_d$ then
        foreach Charging operation $i_j$ in $T_d$ do
            if $i_j$ not in current_schedule then
                current_schedule.add($i_j$);
                permutations ⟵ generate_permutations(current_schedule);
                /* Permutations generated using Heap's Algorithm
                   (HEAP, 1963)                                        */
                best_permutation_cost ⟵ ∞;
                best_permutation ⟵ $\emptyset$;
                foreach Permutation p in permutations do
                    if p is feasible then
                        /* Permutation is feasible if all its
                           charging tasks $i_k \in p$ starts after their
                           respective release time $h_{i_k}^R$ and ends before
                           their respective due time $h_{i_k}^D$          */
                        if $eval(p) <$ best_permutation_cost then
                            /* Permutation evaluated using
                               Equation 2.46                           */
                            best_permutation ⟵ $p$;
                            best_permutation_cost ⟵ $eval(p)$;
                        end
                    end
                end
                if best_permutation $\neq \emptyset$ then
                    current_schedules_set.push(best_permutation);
                end
                current_schedule.remove($i_j$);
            end
        end
    end
end
```

Annexe C – A matheuristic for a multi-day electric bus assignment and recharge scheduling problem

Charging event sequence initialization procedure

Algorithme 7 : Charging event sequence initialization procedure

Input : $B_{d,l}$: Set of sub-blocks on day d associated with an charging event at location l

Input : C_l : Set of chargers at charging location l

Input : K : Number of considered charging events in the selection at each iteration

$\mathbb{E} \longleftarrow B_{d,l}$: Set of charging events associated with a sub-block on day d starting at location l;

$availability$: Array of size $|C_l|$ indicating the maximum time at which the charger becomes available;

$availability[c] \longleftarrow -\infty, \forall c \in C_l$;

if $l = l_0$ **then**

  Sort $\mathbb{E}$ according to the increasing starting time of the associated sub-block $h^S_{i,k}$;

else

  Sort $\mathbb{E}$ according to the increasing ending time of the preceding sub-block $h^E_{i,k-1}$;

end

while $\mathbb{E} \neq \emptyset$ **do**

  $e \longleftarrow$ A charging event selected randomly from the K first events of $\mathbb{E}$;

  Remove e from $\mathbb{E}$;

  Select charger c such as $\forall\ c' \in C_l, availability[c] \leq availability[c']\}$;

  Assign e at the end of the charging sequence of charger c;

  $(i,k) \longleftarrow$ Sub-block associated with charging event e;

  $availability[c] \longleftarrow h^S_{i,k}$;

end